

USING OF GEOTHERMAL ENERGY IN HEATING AND COOLING OF AGRICULTURAL STRUCTURES

BY

SHABAN GABER ALI GOUDA

B. Sc. Agricultural Sciences (Agricultural Engineering), Moshtohor
Faculty of Agriculture, Benha Univ., 2010

A THESIS

Submitted in Partial Fulfillment of The

Requirements for the Degree of

MASTER OF SCIENCE

IN

AGRICULTURAL SCIENCE

(AGRICULTURAL ENGINEERING)

AGRICULTURAL ENGINEERING DEPARTMENT

FACULTY OF AGRICULTURE, MOSHTOHOR

BENHA UNIVERSITY

2015


USING OF GEOTHERMAL ENERGY IN HEATING AND COOLING OF AGRICULTURAL STRUCTURES

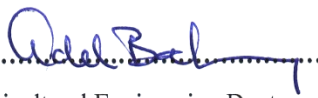
BY

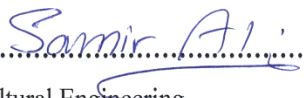
SHABAN GABER ALI GOUDA

B. Sc. Agricultural Sciences (Agricultural Engineering), Moshtohor
Faculty of Agriculture, Benha Univ., 2010

Under the supervision of:

Prof. Dr. Zakaria A. El-Haddad 
Professor Emeritus of Agricultural Engineering,
Faculty of Agriculture, Moshtohor, Benha University

Prof. Dr. Adel H. Bahnasawy 
Professor and Head of Agricultural Engineering Dept.,
Faculty of Agriculture, Moshtohor, Benha University

Prof. Dr. Samir A. Ali 
Professor of Agricultural Engineering,
Faculty of Agriculture, Moshtohor, Benha University

2015

Approval Sheet

USING OF GEOTHERMAL ENERGY IN HEATING AND COOLING OF AGRICULTURAL STRUCTURES

BY


SHABAN GABER ALI GOUDA

B. Sc. Agricultural Sciences (Agricultural Engineering), Moshtohor
Faculty of Agriculture, Benha Univ., 2010

This Thesis for Master has been Approved by:

Prof. Dr. Mohamed Hashem Hatem.....

Professor Emeritus of Agricultural Engineering,
Faculty of Agriculture, Cairo University.

Prof. Dr. Zakaria A. El-Haddad

Professor Emeritus of Agricultural Engineering,
Faculty of Agriculture, Moshtohor, Benha University.

Prof. Dr. Adel H. Bahnasawy

Professor and Head of Agricultural Engineering Dept.,
Faculty of Agriculture, Moshtohor, Benha University.

Prof. Dr. Samir A. Ali

Professor of Agricultural Engineering,
Faculty of Agriculture, Moshtohor, Benha University.

Dr. Taha H. Ashour

Associate Professor of Agricultural Engineering,
Faculty of Agriculture, Moshtohor, Benha University.

Date of Examination: / / 2015

DEDICATION

I dedicate this work to my parents who motivates me to set higher targets and encourage me to finish this work. I also dedicate this work to my brother, my sisters and my wife.

ACKNOWLEDGEMENTS

First of all, I would like to express my deepest thanks to **ALLAH** (God) for helping me to carry out and complete this work.

The author is greatly indebted to his supervisors **Prof. Dr. Zakaria A. El-Haddad**, Professor Emeritus of Agricultural Engineering, Faculty of Agriculture, Moshtohor, Benha University, **Prof. Dr. Adel H. Bahnasawy**, Professor and Head of Agric. Eng. Dept., Faculty of Agriculture at Moshtohor, Benha University, and **Prof. Dr. Samir A. Ali**, Professor, Agric. Eng. Dept., Faculty of Agriculture at Moshtohor, Benha University for their valuable guidance supervision, encouragement, constructive criticism and giving every possible help throughout the execution of this work.

Thanks are extended to all staff member in the Department of Agricultural Engineering, Faculty of Agriculture at Moshtohor, Benha University: who were so willing interrupted their own work to assist me throughout the course of this study.

CONTENTS

Title	Page
LIST OF TABLES	
LIST OF FIGURES	
LIST OF SYMBOLS AND ABBREVIATION	
ABSTRACT	
1. INTRODUCTION.....	1
2. LITERATURE REVIEW.....	4
2.1. Global Energy Situation.....	4
2.2. Geothermal Energy.....	5
2.2.1. Geothermal potential energy in the world.....	5
2.2.2. Geothermal energy in Egypt.....	7
2.2.3. Utilization of geothermal energy.....	8
2.2.3.1. Direct use of geothermal energy.....	8
2.3. Geothermal Energy System.....	13
2.3.1. Sub-surface soil temperature.....	13
2.3.1.1. Ground thermal properties.....	15
2.3.1.2. Soil temperature model.....	16
2.3.2. Earth to air heat exchanger.....	21
2.3.2.1. Design consideration of earth tube heat exchanger.....	21
a) Soil type.....	21

b) Tube depth.....	22
c) Tube material.....	24
d) Tube diameter.....	25
e) Tube Length.....	27
f) Air velocity.....	28
g) Air flow rate.....	28
h) Number of tube.....	29
i) Spacing between tubes.....	29
j) Fan position.....	30
k) Control mode.....	30
2.3.2.2. Types of ETAHE.....	30
2.3.2.3. ETAHE applications.....	34
2.3.2.4. ETAHE economics.....	37
2.4. Greenhouses.....	38
2.4.1. Greenhouse heat balance.....	40
3. MATERIALS AND METHODS.....	42
3.1. Materials	42
3.1.1. System description.....	41
3.1.2. Instruments.....	43
a) Scanning thermometer.....	43
b) Electric dry oven.....	44

3.2. Methods	45
3.2.1. Field experiment	45
3.2.2. Measurements.....	45
4. MODEL DEVELOPMENT.....	47
4.1. Geothermal Energy Model.....	47
4.1.1. Soil temperature model.....	44
4.1.2. Earth to air heat exchanger model (ETAHE)..	49
4.1.2.1. Heat transfer between soil and air.....	50
(i) Thermal resistance due to convection heat transfer between the air in the pipe and the pipe inner surface (R_c) calculation.....	51
(ii) Thermal resistance due to conduction heat transfer between the pipe inner and outer surface (R_p) calculation.....	53
(iii) Thermal resistance due to conduction heat transfer between the pipe outer surface and the undisturbed soil (R_s) calculation.....	53
4.1.2.2. Calculation the length of ETAHE.....	53
4.1.2.3. Air flow rate.....	54
4.1.2.4. Fan power.....	54
4.1.2.5. Outlet fluid temperature from the ETAHE	55
4.1.2.6. Efficiency of ETAHE.....	55
4.1.3. Greenhouse Model.....	56
4.1.3.1.Greenhouse heating and cooling requirements.....	56
4.1.4. Data inputs for model validation and experimentation.....	67

4.1.4.1. Input data of soil temperature model.....	67
4.1.4.2. Input data of earth to air heat exchanger model.....	68
4.1.4.3. Description of greenhouse as a case study.	69
5. RESULTS AND DISCUSSIONS.....	71
5.1. Model validation.....	71
5.1.1. Soil temperature model validation.....	71
5.1.2. Earth to air heat exchanger model validation....	76
5.2. Model Experimentation.....	79
5.2.1. Soil temperature at various depths.....	79
5.2.1.1. Influence of various parameters on ETAHE system.....	82
5.2.1.2. Influence of pipe length	82
5.2.1.3. Influence of pipe diameter.....	86
5.2.2.3. Influence of air velocity.....	89
5.2.1.4. Influence of pipe material.....	93
5.2.2. Greenhouse as a case study.....	96
6. SUMMARY AND CONCLUSION.....	97
7. REFERENCES.....	101
8. ARABIC SUMMARY.....	-

LIST OF TABLES

No.	Title	Page
2.1	Thermal properties of selected soils, rocks, and backfills	17
3.1	Specifications of scanning thermometer.	41
3.2	Specifications of the electric oven.	42
4.1	Suggested heat transmission coefficients.	58
4.2	Construction U-Factor multipliers.	59
4.3	Suggested Design Air Changes (<i>N</i>) (1/hour).	60
4.4	Transmissivity of glazing materials.	61
4.5	Input parameters for calculating soil temperature.	67
4.6	Input parameters for comparative validation of ETAHE model.	68
4.7	Details of greenhouse specifications and other details used for ETAHE model.	70
5.1	Measured data and predicted soil temperature.	72
5.2	The predicted soil temperatures and measured by Kassem, (1999) .	74
5.3	ETAHE model validation at ambient air temperature 25.56 °C.	77
5.4	ETAHE model validation at ambient air temperature 20.55°C.	78
5.5	Predicted soil temperature at various depths.	80
5.6	Influence of pipe length on pressure drop, inlet temperature and efficiency of ETAHE at 0.15 pipe diameter and 8 m/s air velocity.	83

5.7	Influence of pipe diameter on pressure drop, inlet temperature and efficiency of ETAHE at 60 m pipe length and 8 m/s air velocity.	87
5.8	Influence of air velocity on pressure drop, inlet temperature and efficiency of ETAHE at 0.15 m pipe diameter and 60 m pipe length.	90
5.9	Influence of pipe material on inlet air temperature and efficiency of ETAHE at 0.15 m pipe diameter and 60 m pipe length.	93
5.10	The results obtained from geothermal energy model for greenhouse at 11 m/s air velocity and PVC pipe material.	95

LIST OF FIGURES

No.	Title	Page
2.1	Growth curves for some crops.	9
	Heating systems in geothermal greenhouses. Heating installations with natural air movement ((natural convection): (a) aerial pipe heating; (b) bench heating; (c) low position heating pipes for aerial heating. (d) Soil heating. Heating installations with forced air movement (forced convection): (e) lateral position; (f) aerial fan; (g) high position ducts; (h) low-position ducts.	10
2.2	Effect of temperature on growth or production of food animals.	11
2.3	Geothermal energy uses.	12
2.4	Energy flows in ground.	15
2.5	Classification of earth to air heat exchanger.	31
2.6	An opened loop mode ETAHE	32
2.7	A closed loop mode ETAHE	32
2.8	ETAHE horizontal type.	32
2.10	Borehole heat exchanger (Double U-pipe).	34
2.11	Cross sections of different types of borehole heat exchangers.	34
2.12	Energy exchange between a greenhouse and the surroundings.	41
2.13	Heat loss/gain from a greenhouse.	41

3.1	Description of experiment.	42
3.2	Image of scanning thermometer.	44
3.3	J-type thermocouple. Flow chart of soil temperature model.	44
4.1	Geothermal energy system structure.	47
4.2	Flow chart of soil temperature model.	63
4.3	Flow chart of ETAHE model.	64
4.4	Heat balance for greenhouse.	57
4.5	Flow chart of greenhouse model	66
5.1-a	The predicted and measured soil temperatures at 2 m depth.	72
5.1-b	The predicted and measured soil temperatures at 3 m depth.	73
5.1-c	The predicted and measured soil temperatures at 4 m depth.	73
5.2-a	The predicted soil temperatures compared to that measured by Kassem, (1999) at 1.5 m.	75
5.2-b	The predicted soil temperatures compared to that measured by Kassem, (1999) at 2 m.	75
5.3	ETAHE Model validation at ambient air temperature 25.56 °C.	77
5.4	ETAHE model validation at ambient air temperature 20.55°C.	78
5.5	Predicted soil temperature at various depths.	81

5.6	Amplitude of predicted soil temperature at various depths.	81
5.7	Influence of pipe length on inlet air temperature in heating and cooling modes.	84
5.8	Influence of pipe length on ETAHE efficiency.	84
5.9	Influence of pipe length on pressure drop.	85
5.10	Influence of pipe diameter on inlet air temperature in heating and cooling modes.	87
5.11	Influence of pipe diameter on ETAHE efficiency.	88
5.12	Influence of pipe diameter on pressure drop.	88
5.13	Influence of air velocity on inlet air temperature in heating and cooling modes.	91
5.14	Influence of air velocity on ETAHE efficiency.	91
5.15	Influence of Air velocity on pressure drop.	92
5.16	Influence of pipe material on inlet air temperature.	94
5.17	Influence of pipe material on efficiency of ETAHE.	94

LIST OF SYMBOLS AND ABBREVIATION

$T_{(t,z)}$	Undisturbed ground temperature at time (t) and depth (z), °C.
T_{mean}	The mean ground surface temperature, °C.
T_{ma}	Mean ambient air temperature, °C.
A_s	The annual amplitude of the ground surface temperature, °C.
A_a	Annual amplitude of the ambient air temperature, °C.
t	Time in year (days) from starting date of year, number.
t_o	Phase constant (days) since the beginning of the year of the highest average ground surface temperature or ambient air temperature, number.
ω	Annual frequency, rad/day.
α	Thermal diffusivity of soil, m ² /day.
z	Depth of soil, m.
k_s	Soil thermal conductivity, W/(m.°C).
ρ_s	Soil density, kg/m ³ .
w	Moisture content of soil, % (dry basis).
c_s	Dry soil specific heat, kJ/(kg.°C).
c_w	Specific heat of water, kJ/(kg.°C).
q	Heat loss or gain per unit length of system, W/m.
T_f	Fluid temperature, °C.

T_s	Average annual soil temperature, °C.
T_{out}	Outlet air temperature, °C.
R_t	Total thermal resistance, (m·°C)/W.
R_c	Thermal resistance due to convection heat transfer between the air in the pipe and the pipe inner surface, (m·°C)/W.
h_c	Convective heat transfer coefficient at the inner pipe surface, W/m ² °C.
Nu	Nusselt number.
k_a	Thermal conductivity of air, W/(m·°C).
ρ_a	Density of air, kg/m ³ .
μ_a	Dynamic viscosity of air, Pa.s.
v	Air velocity, m/s.
D	Diameter of the pipe, m.
Pr	Prandtl number.
c_a	Specific capacity of air, kJ/(kg·°C).
R_p	Thermal resistance due to conduction heat transfer between the pipe inner and outer surface, (m·°C)/W.
r_1	Inner pipe radius, m.
r_2	Pipe thickness, m.
r_3	Distance between the pipe outer surface and undisturbed soil (assumed to be equal to the radius of the pipe), m.
k_p	Pipe thermal conductivity, W/(m·°C).

R_s	Thermal resistance due to conduction heat transfer between the pipe outer surface and the undisturbed soil, (m.°C)/W.
l	Length of ETAHE, m.
\dot{m}	Mass flow rate of the air, kg/s.
A_p	Cross section area of pipe, m ² .
P_f	Fan air power, W.
ΔP	Fan total pressure difference, Pa.
η_{fan}	Total fan efficiency, %.
f	Friction factor, -
Δt_m	Logarithmic average temperature difference, °C.
η_{ETAHE}	Efficiency of ETAHE, %.
Q_f	Furnace heat (heat losses), W.
Q_{em}	Heat from electric motors, W.
Q_l	Heat from lighting, W.
Q_s	Heat from the sun, W.
Q_c	Heat Loss by conduction through the greenhouse shell, W.
Q_{inf}	Heat Loss by air exchange between inside and outside air, W.
Q_{ev}	Heat Loss by evaporating water, W.
A	Surface area of the greenhouse, m ² .
U	Overall heat transmission coefficient, W/(m ² .°C).
T_i	Inside temperature, °C.

T_o	Outside temperature, °C.
N	Number of air exchanges per hour.
V	Volume of greenhouse, m ³ .
τ	The transmittance of the greenhouse cover to solar radiation
I_s	Intensity of solar radiation on a horizontal surface outside, W/m ² .
A_f	Area of greenhouse floor, m ² .
E	Ratio of evapotranspiration to solar radiation.
F	Floor use factor ratio of ground covered by plants to total ground area,-
ETAHE	Earth to air heat exchanger.

ABSTRACT

This study aimed to using geothermal energy in heating and cooling of agricultural structures. The greenhouse is taken here as a case study. Geothermal energy system was analysed and restructured as three sub models: soil temperature model, ETAHE model and greenhouse model. Soil temperature model was developed using previous researches and adjusted to suit Egyptian conditions. It was validated against two sets of data. The results show good agreement with measurements in both cases. It was found that the root mean squares of deviations of the first set at 1.5 and 2 m depths were 1.93, 1.85 °C respectively and for the second set at 2, 3 and 4 m depths were 2.65, 1.65 and 0.39 °C respectively. This soil temperature model was used as a component of ETAHE model. Similarly an earth to air heat exchanger (ETAHE) model was developed. Its results were validated against the results of three other studies. The current model gave good agreement with these studies. It can be suitably used to predict the thermal performance of ETAHE system. Using ETAHE model, a parametric analysis was carried out to investigate the effect of pipe diameter, pipe length, pipe material and air velocity inside the pipe on the earth tube inlet air temperature, the efficiency of ETAHE system and pressure drop under Egyptian conditions during both cooling and heating seasons. The results illustrate that the optimal values of pipe length used as inputs to design an ETAHE should be greater than 30 m and don't exceed 90 to 150 m. The optimum diameter was found to be in the range of 0.10 m to 0.30 cm. The diminution of air velocity causes an increase of thermal efficiency and a diminution of pressure losses. Plastic or metallic materials of pipe lead to very similar energy performances. The developed greenhouse model is used to predict the heating and cooling loads for a typical gable even span greenhouse of 256 m² floor area was considered, to be 42.91 kWh

and 170.39 kWh respectively. Experimentation with the model has shown that, to minimize the installation cost of ETAHE system for heating and cooling greenhouse under consideration, it is better to use smaller pipe diameters (from 0.10 to 0.30 m), because pipe diameter larger than this range leads to a little improvement in performance of ETAHE system and increases the installation cost. It also preferable to use a smaller air velocity which can be ranged from 5 to 15 m/s, because the air velocity less than 5 m/s required longer pipes and this leads to increasing the costs and the air velocity larger than 15 m/s required high fan power and reduces the efficiency of the system. The results indicated that, using of an ETAHE system for heating greenhouse was more efficient and low cost compared to using it for cooling in all cases of pipe diameters and air velocities. In case of using it for cooling, the remaining cooling requirements could be obtained by other cooling systems, e.g. evaporative cooling systems (fan-pad, fog/mist and roof evaporative cooling systems).

Keywords: geothermal energy, soil temperature, earth to air heat exchanger model, agricultural structures, greenhouse, heating and cooling requirements.

INTRODUCTION

1. INTRODUCTION

The global energy oil production is unstable and will diminish within a few years. Therefore, the energy prices are expected to rise and new energy systems are needed. In addition to this energy crisis the fossil fuels seems to be the main reason for climate change. There is a global political understanding that we need to replace fossil fuels by renewable energy systems in order to develop a stable and sustainable energy supply. About half of the global energy consumption is used for space heating and space cooling systems (**Kharseh, 2009**).

The global energy consumption, which increased ~84% during the last thirty years, exceeded 1.4×10^{11} MWh in 2008. It is projected to increase another ~39% until 2030. Heating and cooling, for industrial, commercial, and domestic use, represent 30-50% of global energy consumption i.e. 5.6×10^{10} MWh/year and an emission of 1.4×10^{10} ton CO₂/year. Consequently, implementing more efficient heating/cooling systems for buildings should make a significant contribution in saving energy and environment (**Kharseh, 2009**).

Egypt is the largest oil and natural gas consumer in Africa. Natural gas and oil are the primary fuels used to meet Egypt's energy needs, accounting for 94% of the country's total energy consumption in 2013. Egypt's total primary energy consumption was 1.7 million barrels per day of oil equivalent in 2013 (**BP, 2014**).

Agricultural and irrigation sector in Egypt consumed 178271 metric ton which represent 6.3 % from total consumption of petroleum products in 2007/2008 according to Egyptian ministry of petroleum. Greenhouses sector represented 3×10^7 m² of area for winter season and 3×10^6 m² of area for springer season which required fuel with cost 42937000 LE (**CAPMAS, 2013**).

Agriculture is the sole provider of human food. Most farm powers are supplied by fossil fuels, which contribute to greenhouse gas emissions and, in turn, accelerate climate change. Such environmental damage can be mitigated by the promotion of renewable resources such as solar, wind, biomass, tidal, geothermal, small-scale hydro, biofuels and wave-generated power. These renewable resources have a huge potential for the agriculture industry. The farmers should be encouraged by subsidies to use renewable energy technologies. The concept of sustainable agriculture lies on a delicate balance of maximizing crop productivity and maintaining economic stability, while minimizing the utilization of finite natural resources and detrimental environmental impacts (**Chel and Kaushik, 2011**).

Geothermal energy is one of renewable energy sources which has a potential use in Egypt. Although Egypt is not characterized by abundant igneous activity, its location in the northeastern corner of the African plate suggests that it possesses geothermal resources, especially along its eastern margin. **Farghally *et al.* (2010) and Haytham *et al.* (2013)** mentioned that the temperature of 150 °C may be found in the reservoir in the Gulf of Suez and red coastal zone.

It is a clean, renewable resource because the heat emanating from the interior of the earth is essentially limitless. The source of geothermal energy, the earth's heat, is available 24 hours a day, 365 days a year. Solar and wind energy sources, in contrast, are dependent upon a number of factors, including daily and seasonal fluctuations and weather variations.

Maintaining a comfortable temperature for plants inside a greenhouse requires a significant amount of energy. Separate heating and cooling systems are often used to maintain the desired air temperature inside the greenhouse, and the energy required to operate these systems commonly comes from electricity, fossil fuels, or biomass. The other

option is to consider using renewable energy resources such as geothermal energy which is available on-site, and in massive quantities (**Alghannam, 2012**).

The utilization of geothermal energy in Egypt is still far away from the economic usage. In most countries, there is no geothermal studies or researches of utilization of geothermal energy in agriculture, only geothermal potential estimations are available. It is time now to investigate the possibility of using geothermal energy for heating and cooling of agricultural structures. To achieve that the specific objectives of this work are:

1. Develop, validate and test a soil temperature model.
2. An earth- to air heat exchanger model was constructed.
3. Greenhouse heating and cooling requirements were determined as a case study.

LITERATURE

REVIEW

2. LITERATURE REVIEW

2.1. Global energy situation

Global primary energy consumption increased by 2.3% in 2013, an acceleration over 2012 (+1.8%). Growth in 2013 accelerated for oil, coal, and nuclear power. But global growth remained below the 10-year average of 2.5% according to the BP 2014 Statistical Review of World Energy.

Egypt is the largest oil and natural gas consumer in Africa. Natural gas and oil are the primary fuels used to meet Egypt's energy needs, accounting for 94% of the country's total energy consumption in 2013. Egypt's total primary energy consumption was 1.7 million barrels per day of oil equivalent in 2013, according to the BP 2014 Statistical Review of World Energy. According to the Middle East Economic Survey (MEES), Egypt spent \$26 billion on fossil-fuel subsidies in 2012, ranking as the eighth-highest spender of fossil fuel subsidies in the world. Energy subsidies, which account for 20% to 25% of government spending, continue to cut into Egypt's budget. Energy subsidies have contributed to Egypt's high budget deficit, and EGPC accumulated \$7.5 billion, as of June 2014, in outstanding arrears to foreign oil companies (EIA, 2014).

Agricultural and irrigation sector in Egypt consumed 178271 metric ton, which represent 6.3 % from total consumption of petroleum products in 2007/2008 according to the Egyptian Ministry of Petroleum. Greenhouses sector represented 3×10^7 m² of area for winter season and 3×10^6 m² of area for springer season which required fuel with cost of 42937000 LE (CAPMAS, 2013).

2.2. Geothermal energy

Geothermal energy is the thermal energy in the earth's crust: thermal energy in rock and fluid (water, steam, or water containing large amounts of dissolved solids) that fills the pores and fractures in the rock, sand, and gravel. Calculations show that the earth, originating from a completely molten state, would have cooled and become completely solid many thousands of years ago without an energy input beyond that of the sun. It is believed that the ultimate source of geothermal energy is radioactive decay within the earth. Through plate motion and volcanism, some of this energy is concentrated at high temperature near the surface of the earth. Energy is also transferred from deeper parts of the crust to the earth's surface by conduction and by convection in regions where geological conditions and the presence of water allow. Because of variation in volcanic activity, radioactive decay, rock conductivities, and fluid circulation, different regions have different heat flows (through the crust to the surface), as well as different temperatures at a particular depth. The normal increase of temperature with depth (i.e., the normal geothermal gradient) is about 24 K/km of depth, with gradients of 9 to 48 K/km being common. Areas that have higher temperature gradients and/or higher-than-average heat flow rates constitute the most interesting and viable economic resources. However, areas with normal gradients may be valuable resources if certain geological features are presented (ASHRAE, 2011).

2.2.1. Geothermal potential energy in the world

For centuries geothermal springs have been used for bathing, healing and cooking. Only in the early 20th century did people start to consider the heat from inside the earth as a practical source of energy with huge potential. Geothermal energy is now used to produce electricity on a significant scale, as well as for direct use applications

like space heating, greenhouses, and aquaculture. The main advantages of geothermal energy are that it is clean (emits little or no greenhouse gases) and indigenous, decreasing the need for imported fuels and hence the dependency on foreign oil. The exploitable geothermal resources are found throughout the world and are being utilized in at least 78 countries. Electricity is produced from geothermal in 24 countries spread over all continents. Six countries obtain 10-30% of their electricity from geothermal (IGA, 2010).

Geothermal energy has become established as a reliable and environmentally benign source of power. Installed capacity in 2010 is the equivalent of 10-15 typical nuclear power plants, with almost no atmospheric emissions or hazardous wastes. Proven high availability and load factors, and no dependence on sunlight or weather, makes geothermal energy a key resource in a sustainable energy future. The growth of geothermal utilization for power generation has averaged roughly 5.5% per year over the last 30 years, and the geothermal installed capacity in the world has been increased by about 1000 MWe every 5 years, Fig. 2.1 (IGA, 2010).

For countries which having direct utilization of geothermal energy started with 28 countries reported in 1995 increased to 58, 72 and 78 countries reported in years 2000, 2005 and 2010 respectively. An estimate of the installed thermal power for direct utilization at the end of 2009, reported from World Geothermal Congress in Bali, Indonesia (2010) is 48,493 MWt, almost a 72% increased over the 2005 data, growing at a compound rate of 11.4% annually with a capacity factor of 0.28. The distribution of thermal energy used by category is approximately 47.2% for ground-source heat pumps, 25.8% for bathing and swimming (including balneology), 14.9% for space heating (of which 85% is for district heating), 5.5% for greenhouses and open

ground heating, 2.8% for industrial process heating, 2.7% for aquaculture pond and raceway heating, 0.4% for agricultural drying, 0.5% for snow melting and cooling, and 0.2% for other uses. Energy savings amounted to 250 million barrels (38 million tonnes) of equivalent oil annually, preventing 33 million tonnes of carbon and 107 million tonnes of CO₂ being released to the atmosphere (**Lund, 2010 and Lund *et al.*, 2011**).

2.2.2. Geothermal energy in Egypt

The geothermal resources in Egypt are in the lower temperature ranges that are more widespread than the higher temperature resources used for electricity generation (**Hanaa *et al.*, 2010**).

Lashin and Nassir (2010) reported that the geothermal activity in Egypt is recognized in different areas, in terms of small hot springs exposed at the surface or thermal deep wells. Nearly all the hot springs are detected around the coastal parts of the Gulf of Suez and around the Cairo-Suez road. The author evaluated the geothermal potentiality around the coastal areas of the Gulf of Suez, using the available logging and geothermometer data sets. The available temperature and well logging data of some oil fields around the coastal area of the Gulf of Suez were analyzed. It was found that, the geothermal gradient around the Gulf of Suez is generally medium to high and tends to be much higher (35 °C /km to 44 °C /km) in certain areas. A geothermal reserve study is carried out for Hammam Faraun hot spring. The estimated geothermal potential was found to be 12.4 MWt.

Farghally *et al.* (2010) studied the geothermal hot water and space heating system in Egypt, and found that the geothermal hot water and space heating system is the best and clean system to satisfy the energy needs in remote area buildings. They conducted a design analysis

of the geothermal heating system components and applied it to the Umm Huweitat well in eastern desert as a case study.

2.2.3. Utilization of geothermal energy

Geothermal energy has traditionally been classified by use into two categories, namely: electrical generation and direct use (**Thorhallsson and Ragnarsson, 2008**).

ASHRAE (2011) has identified three categories according to soil temperature: high-temperature ($>150^{\circ}\text{C}$) electric power production, intermediate- and low-temperature ($< 150^{\circ}\text{C}$). Direct-use applications, and ground-source heat pump applications (generally $< 32^{\circ}\text{C}$).

2.2.3.1. Direct use of geothermal energy

Direct-use of geothermal energy is one of the oldest, most versatile and a common form of utilization of geothermal energy (**Dickson and Fanelli, 2003**).

Direct use of geothermal energy is where the heat itself is used, such as for space heating, bathing or in industry. This covers a variety of uses where there is need for heat. The application temperature range is wide and the thermal efficiency of direct use can be in the range 50-80%. In a few cases the two classes go together, the electricity is generated first and then the heat goes to direct use, so called co-generation. Geothermal house heating is applied in the cold regions of the world and heating of greenhouses is another popular application found even in hot regions. Normally conventional equipment and materials can be used, with a few exceptions. The main design challenge is the use of lower temperature sources than is the norm. Where the source temperature is low it is possible to upgrade it by the use of electrically driven heat pumps (**Thorhallsson and Ragnarsson, 2008**).

The agricultural applications of geothermal fluids consist of open-field agriculture and greenhouse heating. Thermal water can be used in open-field agriculture to irrigate and/or heat the soil. The greatest drawback in irrigating with warm waters is that, to obtain any worthwhile variation in soil temperature, such large quantities of water are required at temperatures low enough to prevent damage to the plants that the fields would be flooded (**Barbier and Fanelli, 1977**). The cultivation of vegetables and flowers out-of-season, or in an unnatural climate, can now draw on a widely experimented technology. Various solutions are available for achieving optimum growth conditions, based on the optimum growth temperature of each plant (Fig. 2.1) and on the quantity of light, on the CO₂ concentration in the greenhouse environment, on the humidity of the soil and air and on air movement.

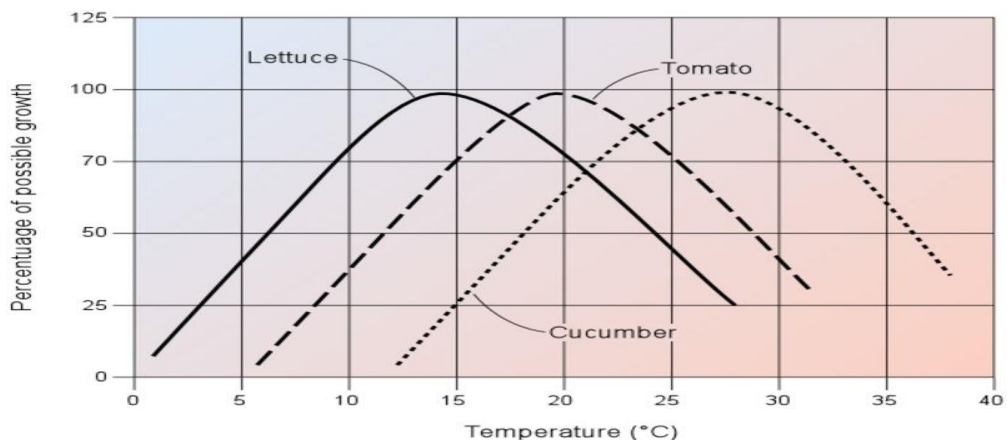


Fig. 2.1 Growth curves for some crops (**Beall and Samuels, 1971**).

The walls of the greenhouse can be made of glass, fiberglass, rigid plastic panels or plastic film. Glass panels are more transparent than plastic and will let in far more light, but will provide less thermal insulation, are less resistant to shocks, and are heavier and more expensive than the plastic panels. The simplest greenhouses are made of single plastic films, but recently some greenhouses have been

constructed with a double layer of film separated by an air space. This system reduces the heat loss through the walls by 30 - 40%, and thus greatly enhances the overall efficiency of the greenhouse. Greenhouse heating can be accomplished by forced circulation of air in heat exchangers, hot-water circulating pipes or ducts located in or on the floor, finned units located along the walls and under benches, or a combination of these methods (Fig. 2.2). Exploitation of geothermal heat in greenhouse heating can considerably reduce their operating costs, which in some cases account for 35% of the product costs, such products are vegetables, flowers, house-plants and tree seedlings (**Dickson and Fanelli, 2004**).

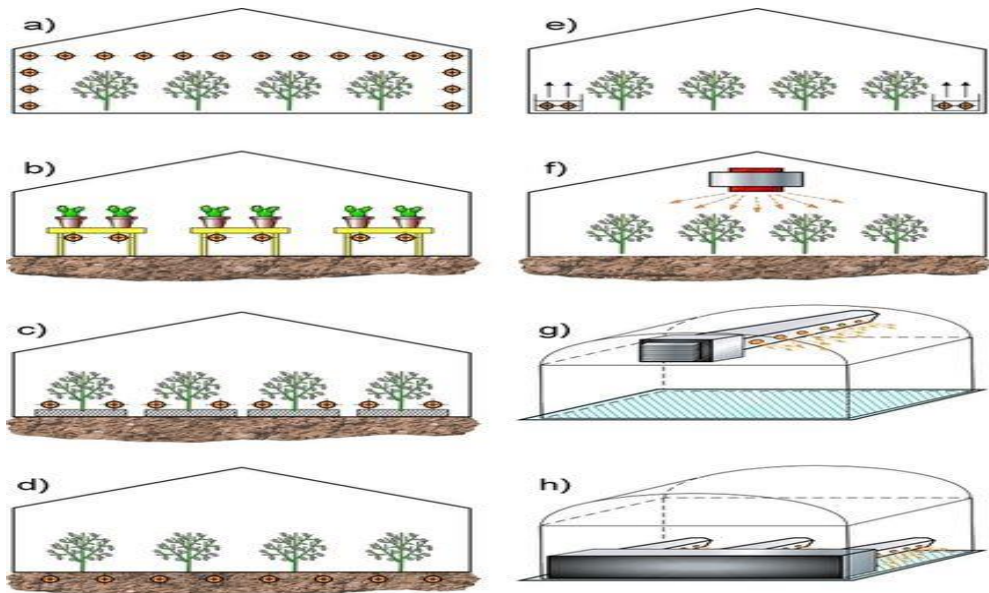


Fig. 2.2 Heating systems in geothermal greenhouses. Heating installations with natural air movement ((natural convection): (a) aerial pipe heating; (b) bench heating; (c) low position heating pipes for aerial heating. (d) Soil heating. Heating installations with forced air movement (forced convection): (e) lateral position; (f) aerial fan; (g) high position ducts; (h) low-position ducts.

Farm animals and aquatic species, as well as vegetables and plants, can benefit in quality and quantity from optimum conditioning of their environmental temperature (Fig. 2.3). In many cases geothermal waters could be used profitably in a combination of animal husbandry and geothermal greenhouses. The energy required to heat a breeding installation is about 50% of that required for a greenhouse of the same surface area, so a cascade utilization could be adopted. Breeding in a temperature-controlled environment improves animal health, and the hot fluids can also be utilized to clean, sanitize and dry the animal shelters and waste products (**Barbier and Fanelli, 1977**).

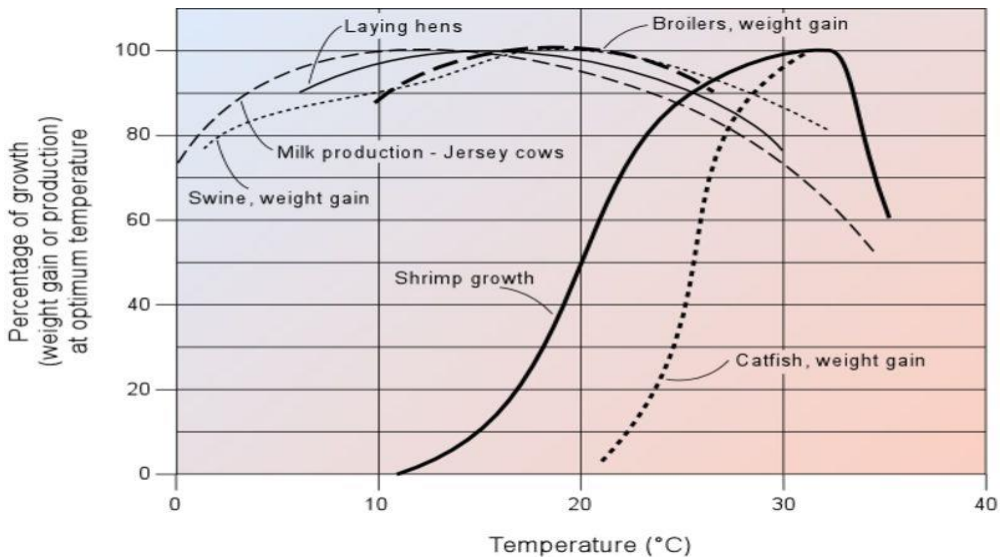


Fig. 2.3 Effect of temperature on growth or production of food animals (**Beall and Samuels, 1971**).

Aquaculture, which is the controlled breeding of aquatic forms of life, is gaining world-wide importance nowadays, due to an increasing market demand. Control of the breeding temperatures for aquatic species is of much greater importance than for land species, as can be seen in Fig. 2.3, which shows that the growth curve trend of aquatic species is

very different from that of land species. By maintaining an optimum temperature artificially we can breed more exotic species, improve production and even, in some cases, double the reproductive cycle (**Barbier and Fanelli, 1977**). The species that are typically raised are carp, catfish, bass, tilapia, mullet, eels, salmon, sturgeon, shrimp, lobster, crayfish, crabs, oysters, clams, scallops, mussels and abalone. Aquaculture also includes alligator and crocodile breeding, as tourist attractions and for their skins, which could prove a lucrative activity. Past experience in the United States has shown that, by maintaining its growth temperature at about 30 °C, an alligator can be grown to a length of about 2 m in 3 years, whereas alligators bred under natural conditions will reach a length of only 1.2 m over the same period. These reptiles have been bred on farms in Colorado and Idaho for some years now, and the Icelanders are planning something similar. The temperatures required for aquatic species are generally in the 20 - 30 °C range. The size of the installation will depend on the temperature of the geothermal source, the temperature required in the fish ponds and the heat losses from the latter (**Dickson and Fanelli, 2004**). Fig. 2.4 illustrates the different uses of geothermal energy.

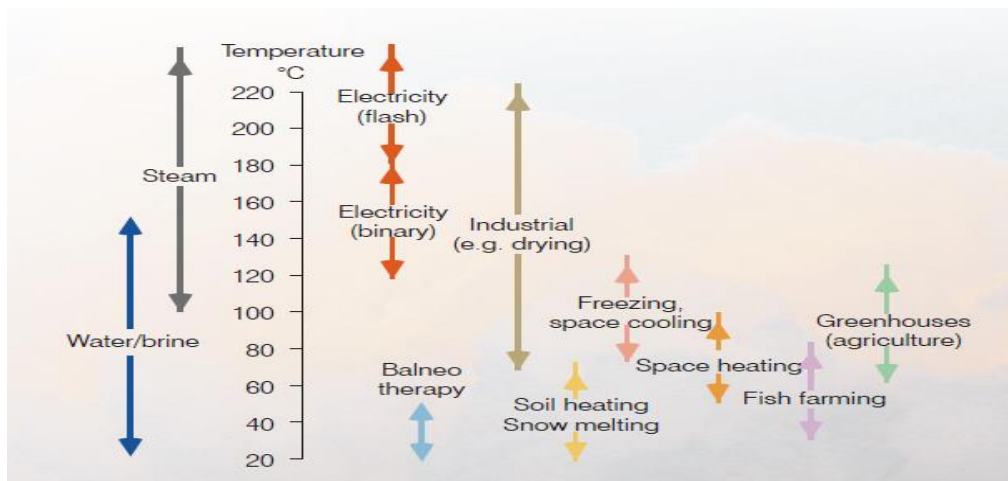


Fig. 2.4 Geothermal energy uses (**IGA, 2010**).

2.3. Geothermal energy system

The temperature at a certain depth in the ground remains nearly constant throughout the year and the ground capacitance is regarded as a passive means of heating and cooling of buildings. To exploit effectively the heat capacity of the ground, a heat-exchanger system has to be constructed. This is usually an array of buried pipes running along the length of a building, a nearby field or buried vertically into the ground. A circulating medium (water or air) is used in summer to extract heat from the hot environment of the building and dump it to the ground and vice versa in winter. A heat pump may also be coupled to the ground heat exchanger to increase its efficiency (**Florides and Kalogirou, 2007**).

Geothermal energy system consists of three models as follow: a) Soil temperature model. b) Earth to air heat exchanger model and c) Agricultural building model.

2.3.1. Sub-surface soil temperature

Soil temperature is an important parameter in solar and geothermal energy applications such as the passive heating and cooling of buildings and agricultural greenhouses (**Mihalakakou, 2002**). Ground temperature is also an important parameter for the passive heating and cooling of buildings (**Labs, 1992**). In many engineering applications it is necessary to know the soil temperature at different depths in order to determine the system design parameters. Although soil temperature is considered to be constant at certain depths, it varies especially near surface levels. It is well known that in systems such as Ground Source Heat Pumps (GSHPs), Earth-to-Air Heat Exchangers (EAHEs) etc. the depth at which heat exchangers are to be installed has vital importance on dimensions, performance and installation costs of

the system (**Ozgener, 2011; Ozgener and Ozgener, 2011 and Ozgener and Ozgener, 2010**).

The ambient climatic conditions affect the temperature profile below the ground surface (Fig. 2.5) and has to be considered when designing a heat exchanger (**Florides and Kalogirou, 2007**).

The ground temperature distribution is affected by the structure and physical properties of the ground, the ground surface cover (e.g., bare ground, lawn, snow, etc.) and the climate interaction (i.e., boundary conditions) determined by air temperature, wind, solar radiation, air humidity and rainfall (**Popiel *et al.*, 2001**).

From the point of view of the temperature distribution, (**Chow *et al.*, 2011 and Popiel *et al.*, 2001**) distinguish three ground zones:

- **Surface zone** reaching a depth of about 1m, in which the ground temperature is very sensitive to short time changes of weather conditions.
- **Shallow zone** extending from the depth of about 1–8 m (for dry light soils) or 20m (for moist heavy sandy soils), where the ground temperature is almost constant and close to the average annual air temperature; in this zone the ground temperature distributions depend mainly on the seasonal cycle weather conditions.
- **Deep zone** (below about 8–20 m), where the ground temperature is practically constant (and very slowly rising with depth according to the geothermal gradient).

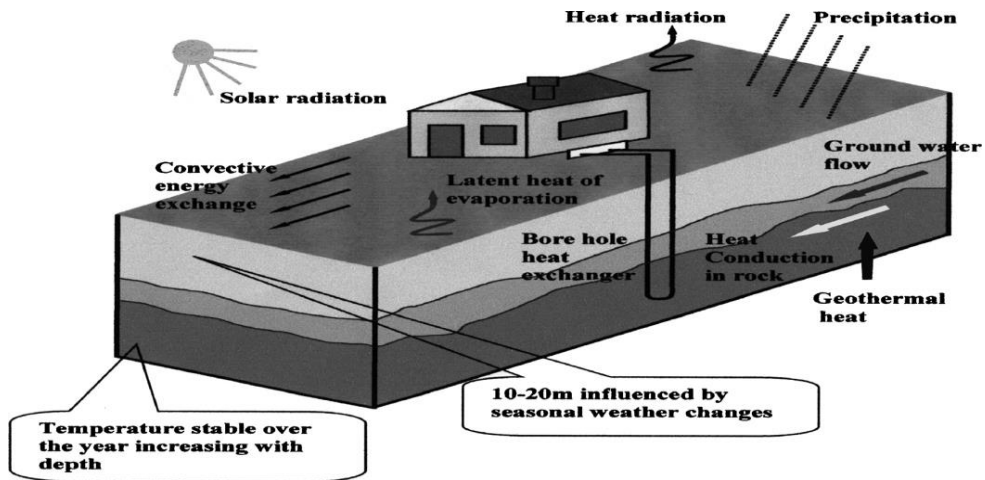


Fig. 2.5 Energy flows in ground.

2.3.1.1. Ground thermal properties

Soil thermal properties, including thermal conductivity, heat capacity, and thermal diffusivity, play an important role in the surface energy partitioning and resulting temperature distribution (**Chung and R, 1987**).

The performance of an earth to air heat exchanger (ETAHE) is directly related to the thermal properties of the ground. The ground has thermal properties that give it a high thermal inertia. The heat transfer mechanisms in soils are, in order of importance: conduction, convection and radiation. Conduction occurs throughout the soil but the main flow of heat is through the solid and liquid constituents. Convection is usually negligible, with the exception of rapid water infiltration after irrigation or heavy rain. Radiation is important only in very dry soils, with large pores, when the temperature is high. Therefore, the main parameters influencing the thermal behavior of the soil are the thermal conductivity and heat capacity which can be jointly expressed under the term of thermal diffusivity:

$$\alpha = \frac{k_s}{\rho_s c_s} \quad (2.1)$$

Where, (α) is the thermal diffusivity (m^2/s), (k_s) is the thermal conductivity ($\text{W}/(\text{m}\cdot^\circ\text{C})$), (ρ_s) is the density (kg/m^3) and (c_s) is the specific heat of the soil ($\text{kJ}/(\text{kg}\cdot^\circ\text{C})$). Thermal diffusivity determines the thermal behavior of the soil. The temperature field in the ground depends on the soil type and the moisture contained, respectively. In most cases there is no detailed information about soil characteristics available and the moisture varies throughout the year (**Zhao, 2004**). However, (**ASHRAE, 2011**) gives the thermal properties of selected soils, rocks, and backfills as shown in Table 2.1.

2.3.1.2. Soil temperature model

In many cases a detailed investigation of the soil properties and long term soil temperature measurements at different depths of the research area are needed in order to determine design parameters and feasibility of a system. However, researchers are in the need of more practical tools to obtain a detailed site survey which is not always possible. Despite its importance in scientific research and operations, relatively few data are available on soil temperature. Even when available, the data are often scattered and incomplete. These problems could be attributed to the substantial investment of money and time, and relatively large network of data acquisition system needed for detailed characterization of soil temperature at different depths and times (**Ogunlela, 2003**).

Kassem (1999) measured soil temperature at different depths of 0, 0.5, 1.0, 1.5 and 2 m to determine the specific depth of earth at which the relative temperature remains sufficiently constant with damped variation for effective heating and cooling modes performance respectively. The results showed that soil temperature was almost constant at 2 m depth of soil.

Table 2.1 Thermal properties of selected soils, rocks, and backfills
(ASHRAE, 2011).

	Dry Density, kg/m ³	Conductivity, W/m. k	Diffusivity, m ² /day
Soils			
Heavy clay, 15% water	1925	1.4 to 1.9	0.042 to 0.061
Heavy clay, 5% water	1925	1.0 to 1.4	0.047 to 0.061
Light clay, 15% water	1285	0.7 to 1.0	0.055 to 0.047
Light clay, 5% water	1285	0.5 to 0.9	0.056 to 0.056
Heavy sand, 15% water	1925	2.8 to 3.8	0.084 to 0.1 1
Heavy sand, 5% water	1925	2.1 to 2.3	0.093 to 0.14
Light sand, 15% water	1285	1.0 to 2.5	0.047 to 0.093
Light sand, 5% water	1285	0.9 to 1.9	0.055 to 0.12
Rocks			
Granite	2650	2.3 to 3.7	0.084 to 0.13
Limestone	2400-2800	2.4 to 3.8	0.084 to 0.13
Sandstone		2.1 to 3.5	0.65 to 0.1 1
Wet shale,	2570- 2730	1.4 to 2.4	0.065 to 0.084
Dry shale		1.0 to 2.1	0.055 to 0.07
Grouts/Backfills			
Bentonite (20 to 30% solids)		0.73 to 0.75	
Neat cement (not recommended)		0.69 to 0.78	
20% bentonite/80% SiO ₂ sand		1.47 to 1.64	
10% bentonite/90% SiO ₂ sand		1.00 to 1.10	
30% concrete/70% SiO ₂ sand,		2.08 to 2.42	
15% bentonite/85% SiO ₂ sand		2.08 to 2.42	

Popiel *et al.* (2001) present the temperature distributions measured for two differently covered ground surfaces, a bare surface and a surface covered with short grass. They found that air conditioning application the surface covered with short grass is recommended. However, in winter, the temperature distributions were almost the same.

Ben Jmaa Derbel and Kanoun (2010) presented a mathematical model to predict the sub-surface soil temperature of the region of Sfax-Tunisia and validated by measured ground temperatures they conducted an experiment in order to record the ground temperature at different depths during 2006 in a suburb of Sfax (Tunisia) which represents an example of the South-Mediterranean climate. The temperature of the soil calculated using a thermal model taking into account properties of the soil and meteorological conditions. Experimental results were compared with theoretical predictions. In order to estimate the influence of the soil properties on the ground temperature, different soil thermal conductivities are tested. The validation process shown that the proposed model does agree with experimental results with respect to the given input parameters where for each considered depth, an agreement between measured and predicted values with an accuracy of ± 1.5 °C. The mathematical model of the sub-surface soil temperature is based on the heat conduction theory applied to a semi-infinite homogeneous solid. Predictions of soil temperature exhibit a sinusoidal pattern due to the annual fluctuations.

Heat conduction in the soil is governed by the following differential equation:

$$\frac{\partial^2 T}{\partial z^2} - \frac{1}{\alpha} \frac{\partial T}{\partial t} = 0 \quad (2.2)$$

Where:

- α is the thermal diffusivity of soil, m²/day.
- z is the depth of soil, m.

The corresponding boundary conditions at $z = 0$ were the following:

$$T_{(t,0)} = T_{mean} + A_s \cos(\omega(t - t_o)) \quad (2.3)$$

Where:

T_{mean} is the mean ground surface temperature, °C.

A_s is the annual amplitude of the ground surface temperature, °C.

ω is the annual frequency, rad/day.

t is the time in year (days) from starting date of year, number.

t_o is the phase lag constant (days) since the beginning of the year of the highest average ground surface temperature or ambient air temperature, number.

and for the infinite depth $z \rightarrow \infty$, $T_{(\infty,t)} = T_{mean}$.

By analytical solution of Eq. 2.2, the temperature at any depth z and time t can be found by the following expression:

$$T_{(t,z)} = T_{mean} + A_s \cdot e^{-z \sqrt{\frac{\pi}{365 \cdot \alpha}}} \cdot \cos\left(\frac{2\pi}{365} \left(t - t_o - \frac{z}{2} \sqrt{\frac{365}{\pi \cdot \alpha}}\right)\right) \quad (2.4)$$

Kusuda and Archenbach (1965) and Labs (1992) have mathematically modelled the annual sub-surface soil temperature based on heat conduction theory applied to a semi-infinite homogenous solid. Predictions of soil temperature exhibit a sinusoidal pattern due to the annual temperature fluctuation. The prediction accuracy of the undisturbed soil temperature is very sensitive to the values of the input parameters. From the analytical solution of Eq. 2.2 the temperature at any depth z and time t can be found by the following expression:

$$T_{(t,z)} = T_{mean} - A_s \cdot e^{-z \sqrt{\frac{\pi}{365 \cdot \alpha}}} \cdot \cos\left(\frac{2\pi}{365} \left(t - t_i - \frac{z}{2} \sqrt{\frac{365}{\pi \cdot \alpha}}\right)\right) \quad (2.5)$$

Where, t_i is the phase constant (days) since the beginning of the year of the lowest average ground surface temperature or ambient air temperature, number. However, when the variables are determined from

field measurements, the model generally yields errors of no more than $\pm 1.1^\circ\text{C}$ (Labs, 1992).

AL-Ajmi *et al.* (2006) predicted Kuwaiti sub-surface soil temperature using Eq. 2.5, after modifying it as a follow:

$$T_{(t,z)} = 27 - 13.3e^{-0.31z} \cdot \cos\left(\frac{2\pi}{8760}(t - 552 - 428.31z)\right) \quad (2.6)$$

Where, 27°C is the annual mean ground temperature (T_{mean}), 13.3°C is annual surface temperature amplitude (A_s); 552 h is the phase constant (t_0) and soil thermal diffusivity (α) was $0.0038\text{ m}^2/\text{h}$. They validated this equation against measured soil temperature values and found that a good agreement of an accuracy of $\pm 1^\circ\text{C}$.

Sharan and Jadhav (2002) measured ground temperature at Ahmedabad using a special thermal probe up to the depth of three meters on hourly basis for one year. Using that data they developed an analytical expression for temperature regime in Ahmedabad region.

$$T_{(t,z)} = 27 + 10 \cdot e^{-z\sqrt{\frac{\pi}{365\alpha}}} \cdot \cos\left(\frac{2\pi}{365}(t - 105) - z\sqrt{\frac{\pi}{365\alpha}}\right) \quad (2.7)$$

Where, 27°C is the annual mean air temperature for ten years at Ahmedabad, India; 10°C is annual surface temperature amplitude; (t) is the time with day and 105 is the phase lag. They validated this model against measured soil temperature values and found that good agreement of an accuracy of ± 0.67 , ± 0.44 and $\pm 0.24^\circ\text{C}$ for wet loam soil at 1, 2 and 3 m depth respectively; for dry loam soil an accuracy of $\pm 0.48 \pm 0.23$ and $\pm 0.11^\circ\text{C}$ at 1, 2 and 3 m depth respectively.

Ogunlela (2003) modelled soil temperature variations with depth and time using transient heat flow principles with the assumptions that the heat flow was one -dimensional, the soil was homogeneous and that the thermal diffusivity was constant. Average conditions were also

assumed in the simulations. Predictive equations were developed for the annual and diurnal (daily) soil temperature variations.

$$T_{(t,z)} = T_{mean} + A_s \cdot e^{-z \sqrt{\frac{\pi}{365 \cdot \alpha}}} \cdot \sin\left(\frac{2\pi}{365}(t - t_o) - z \sqrt{\frac{\pi}{365 \cdot \alpha}}\right) \quad (2.8)$$

Where, t_o is the phase constant (days) since the beginning of the year of the highest average ground surface temperature or ambient air temperature, number.

Mihalakakou *et al.* (1992) analyzed a seventy-four years of ground temperature measurements at various depths at the National Observatory of Athens to develop a simple accurate models for the prediction of the annual variation of the ground temperature at the earth's surface and at various depths. Algorithms to predict the daily variation at the ground surface were also proposed. Finally the results of the overall analysis were compared with the corresponding data from other known sets of measurements. In all cases the predicted values are in close agreement with the corresponding measurements. The overall analysis is useful for the prediction of the performance of buildings in direct contact with the soil as well as for the prediction of the efficiency of the earth-to-air heat exchangers.

2.3.2. Earth to air heat exchanger

An earth tube is a long, underground metal or plastic pipe through which air is drawn. As air travels through the pipe, it gives up or receives some of its heat to/from the surrounding soil and enters the room as conditioned air during the cooling and heating period (**Lee and Strand, 2008**).

2.3.2.1. Design consideration of earth tube heat exchanger:

a) Soil type

Ascione *et al.* (2011) found that the best energy performances have been obtained for wet and heavy soil. As regards the material surrounding the buried tube, a good contact between soil and tubes has to be ensured, by means of compacted clay or sand. These kinds of soil are also suitable for a correct tube installation.

Deglin *et al.* (1999) found that for two extreme soil types: saturated silt and dry sand. In dry sand, the performance of the exchanger decreases much faster than in saturated silt. It is evident that the most suitable soils are those with good thermal conductivity, such as silt soils saturated in water, and found that the greatest thermal efficiency is provided by saturated loam, The higher the soil moisture, the higher is the thermal conductivity and the latent heat transfer in winter.

Ghosal and Tiwari (2006) found that the greenhouse air temperatures are highest, both in the typical winter and summer day, in sandy soil followed by sandy loam, gravelly sand and silt loam with the same operational parameters of the earth to air heat exchanger experiment.

Thevenard (2007) reported that wet soil is preferable to dry soil because of better thermal conductivity; peat and dry sand should be avoided. The author suggest surrounding the pipes with compacted clay to ensure good thermal contact between the pipes and the earth.

b) Tube depth

Ascione *et al.* (2011) found that the ideal depth of buried tubes is about 8 m under the ground level. In fact, in this case the time lag is approximately 6 months, so the ground is characterized by the lowest yearly temperatures in summer and the highest in winter. Thus, the

thermal recovery is optimal in both the seasons. The depth of 6-9 m is also preferable compared to major depths characterized by ground temperature almost constant during the year. The depth of 3 m under the ground level implies a better thermal exchange compared to the depth of 1 m (not satisfactory depth), while a further deepness (4 m) allows only a minimal improvement. Thus, if the excavation costs are low (unleashed soils), a deeper tube can be useful, while, in presence of rock, a depth of 3 m is the best compromise.

Deglin *et al.* (1999) used three pipes having a 251 mm diameter and buried at 1.5, 2.25 and 3.0 m to measure the effect of depth on the performance of the exchanger, and found that in summer, the temperature measured for the pipe at a depth of 3.0 m was 2 °C lower than in the case of the pipe at 1.5 m. In winter, the difference is less significant, although the variation between the outside temperature and that of the outgoing air is greater, and mentioned that the greater the depth, the smaller is the effect of a variation in the outside climate on the soil, but the higher the costs of the installation.

Lee and Strand (2008) and Lee and Strand (2006) illustrated that as the pipe depth increases, the inlet air temperature decreases, regardless of the location, indicating that earth tube should be placed deeply as possible. However, the trenching cost and other factors should be considered when installing earth tubes.

Abdullahi *et al.* (2007) studied the potential of earth-air heat exchangers for low energy cooling of buildings and found that outlet air temperature decreases with pipe depth.

Ghosal and Tiwari (2006) studied the effects of the depth of ground for installation of the earth to air heat exchanger on the hourly variations of greenhouse air temperature for typical winter and summer days and found that with an increase in the depths of ground, the temperatures of the greenhouse air go on increasing and decreasing in

the winter and in the summer, respectively. This is due to the higher and lower outlet air temperatures in the winter and in the summer, respectively, with the increase in the depth of ground.

Mihalakakou *et al.* (1996) studied the heating potential of buried pipes techniques and evaluated the effect of the main design parameters on the system's heating capacity influencing the pipe depth below the surface of the earth. They found that there was a considerable increase of the system's heating capacity potential with increasing depth.

Santamouris *et al.* (1995) studied use of buried pipes for energy conservation in cooling of agricultural greenhouses and performed a parametric analysis for a typical 1000 m² glass greenhouse with four plastic pipe located in Athens and found that the indoor air temperature decreases with increasing depth up to 4 m.

Thevenard (2007) reported that deeper positioning of the tubes ensures better performance. Typical depths are 1.5 to 3.0 m. The tubes can be positioned under the building or in the ground outside the building foundation.

c) Tube material

Ascione *et al.* (2011) found that concrete, plastic or metallic materials lead to very similar energy performances. In fact, due to the small thickness of the tubes (5 mm in the case of PVC, 7 mm for the metallic material, 7 cm for the concrete), the different thermal conductivity values scarcely influence the heat exchange, if the right depths and lengths are used. Note that the concrete tubes require a further internal coating to avoid possible radon infiltrations; furthermore, hygienic conditions inside the tubes must be assured, for example by using antimicrobial coatings. Finally the tube material (usually, PVC, metal or concrete) on the energy performance is negligible.

Thevenard (2007) mentioned that this is actually of little importance from a thermal point of view, as the conductivity of the soil surrounding the pipe is the limiting factor. PVC or concrete have been used. The material has to be strong enough to withstand crushing when the pipe is buried. Corrugation (as in corrugated PVC) gives a stronger structural strength but should be avoided as it traps water in the pipes. The pipes should not be perforated so that water does not seep through.

d) Tube diameter

Deglin *et al.* (1999) studied three pipes buried at 1.5 m (diameters of 251, 315 and 402 mm) of the experimental installation were used to measure the effect of pipe diameter on the performance of the exchanger. At the same time, the other pipes of the installation were obstructed and shown that small pipes are thermally more efficient but cause greater pressure losses and require larger installations. A compromise has to be found between the cost of the installation and its thermal efficiency.

Lee and Strand (2008) and Lee and Strand (2006) illustrated that as the pipe radius increases, the earth tube inlet air temperature also increases, regardless of the location. This is due to the fact that higher pipe radius results in a lower convective heat transfer coefficient on the pipe inner surface and a lower overall heat transfer coefficient of earth tube system. Therefore, a smaller pipe radius should be used for the better performance of the earth tube.

Abdullahi *et al.* (2007) studied the potential of earth-air heat exchangers for low energy cooling of buildings and found that the pipe outlet temperature increases with increased pipe diameter.

Ghosal and Tiwari (2006) found that an increase in diameter results in lower and higher greenhouse air temperatures in the winter and the summer, respectively. This result is mainly caused by the decrease in

the transfer of heat from the earth or lower convective heat transfer coefficient due to the increase of pipe surface and slower air flow.

Kondili and Kaldellis (2006) studied a four typical polyethylene pipe diameters with values ranging between 30 and 100 mm. the geothermal fluid quantity needed is reduced (lower heat loss) as the network diameter is decreased. On the other hand, by reducing the network diameter the corresponding electricity consumption (absorbed by the system pump) is substantially amplified, especially for $d = 30$ mm, due to the system velocity and the corresponding pressure loss increase. In order to get a clear cut picture, the annual electricity consumption and the geothermal fluid quantity used as a function of the transportation network diameter were presented. Taking into consideration that the geothermal fluid quantity required represents only a small portion ($\leq 20\%$) of the available geothermal potential, the optimum network diameter should be equal to $d_o = 50$ mm, in order to minimize the electricity consumption of the installation.

Mihalakakou *et al.* (1996) found that a reduction of the pipe radius from 150 to 100 mm increases the air temperature at the pipe's exit by 0.9-1.8 °C. However, in general terms, an increase of the buried pipe's radius represents a reduction of the convective heat transfer coefficient and an increase of the pipe surface so providing a lower air temperature at the pipe's outlet, thus reducing the heating capacity of the system.

Santamouris *et al.* (1995) found that an increase of the pipe radius results to higher indoor air temperature. This was caused by an increase of the air temperature at the pipe's outlet, as a result of the lower convective heat transfer coefficient caused by the increase of the pipe radius.

Thevenard (2007) reported that smaller diameters are preferred from a thermal point of view, but they also correspond (at equal flow

rate) to higher friction losses, so it becomes a balance between increasing heat transfer and lowering fan power. Typical diameters are 10 cm to 30 cm but can be as large as 1 m for commercial buildings.

e) Tube Length

Ascione *et al.* (2011) studied the earth-to-air heat exchangers (EAHX) for Italian climates and found that the thermal exchange between the ground and the air crossing the tube increases with the length of the buried tubes. Values of about 10 m are unsatisfactory while significant advantages do not occur for lengths over 70 m. For the climates here considered, lengths of about 50 m were preferable, which optimize heat exchange and first costs.

Deglin *et al.* (1999) showed that the length determines the thermal efficiency of the installation but the maximum length of pipe is limited by cost and pressure losses. A thermal efficiency of 100% requires a pipe of infinite length.

Lee and Strand (2008) and Lee and Strand (2006) illustrated that as the pipe length increases, the inlet air temperature decreases, regardless of the location. This is due to the fact that the longer pipe provides a longer path over which heat transfer between the pipe and the surrounding soil can take place given the same overall heat transfer coefficient of earth tube. Therefore, a longer pipe should be used if the trenching cost is not prohibitive.

Abdullahi *et al.* (2007) found that outlet air temperature decreases with length of pipe.

Ghosal and Tiwari (2006) found that with the increase of the length of buried pipes from 30 m to 50 m, the temperatures of the air inside the greenhouse go on increasing in the winter period and decreasing during the summer period.

Mihalakakou et al. (1996) found that an increase of pipe length from 30 to 70 m provides a significant increase of the exit air temperature and, therefore, an improvement of the system's heating capacity.

Santamouris et al. (1995) concluded that the indoor air temperature decreases with increasing pipe length.

Thevenard (2007) reported that length can typically range from 10 to 100 m. Longer tubes correspond to more effective systems, but the required fan power and the cost also increase.

f) Air velocity

Ascione et al. (2011) concluded that low speeds (about 8 m/s) of the airflow inside the tubes are preferable, as the pressure drops and fan electric energy requirements decrease.

Lee and Strand (2008) and Lee and Strand (2006) indicated that an earth tube with a lower air velocity will perform better since the air spends more time in the tube and thus in contact with the lower soil temperature.

Abdullahi et al. (2007) found that the pipe outlet temperature increases with increased air velocity.

Mihalakakou et al. (1996) investigated the impact of air speed on the thermal behavior of the system (buried pipes techniques). The overall analysis demonstrated that a higher air velocity leads to a slight decrease of air temperature at the pipe exit and then to a reduction of the system's heating capacity.

Santamouris et al. (1995) found that the greenhouse indoor air temperature increases with increasing air velocity inside the pipes.

g) Air flow rate

Ascione et al. (2011) found that in the considered climates, the achievable thermal energy savings increase when raising the airflow rate

crossing the earth to air heat exchangers. They concluded that the ventilation airflow rate, 1 or 2 air changes per hour (ACH) were equivalent and preferable in terms of total primary energy requirements.

Ghosal and Tiwari (2006) found that an increase in mass flow rate causes the decrease and increase of the greenhouse air temperatures in the winter and the summer, respectively.

Thevenard (2007) mentioned that lower flow rates are beneficial to achieve higher or lower temperatures, and also because they correspond to lower fan power. However, a compromise has to be made between pipe diameter, desired thermal performance, and flow rate.

h) Number of tubes

Thevenard (2007) reported that the number of tubes is dictated by air flow requirements, the length of the tubes and the required thermal performance.

To meet given air conditioning requirements of a given building space, air through one tube may not be adequate or the size of the required tube may be too large. In such a case one may use more than one tube, buried in the ground, parallel to each other, to meet the given load requirements, taking into account the influence of the tubes on each other. To prevent interference between the individual tubes, the distance between them should be at least 1 m (**Paepe and Janssens, 2003**).

i) Spacing between tubes

Deglin et al. (1999) found that the thickness of the active cylinder of soil around the pipe depends on the heat storage capacity and the thermal conductivity of the soil. Calculations show that, in the case of saturated silt, approximately 75% of the heat transfer comes from the first 45 cm of soil. This same percentage is reached at only approximately 30 cm for dry sand. The effect of the spacing between the

pipes becomes significant where there is a long period of extreme external temperature.

Thevenard (2007) mentioned that spacing should be large enough that tubes are thermally independent, typically at least 1 m apart. Tubes can also be placed in a radial pattern.

j) Fan position

Earth to air heat exchangers can use intake fans, exhaust ones or both, depending on the complexity of the air ducts. The exclusively use of exhaust fans requires a careful sizing of the ventilation the higher energy costs due to system, so that the room extraction grilles can guarantee the correct incoming airflow rates in all the building zones. The use of intake fans instead of exhaust ones are negligible (**Ascione *et al.*, 2011**). Preferred location for the fan is at the exit end of the tunnel. However, other practical considerations may determine whether the fan is installed at the entry or the exit (**Goswami and Biseli, 1993**).

k) Control mode

Thevenard (2007) mentioned that the system should be bypassed when the outside temperature is typically between 15 and 22 °C (one can also take the earth temperature into account to decide when to turn the system off). Windows need to be closed for the system to contribute properly to the heating or air conditioning of the building.

Ascione *et al.* (2011) studied a five different control modes of the earth to air heat exchangers, in which the daily working period was varied and found that the best solution consists in a long use.

2.3.2.2. Types of ETAHE

The classification of EATHE is shown using a tree diagram in Fig. 2.6 First, it is classified by the open (Fig. 2.7), closed (Fig. 2.8) and other system where open means fresh atmospheric air entering to the

tunnel from open sky space; in a closed system, the air is recycled into the room and in other system, the bore hole geothermal heat is used for heating and cooling the buildings. Normally it is single well, but multiwell is used for higher heating–cooling effect for long duration. Horizontal system may be divided into parallel, series and trench collector type, and vertical heat ground exchangers are single bore or multiple bore types (Kaushik *et al.*, 2013).

Mands and Sanner (2005) classified the shallow geothermal (0–3 m depth) energy sources or ground source heat pumps by horizontal and vertical.

I. Horizontal type

The horizontal type has a number of pipes connected together either in series or in parallel. This configuration is usually the most cost-effective when adequate yard space is available and trenches are easy to dig. The trenchers have a depth of 1–2 m in the ground and usually a series of parallel plastic pipes is used shown in Fig. 2.9.

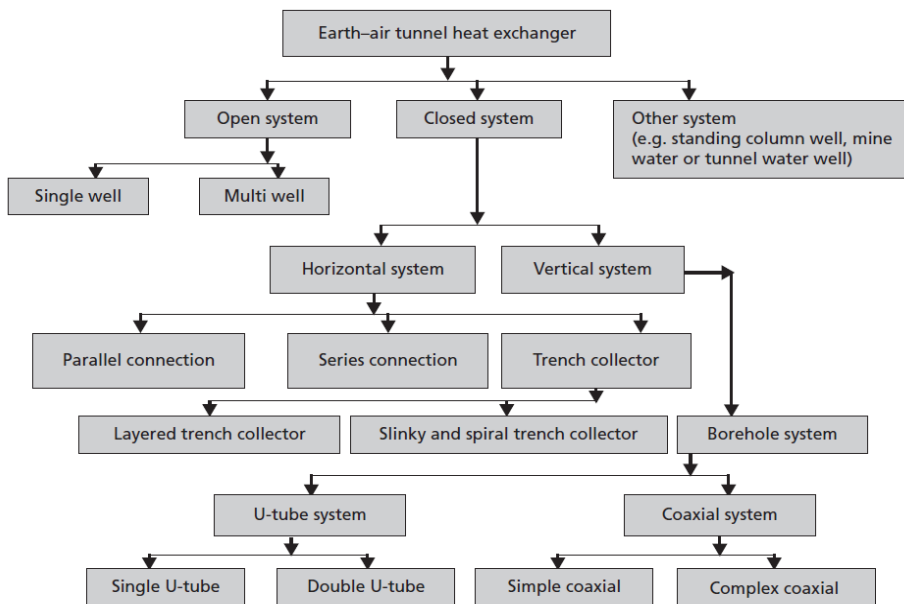


Fig. 2.6 Classification of earth to air heat exchanger.

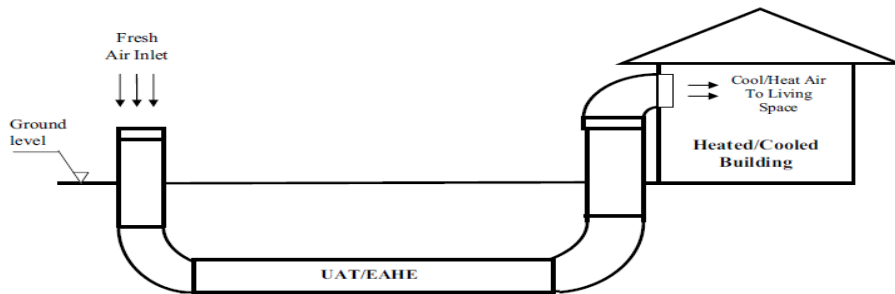


Fig. 2.7 An opened loop mode ETAHE (Ozgener, 2011).

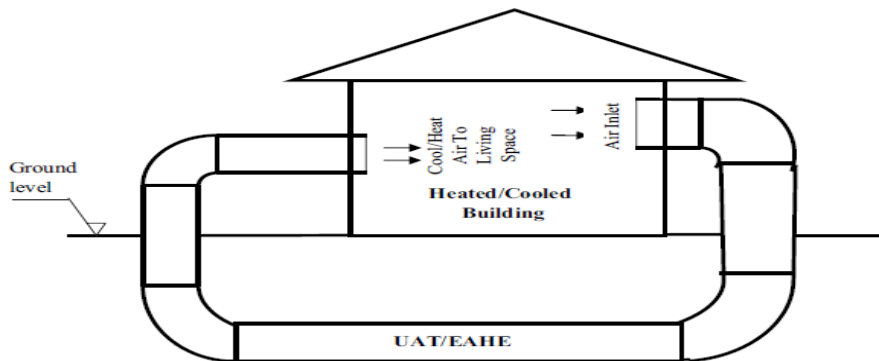


Fig. 2.8 A closed loop mode ETAHE (Ozgener, 2011).

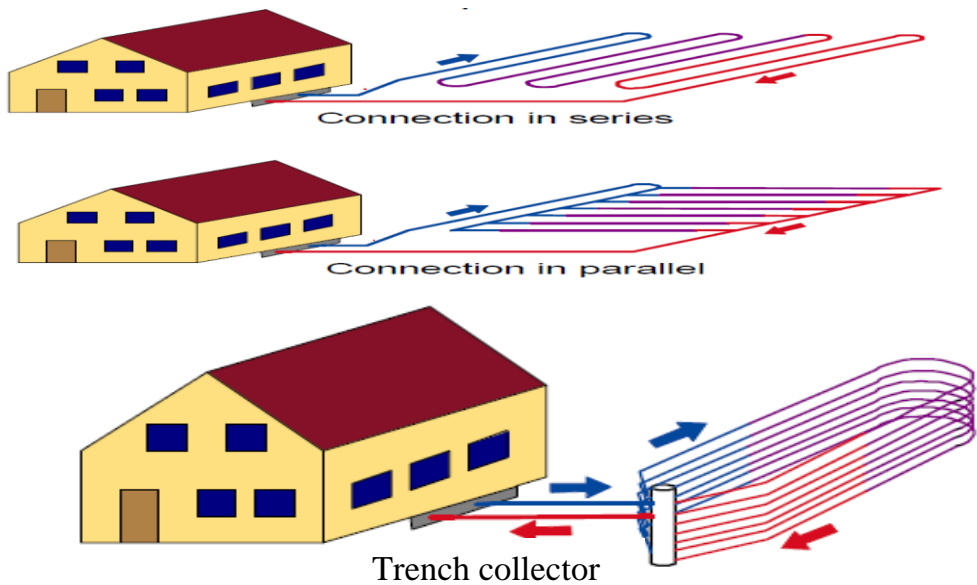


Fig. 2.9 ETAHE horizontal type.

II. Vertical type

Vertical ground heat exchangers or borehole heat exchangers are widely used when there is a need to install sufficient heat exchange capacity under a confined surface area such as when the earth is rocky close to the surface, or where minimum disruption of the landscape is desired. This is possible because the temperature below a certain depth remains constant over the year. In a standard borehole, which in typical applications is 50–150 m deep, plastic pipes (polyethylene or polypropylene) are installed, and the space between the pipe and the hole is filled with an appropriate material to ensure good contact between the pipe and the undisturbed ground and reduce the thermal resistance. Vertical loops are generally more expensive to install, but require less piping than horizontal loops because the earth deeper down is cooler in summer and warmer in winter, compared to the ambient air temperature. Several types of borehole heat exchangers were tested and are widely used. These are classified in two basic categories as shown in Figs. 2.10 and 2.11 (**Mands and Sanner, 2005**):

1. U-pipes, consisting of a pair of straight pipes, connected with a U-turn at the bottom. Because of the low cost of the pipe material, two or even three of such U-pipes are usually installed in one hole.
2. Concentric or coaxial pipes, joint either in a very simple way with one straight pipe inside a bigger diameter pipe or joint in complex configurations.

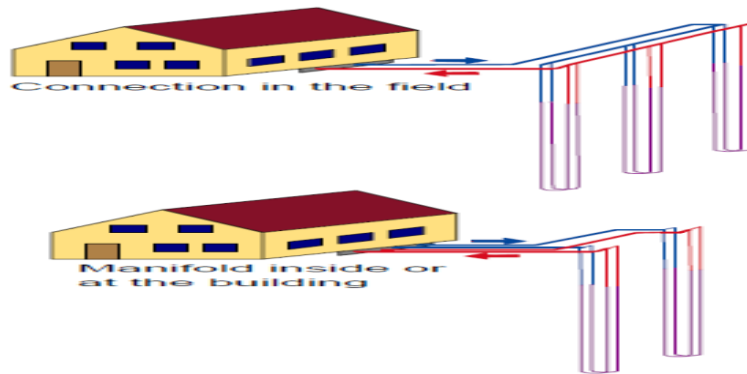


Fig. 2.10 Borehole heat exchanger (Double U-pipe).

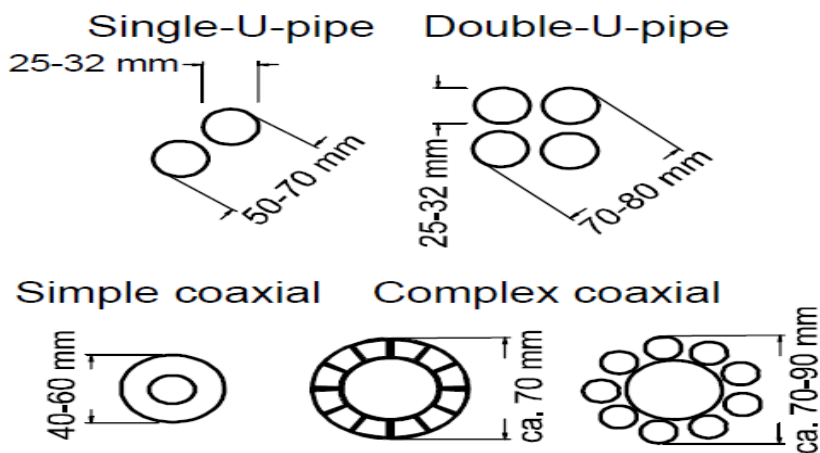


Fig. 2.11 Cross sections of different types of borehole heat exchangers.

2.3.2.3. ETAHE applications

High temperature during the summer season and low temperature in winter are also adverse to greenhouse crops. The ETAHE, which is one of the passive solar systems, has been installed in greenhouses as a heating and cooling system over last thirty years. The ground potential of the earth can also be used for cooling the greenhouses in summer conditions and heating in winter conditions due to its constant year round temperature (26–28 °C). In this case, hot and cold greenhouse air is

circulated through the buried pipe (2–4 m depth) for dissipation of heat or gain a heat to the underground soil (**Sethi and Sharma, 2008**).

Sharan *et al.* (2005) developed earth-tube-heatexchanger (ETHE) for controlling the hot arid environment of Kutch, India. they reported that ETHE limits the greenhouse temperature with crop up to 36 °C with shading on top of the greenhouse.

Ghosal *et al.* (2004) developed a simplified analytical model to study round the year effectiveness of a recirculation type earth to air heat exchanger in a greenhouse located in New Delhi, India. The average temperature of greenhouse was 3–4 °C less in summer than control greenhouse.

Ghosal and Tiwari (2006) developed a thermal model to investigate the potential of using the stored thermal energy of the ground for greenhouse cooling with the help of an Earth to Air Heat Exchangers (EAHES); with the experimental parameters of the EAHES, were found to be, on average 5–6 °C lower in the summer than those of the same greenhouse without the EAHES.

Sethi and Sharma (2008) studied an Earth to Air Heat Exchangers (EAHES) in various sizes of greenhouse and found that it can cover 28–62% heating needs or can raise the inside air temperature by 3–9 °C for various size greenhouses at different locations.

Al-Ajmi *et al.* (2006) concluded that an earth–air heat exchangers for domestic buildings in a desert climate have the potential for reducing cooling energy demand in a typical house by 30% over the peak summer season.

Kumar *et al.* (2003) developed a numerical model to predict energy conservation potential of earth–air heat exchanger system and passive thermal performance of a building. The model was validated against experimental data of a similar tunnel in Mathura (India). It could

be seen that cooling potential of 80 m earth tunnel was found adequate (19 kW) to maintain an average room temperature 27.65 °C.

Ascione *et al.* (2011) evaluated the energy performances achievable using an earth to air heat exchanger for an airconditioned building for both winter and summer. They concluded that the earth to air heat exchanger shown the highest efficiency for cold climates both in winter and summer.

Darkwa *et al.* (2011) evaluated the concept of using earth-tube ventilation system as an energy saving technology theoretically and practically. The results shown that the system has the potential to become an effective energy saving technology in buildings. For instance in March and July 2010 the E-tube system was able to contribute 62% and 86% of the peak heating and cooling loads respectively and also achieved corresponding COPs of 3.20 and 3.53. Further investigation into the impact of these factors on E-tube ventilation systems is therefore recommended.

Deglin *et al.* (1999) studied subsoil heat exchangers and the potential to improve ambient conditions in livestock buildings by developing a three-dimensional non-steady-state heat flow model in order to simulate the heat transfer between the air circulating in the tubes and the surrounding ground. By combining the results of this heat flow model with those of an experimental subsoil heat exchanger, they studied the influence of various parameters, such as the type of ground and the air speed, as well as the characteristics of the pipes (diameter, length, depth and spacing), on the efficiency of heat exchange.

Goswami and Biseli (1993) found that underground air tunnels for heating and cooling agricultural and residential buildings can reduce the ambient air temperature from 32.2 °C to one in the range of 26.7 to 28.3 °C. Therefore, these systems are recommended for use in

agricultural buildings where a drop in air temperatures of -13.9 to -12.2 °C is acceptable.

Lee and Strand (2008) developed a new module and implemented in the EnergyPlus program for the simulation of earth tubes for cooling and heating potential in buildings. The model validated against and showed good agreement with both theoretical and experimental data. They found that an earth tube is beneficial turned out to be heavily dependent on the climate of the location.

2.3.2.4. ETAHE economics

The economics of earth tubes are controversial. The economics are reported to be positive for cooling applications, because in some climates earth tubes enable the user to dispense with a dedicated air-conditioning system. The economics are not as good for heating applications because earth tubes by themselves are not sufficient to significantly heat a building and therefore a heating system is still required. In other words, the small heating gain does not justify the additional cost of the earth tubes. However, if earth tubes are used for cooling in the summer, an added benefit is to use them for preheating ventilation air in the winter, either directly or by preheating the inlet air of a heat recovery ventilator (HRV) (**Thevenard, 2007**).

Thevenard (2011) reported that with earth tube system costs typically in the range of \$2,000 to \$3,000, payback is often long given the expected energy savings. One manufacturer mentions between 10 and 20 years as long as excavation costs are kept to a minimum.

Bansal et al. (2012) concluded from the economic analysis of earth to air heat exchanger system that the energy consumption of the blower is an important parameter in the design of earth to air heat exchanger system. Results show that with an energy efficient blower, the

financial payback period of integrated earth to air heat exchangers- evaporative cooling system is about 2 years while the systems with inefficient blower are financially not viable due to much higher payback.

Ascione *et al.* (2011) concluded that the use of an earth to air heat exchanger is suitable (simple payback of 5-9 years) only when the moving earth works are easy and cheap; otherwise, high moving earth costs or expensive tube materials (metals) induce too long payback values.

Stecher and Klingenberg (2008) reported that the earth tube is not cost effective. Various people interviewed during this study have mentioned that excavation expenses are one of the big drivers of the overall cost of the system. Other factors which reduce the economic appeal of earth to air heat exchangers include the fact that the systems tend to work seasonally, that they require sophisticated controls or risk heating and cooling when they should not, and that they overlap the functionality of the heat recovery ventilator (if supplied) in heating and cooling modes.

Goswami and Biseli (1993) found that the payback period is approximately 20 years. Therefore, investment in such as system is not cost effective in Florida.

2.4. Greenhouses

Greenhouse cultivation is necessary in a tropical climate to prevent plants from natural environmental damage, destruction from disease, and insect pests. The agriculturist can also adjust environmental suitability for plants more easily. However, problems with the accumulation of heat can be encountered in the greenhouse during the daytime. The use of an active cooling system may require a higher investment than passive cooling, but some passive cooling techniques

may have a limitation on plant growth, especially in the summer. Frequently, solar radiation during the daytime rises the temperature higher than the optimal level. In monsoon weather condition may be harmful for plants due to the rain and wind storms. The surrounding high relative humidity together with high temperatures encourages disease and insect pests. Most agriculturists will avoid the implementation of air conditioning. On the other hand, the use of shading material together with natural ventilation by opening the roof or side vents can decrease greenhouse temperature moderately (**Mongkon *et al.*, 2014**).

The renewable energy of passive cooling uses underground energy that will be used in a ground heat exchanger or horizontal earth tube system (HETS). The idea of using ground heat exchanger in cooling is also interest although the thermodynamic and heat transfer relation is well-known. In the tropical and subtropical countries, the development of ground heat exchangers has been widely researched in greenhouses in different climates such as the South Asia (**Misra *et al.*, 2013 and Tiwari *et al.*, 2006**).

Greenhouses have to provide optimal climate conditions for healthy plant growth and high production. The design strongly influences not only the mechanical behavior of the greenhouse structure, but also internal climate factors such as temperature, air humidity and light transmittance. The physical properties of the covering material also influence the quality of the indoor microclimate, while its mechanical properties influence the structural design and the mechanical behavior of the greenhouse. For example, glass-covered greenhouses normally have a pitched roof, while plastic film greenhouses can have a pitched roof, a saw-tooth shed roof and a round or Gothic arched roofs. For this reason, functional aspects of the greenhouse structure such as total light transmittance and ventilation, as well as physical properties of the covering material, such as condensation behavior and dirt behavior,

impose design requirements on the greenhouse structure (**Elsner et al., 2000**).

2.3.1. Greenhouse heat balance

A greenhouse is built and operated to produce crops and return a profit to the owner. In many areas of the country, sunlight is the limiting factor in production, especially during the winter; therefore, a greenhouse should provide for optimum use of available sunlight. The amount of sunlight available to plants in a greenhouse is affected by the structural frame, covering material, surrounding topography and cultural features, and orientation of the greenhouse. The amount of sunlight available outside is a function of latitude, time of year, time of day, and sky cover. A greenhouse cover with high transmissivity for solar energy can produce temperatures that are higher than desired in the crop zone. Most surfaces within a greenhouse have high absorptivities for solar energy and, thus, convert incoming radiation to thermal energy. Fig. 2.12 shows energy exchange for a greenhouse during daylight. Heat exchange between a greenhouse and the environment is illustrated in Fig. 2.13. Heat exchange between the greenhouse interior and exterior is the sum of heat available from all sources such as solar, furnace, lighting, electric motors, etc., and the rate of heat loss/gain from the greenhouse (**Aldrich and Bartok, 1994**). The following equation include the heat balance of the greenhouse:

$$\text{Furnace heat} + \text{Electric motor Heat} + \text{Lighting heat} + \text{Solar heat} = \text{Heat loss by conduction through the greenhouse shell} + \text{Heat loss by air exchange between inside and outside air} + \text{Heat loss by evaporating water} \quad (2.9)$$

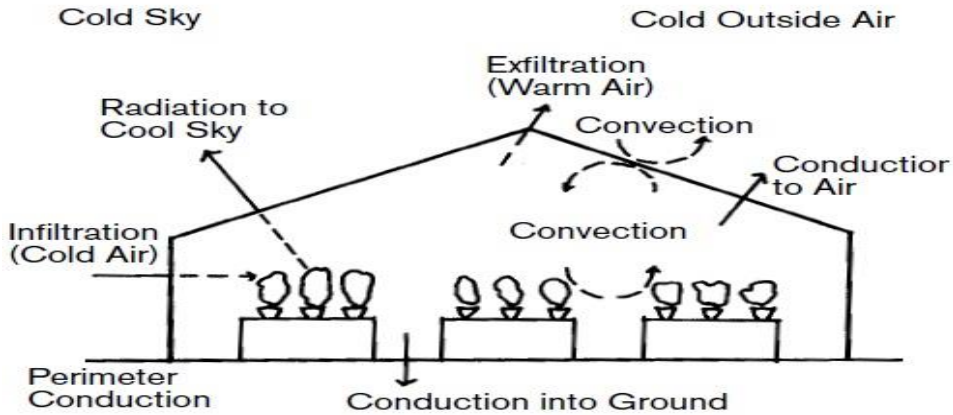


Fig. 2.12 Energy exchange between a greenhouse and the surroundings.

Furnace heat is estimated for night heating when there is no sun, and heat from electric motors and lighting is ignored. Heat used in evaporating water is also ignored (Aldrich and Bartok, 1994 and ASHRAE, 2011).

$$h_f(\text{Furnace heat}) = h_c(\text{Conduction heat}) + h_{sa}(\text{Air exchange heat}) \quad (2.10)$$

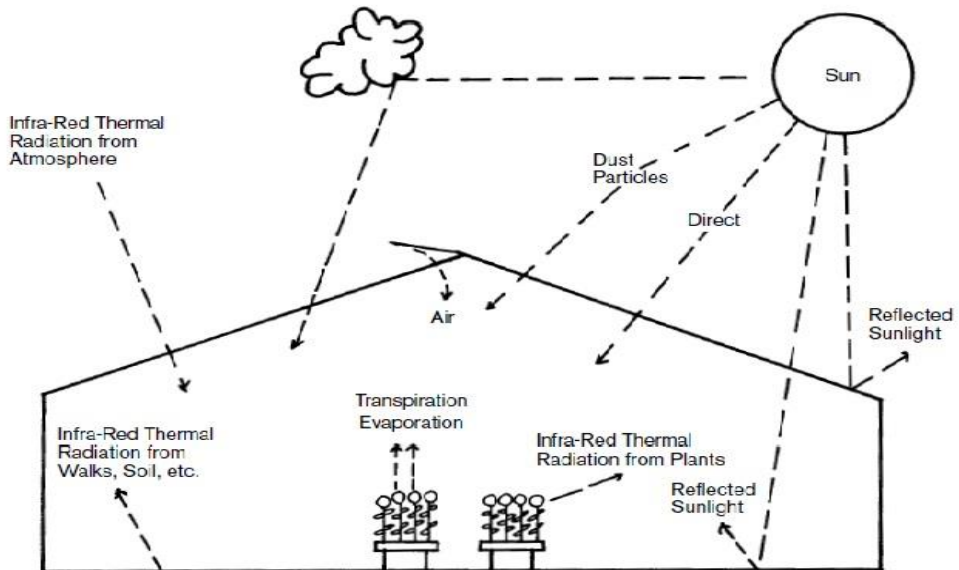


Fig. 2.13 Heat loss/gain from a greenhouse.

MATERIALS
AND METHODS

3. MATERIALS AND METHODS

3.1. Materials

3.1.1. System description

A field experiment was carried out at Faculty of Agriculture, Moshtohor, Benha University (latitude $30^{\circ} 21' N$ and $31^{\circ} 13' E$) during the period of 24th February to 9th March, 2012. Temperatures in the earth at different depths of 2, 3 and 4 m were measured using thermocouples sensors that fixed in a 33.2 mm diameter PVC pipe with 5 m length and installed vertically in the earth, a hole 5 cm in diameter was drilled by an auger. The pipe with thermocouple was placed vertically in the hole and was carefully backfilled and tamped with moist soil. The experimental setup is shown in Fig. 3.1.

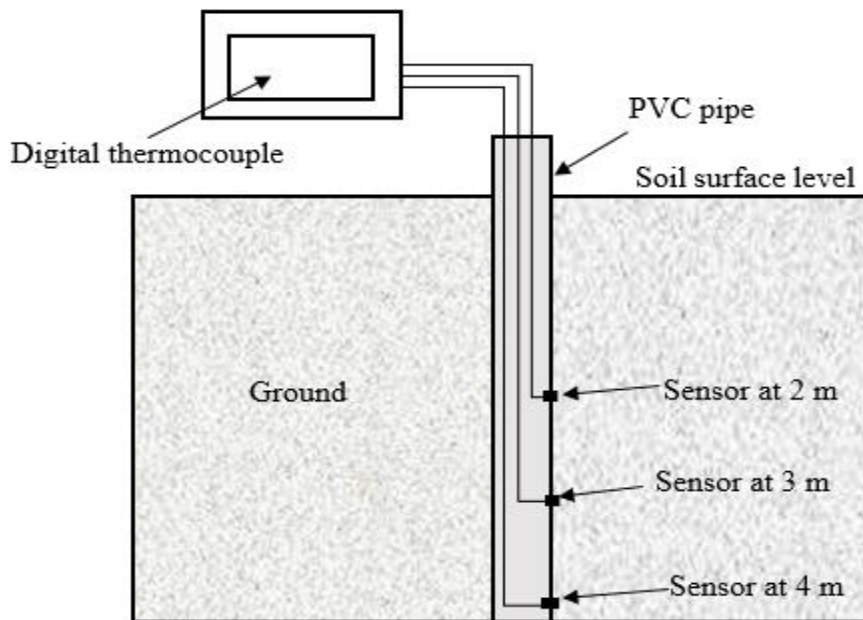


Fig. 3.1 Description of experiment.

3.1.2. Instruments

a) Scanning thermometer

Scanning thermometer was used to measure temperature at different depths in the soil (Fig. 3.2) by used J-type thermocouple sensor (Fig. 3.3). The specifications of this device are listed in Table 3.1.

Table 3.1 Specifications of scanning thermometer.

Origin of manufacture	USA
Model	Digi-Sense 69202-30
Range	-250 to 1800°C (-418 to 3272°F)
Resolution	0.1°/1° selectable to 999.9°; 1° above 1000°
Accuracy	J, K, T, E, N: ±0.1% of reading, ±0.5°C (±0.8°F) above -150°C; ±0.25% of reading, ±1°C (±2°F) below -150°C; R, S, B: ±0.1% of reading, ±2°C (±4°F)
Memory	up to 4680 sets of readings
Sampling Rate	from 4 seconds/12 channels to 99 minutes 59 seconds/12 channels
Software	Included
Display	12-character alphanumeric LCD
Dimensions	L×W×H : 265×215×90 mm
Shipping Weight	700



Fig. 3.2 Image of scanning thermometer.

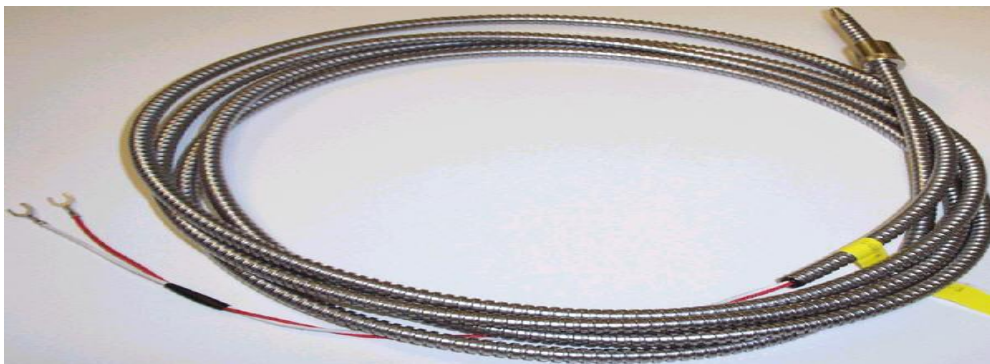


Fig. 3.3 J-type thermocouple.

b) Electric dry oven

Electric dry oven was used to dry of soil samples and determine moisture content according to **Ryan *et al.* (2007)**. The specifications of the device are listed in Table 3.2.

Table 3.2 Specifications of the electric dry oven.

Origin of manufacture	Canada
Model	655F Cat. No. 13-245-655
Temperature range	50 to 300 °C
Power source	Electricity
Accuracy	5 °C

3.2. Methods

3.2.1. Field experiment

This field experiment is designed to validate the soil temperature model. The temperature distribution in the soil at different depths of 2, 3 and 4 m is measured and recorded every 30 minutes through the day and average daily temperature is computed. Sample of soil was taken to determine soil moisture content, dry soil density and soil texture during the drill.

The root mean square of deviation which was determined according to **Ekstrand *et al.* (2011)** by Eq. 3.11 and the normalized root mean square of deviation (Eq. 3.12) were used in statistical analysis.

$$RMSd = \sqrt{\frac{\sum_{i=1}^n (X_m - X_p)^2}{n}} \quad (3.11)$$

$$NRMSd = \frac{RMSd}{X_{mp}} \quad (3.12)$$

Where, RMSd is the root mean square of deviations, NRMSd is the normalized root mean square of deviations, X_m is the measured values, X_{mp} is the mean predicted values and X_p is the predicted values at time/place i .

3.2.2. Measurements

a) Soil temperatures at various depths

The temperature distribution in the soil at different depths of 2, 3 and 4 m is measured and recorded.

b) Moisture content

Moisture content in this study was carried out by drying at 105 °C for approximately 24 hour at constant weight according to **Ryan *et al.* (2007)**.

c) Dry density

Dry density was measured according to **Ryan *et al.* (2007)**.

d) Soil texture

Soil texture was executed according to the international pipette method (**Ryan *et al.*, 2007**).

MODEL

DEVELOPMENT

4. MODEL DEVELOPMENT

4.1. Geothermal energy model

Geothermal energy system as shown in Fig. 4.1 consists of three sub systems: soil temperature, earth to air heat exchanger and agricultural structure (greenhouse here is taken as a case study). For each of three subsystems, a model is to be developed.

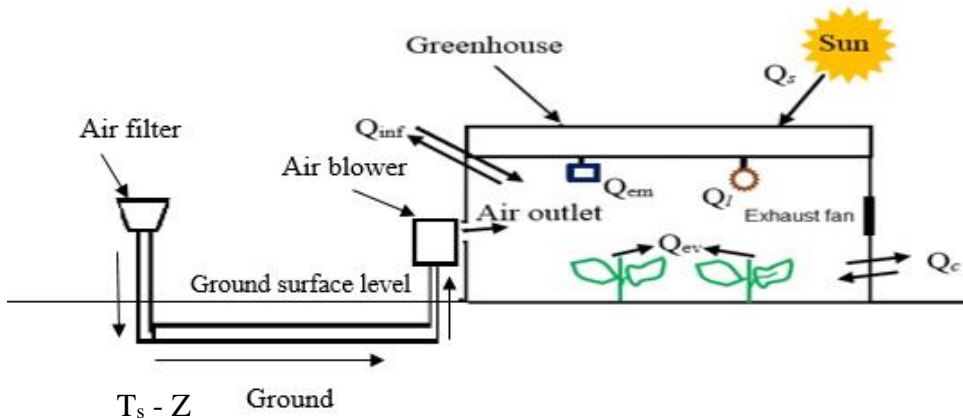


Fig. 4.1 Geothermal energy system structure.

4.1.1. Soil temperature model

As was indicated in the previous review **Kusuda and Archenbach (1965), Labs (1992) and ASHRAE (2012)** agreed that the following Eq. is the best model for prediction soil temperature at various depths and time.

$$T_{(t,z)} = T_{mean} + A_s \cdot e^{-z \sqrt{\frac{\pi}{365 \cdot a}}} \cdot \cos\left(\frac{2\pi}{365} \left(t - t_o - \frac{z}{2} \sqrt{\frac{365}{\pi \cdot a}}\right)\right) \quad (4.13)$$

Where:

T_{mean} is the mean ground surface temperature, °C.

A_s is the annual amplitude of the ground surface temperature, °C.

t is the time in year (days) from starting date of year, number.

t_o is the phase constant (days) since the beginning of the year of the minimum average ground surface temperature.

In this study it was decided to use Eq. 4.13 to predict the soil temperature after developing it for Egyptian conditions. For simplicity, the ground surface temperature is assumed to be equal the air temperature, which is an acceptable assumption for most design calculations as indicated by **ASHRAE (2012)**, also the phase lag is assumed as the phase lag at the maximum air temperature according to **Sharan and Jadhav (2002)** and the annual amplitude of ground surface temperature is assumed to equal the annual amplitude of air temperature.

$$T_{(t,z)} = T_{ma} + A_a \cdot e^{-z \sqrt{\frac{\pi}{365 \cdot \alpha}}} \cdot \cos\left(\frac{2\pi}{365} \left(t - t_o - \frac{z}{2} \sqrt{\frac{365}{\pi \cdot \alpha}}\right)\right) \quad (4.14)$$

Where:

T_{ma} is the mean ambient air temperature, °C.

A_a is the annual amplitude of the ambient air temperature, °C.

t_o is the phase lag constant (days) since the beginning of the year of the maximum ambient air temperature, number.

T_{ma} , t_o and A_a were taken as the average values of ten years from 1997 to 2006 weather data from Sheben El-Knater meteorological station.

Thermal diffusivity (α) for soil in Eq. 4.14 is to be calculated as follows (**ASHRAE, 2012**):

$$\alpha = \frac{24 \times 3600 k_s}{1000 \rho_s [c_s + c_w (w/100)]} = \frac{86.4 k_s}{\rho_s [c_s + 4.18 (w/100)]} \quad (4.15)$$

Where:

k_s is the soil thermal conductivity, W/(m.°C)

c_s is the dry soil specific heat, kJ/(kg.°C)

c_w is the specific heat of water which is equal to 4.18 kJ/(kg.°C).

ρ_s is the soil dry density, kg/m³.

w is the moisture content of soil, % (dry basis).

The thermal conductivity (k_s) in Eq. 4.15 is calculated by the following empirical equation for unfrozen silt and clay soils (**Kersten, 1949**):

$$k_s = 0.144(0.9 \log_{10}(w) - 0.2) \cdot 10^{0.621 \times 10^{-3} \rho_s} \quad (4.16)$$

This equation is valid for moisture content 7% or higher and fine soils, containing 50% or more silt and clay. It gives fit deviation of less than 25% from the measured thermal conductivity values according to **Kersten, (1949)**. When the soil properties isn't the same properties of soil described above, the thermal conductivity factors in Table 2.1 is to be used as an estimate.

The specific heat of dry soil (c_s) in Eq. 4.15 is nearly constant for all types of soil and equal to 0.73 kJ/ kg.°C as reported in **ASHRAE (2012)**. Fig. 4.2 shows the flow chart of soil temperature model.

4.1.2. Earth to air heat exchanger model (ETAHE)

Earth to air heat exchangers are long metallic, plastic or concrete pipes that are laid underground and are connected to the air intake of buildings. Their purpose is to provide some pre-conditioning or full conditioning of the air either pre-heating or full heating in the winter or pre-cooling or full cooling in the summer. The main aim of ETAHE model is to study the influence of pipe length, pipe diameter and air velocity inside the pipe on thermal performance of ETAHE system and determine the required length of the system, fan power and outlet air temperature from the pipe.

For the sake of simplicity, the following assumptions are considered as indicated by **Al-Ajmi *et al.* (2006); Lee and Strand (2006); Lee and Strand (2008) and Ascione *et al.* (2011)**:

- The soil surrounding the pipe is isotropic, with homogenous thermal conductivity in all ground strata.
- The pipe is of uniform cross-section.
- The soil thermal effect surrounding the pipe is negligible after a distance equal to the double of the radius of the pipe from the pipe outer surface.

4.1.2.1. Heat transfer between soil and air

The exchange of heat between the soil and the air passing through a buried pipe is governed by the difference between the air and soil temperatures. The exchange induces a variation in the air temperature and at the same time that of the soil around the pipe (**Deglin *et al.*, 1999**).

The rate of heat transfer is to be calculated by dividing the overall temperature difference by the total thermal resistance as indicated by **ASHRAE (2012)**:

$$q = \frac{(T_f - T_s)}{R_t} \quad (4.17)$$

Where:

q is the heat loss or gain per unit length of system, W/m.

T_f is the fluid temperature, °C.

T_s is the average annual soil temperature, °C.

R_t is the total thermal resistance, (m·°C)/W.

The negative result indicates a heat gain rather than a loss.

In order to calculate the heat transfer between the earth tube and the surrounding soil, the overall thermal resistance (R_t) should be

determined using the following three thermal resistance values (**Lee and Strand, 2008**).

$$R_t = R_c + R_p + R_s \quad (4.18)$$

Where:

R_c is the thermal resistance due to convection heat transfer between the air in the pipe and the pipe inner surface, (m.°C)/W.

R_p is the Thermal resistance due to conduction heat transfer between the pipe inner and outer surface, (m.°C)/W.

R_s is the Thermal resistance due to conduction heat transfer between the pipe outer surface and the undisturbed soil, (m.°C)/W.

(i) Thermal resistance due to convection heat transfer between the air in the pipe and the pipe inner surface (R_c) calculation:

Thermal resistance R_c in Eq. 4.18 is calculated by the following Eq. according to **Al-Ajmi et al. (2006)**; **Ascione et al. (2011)**; **Lee and Strand (2008)** and **Lee and Strand (2006)**:

$$R_c = \frac{1}{2\pi r_1 h_c} \quad (4.19)$$

Where:

r_1 is the inner pipe radius, m.

h_c is the convective heat transfer coefficient at the inner pipe surface, W/m² °C.

The convection heat transfer coefficient (h_c) in Eq. 4.19 inside the pipe is calculated using the following equation according to **Al-Ajmi et al. (2006)**; **ASHRAE (2009)** and **Maerefat and Haghighi (2010)**:

$$h_c = \frac{Nu.k_a}{2r_1} \quad (4.20)$$

Where:

Nu is Nusselt number.

k_a is the thermal conductivity of air, W/(m.°C).

To calculate the convective coefficient it is necessary to know the characteristics of the flow using dimensionless numbers: Nusselt number, Reynolds number and Pradtl Number.

Nusselt number is calculated by the following equation for turbulent flow of air and Re number is higher than or equal to 10000 according to **ASHRAE (2009)**:

$$Nu = 0.023Re^{0.8}.Pr^{0.4} \quad \text{For heating} \quad (4.21)$$

$$Nu = 0.023Re^{0.8}.Pr^{0.3} \quad \text{For cooling} \quad (4.22)$$

Reynolds number in Eqs. 4.21 and 4.22 characterizes the mode of the flow according to **ASHRAE (2009)**:

$$Re = \frac{\rho_a v . D}{\mu_a} \quad (4.23)$$

Where:

ρ_a is the density of air, kg/m³

μ_a is the dynamic viscosity of air, Pa.s

v is the air velocity, m/s

D is diameter of the pipe, m

Prandtl number in Eqs. 4.21 and 4.22 characterize the relationship between the viscosity and the thermal diffusivity of the fluid according to **ASHRAE (2009)**:

$$Pr = \frac{c_a \mu_a}{k_a} \quad (4.24)$$

Where:

Pr is Prandtl number.

c_a is the specific capacity of air, kJ/(kg.°C).

μ_a is the dynamic viscosity of air, Pa.s.

(ii) Thermal resistance due to conduction heat transfer between the pipe inner and outer surface (R_p) calculation:

Thermal resistance (R_p) is calculated by the following equation according to **Al-Ajmi *et al.* (2006); Ascione *et al.* (2011); Lee and Strand (2008) and Lee and Strand (2006):**

$$R_p = \frac{1}{2\pi k_p} \ln\left[\frac{r_1+r_2}{r_1}\right] \quad (4.25)$$

Where:

r_2 is the pipe thickness, m.

k_p is the pipe thermal conductivity , W/(m °C).

(iii) Thermal resistance due to conduction heat transfer between the pipe outer surface and the undisturbed soil (R_s) calculation:

Thermal resistance due to conduction heat transfer between the pipe outer surface and the undisturbed soil (R_s) is calculated by the following Eq. according to **Al-Ajmi *et al.* (2006); Ascione *et al.* (2011); Lee and Strand (2008) and Lee and Strand (2006):**

$$R_s = \frac{1}{2\pi k_s} \ln\left[\frac{r_1+r_2+r_3}{r_1+r_2}\right] \quad (4.26)$$

Where:

r_3 is the distance between the pipe outer surface and undisturbed soil assumed to be equal to the radius of the pipe, m.

4.1.2.2. Calculation the length of ETAHE

Using the previous calculation, the total length of the ETAHE is to be calculated from the following Eq.:

$$l = \frac{q.R_t}{(T_f - T_s)} = \frac{\dot{m}c_a(T_f - T_{out}).R_t}{(T_f - T_s)} \quad (4.27)$$

Where:

l is the length of ETAHE, m.

4.1.2.3. Air flow rate

Air flow rate is to be calculated by the following Eq.:

$$\dot{m} = \rho_a A_p v = \pi \rho_a r_1^2 v \quad (4.28)$$

Where:

\dot{m} is the mass flow rate of the air, kg/s.

A_p is the cross section area of pipe, m².

4.1.2.4. Fan power

The fan energy consumed in blowing air through a pipe is additional energy expenditure in the ETAHE system. The fan air power is given by **Al-Ajmi et al. (2006)**:

$$P_f = \frac{\Delta P A_p v}{\eta_{fan}} \quad (4.29)$$

Where:

P_f is the fan air power, W.

ΔP is the fan total pressure difference, Pa.

η_{fan} is the total fan efficiency, which was assumed to be 0.85.

The pressure drop in a smooth pipe is given by **ASHRAE (2009)** and **Paepe and Janssens (2003)**:

$$\Delta P = f \frac{l}{D} \rho_a \frac{v^2}{2} \quad (4.30)$$

$$f = \frac{64}{Re} \quad \text{if} \quad Re < 2300 \quad (4.31)$$

$$f = (1.82 \log Re - 1.64)^{-2} \quad \text{if} \quad Re \geq 2300 \quad (4.32)$$

Where:

- f is the friction factor, -
- ΔP is the fan total pressure difference, Pa.

4.1.2.5. Outlet fluid temperature from the earth tube

In the earth to air heat exchanger, air is the only heat transporting fluid. The heat released or absorbed by the air is flowing through the tube to the surrounding soil. If the contact of the tube wall with the earth is considered to be perfect and the conductivity of the soil is taken to be very high compared to the surface resistance, then the wall temperature at the inside of the tube can be assumed to be constant and equal to ground temperature. The total heat transferred to the air when flowing through a buried pipe can be written as (ASHRAE, 2011 and Paepe and Janssens, 2003):

$$Q = \dot{m}c_a(T_f - T_{out}) = \frac{l\Delta T_m}{R_t} \quad (4.33)$$

Where:

ΔT_m is the logarithmic average temperature difference, °C.

$$\Delta T_m = \frac{(T_f - T_{out})(T_{out} - T_s)}{\ln\left[\frac{(T_f - T_{out})}{(T_{out} - T_s)}\right]} = \frac{T_f - T_{out}}{\ln\left[\frac{(T_f - T_{out})}{(T_{out} - T_s)}\right]} \quad (4.34)$$

By substitutions from Eq. 4.34 in Eq. 4.33 gives the exponential relation for the outlet temperature of the tube as function of the soil temperature and inlet air temperature:

$$T_{out} = T_s + (T_f - T_s)e^{-\frac{l}{R_t\dot{m}c_a}} \quad (4.35)$$

4.1.2.6. Efficiency of ETAHE

The effectiveness of earth to air heat exchanger can be defined as:

$$\eta_{ETAHE} = \frac{(T_{out}-T_f)}{(T_s-T_f)} \quad (4.36)$$

Using Eq. 4.36 and substitution by Eq. 4.35 the effectiveness becomes:

$$\eta_{ETAHE} = (1 - e^{-\frac{l}{R_t \dot{m} c_a}}) \times 100 \quad (4.37)$$

Where:

η_{ETAHE} is the efficiency of ETAHE, %.

The flow chart of soil temperature model was shown in Fig. 4.2. and Fig. 4.3 shows the flow chart of ETAHE model.

4.1.3. Greenhouse model

4.1.3.1. Greenhouse heating and cooling requirements

Energy balance was performed on the greenhouse to calculate heating or cooling requirements. Energy balance of the greenhouse include solar, furnace, lighting, electric motors, etc., and the rate of heat loss from the greenhouse. The theory used to develop an energy balance for greenhouse is presented as follows. Fig. 4.4 shows the heat loss/gain from a greenhouse described by the following mathematical expression (Aldrich and Bartok, 1994):

$$Q_f + Q_{em} + Q_l + Q_s = Q_c + Q_{inf} + Q_{ev} \quad (4.38)$$

Where:

Q_f is the furnace heat (heat losses), W.

Q_{em} is the heat from electric motors, W.

Q_l is the heat from lighting, W.

Q_s is the heat from the sun, W.

Q_c is the heat loss by conduction through the greenhouse shell, W.

Q_{inf} is the heat loss by air exchange between inside and outside air, W

Q_{ev} is the heat loss by evaporating water, W.

Furnace heat is estimated for night heating when there is no sun, and heat from electric motors and lighting is ignored. Heat used in evaporating water is also ignored according to **Aldrich and Bartok (1994) and ASHRAE (2011)**. Therefore Eq. 4.38 becomes:

$$Q_f = Q_c + Q_{inf} \quad (4.39)$$

The previous equation is used to calculate the heating requirements.

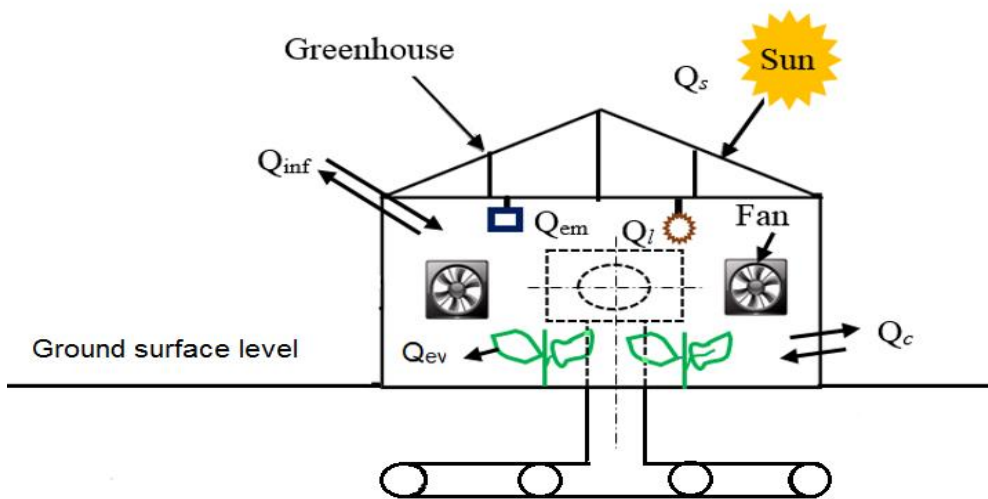


Fig. 4.4 Heat balance for greenhouse.

The largest exchange is by conduction through the greenhouse cover, including glazing and frame. Conduction heat transfer is estimated by the following equation (**Aldrich and Bartok, 1994 and ASHRAE, 2011**):

$$Q_c = AU(T_i - T_o) \quad (4.40)$$

Where:

A is the surface area of the greenhouse, m^2 .

U is the overall heat transmission coefficient, $W/m^2 \cdot ^\circ C$, (Table 4.1).

T_i is the inside temperature, °C.

T_o is the outside temperature, °C.

The type of framing should be considered in determining overall heat loss. Aluminum framing and glazing systems may have the metal exposed to the exterior to a greater or lesser degree, and the heat transmission of this metal is higher than that of the glazing material. To allow for such a condition, the U-factor of the glazing material should be multiplied by the factors shown in Table 4.2.

Table 4.1 Suggested heat transmission coefficients (ASHRAE, 2011).

Cover material	$U, W/(m^2 \cdot ^\circ C)$
Glass	
Single-glazing	6.4
Double-glazing	4.0
Insulating	Manufacturers' data
Plastic film	
Single film ^a	6.8
Double film, inflated	4.0
Single film over glass	4.8
Double film over glass	3.4
Corrugated glass fiber	
Reinforced panels	6.8
Plastic structured sheet ^b	
16 mm thick	3.3
8 mm thick	3.7
6 mm thick	4.1

(a) Infrared barrier polyethylene films reduce heat loss; however, use this coefficient when designing heating systems because the structure could occasionally be covered with non-IR materials.

(b) Plastic structured sheets are double-walled, rigid plastic panels.

Table 4.2 Construction U-factor multipliers (ASHRAE, 2011).

Construction	U-Factor multipliers
Metal frame and glazing system, 400 to 600 mm spacing	1.08
Metal frame and glazing system, 1200 mm spacing	1.05
Fiberglass on metal frame	1.03
Film plastic on metal frame	1.02
Film or fiberglass on wood	1.00

The second major heat transfer mode is air exchange between inside and outside the greenhouse. Heat is transferred in both sensible and latent forms. The sensible heat is transferred by increasing the temperature of incoming air. The latent heat is removed as water vapor from evaporation and transpiration. Sensible heat transfer can be estimated by **Aldrich and Bartok (1994) and ASHRAE (2011)**:

$$Q_{inf} = \rho_{air} V C_p N (t_i - t_o) \quad (4.41)$$

Where:

ρ_{air} is the density of air, kg/m³.

C_p is the specific capacity of air, J/(kg.°C).

N is the number of air exchanges per hour.

V is the volume of greenhouse, m³.

The rate of air exchange between inside and outside is affected by wind and the type and quality of greenhouse construction. Reasonable estimates of air exchange are given in Table 4.3. (**Elsner et al. 2000**).

Table 4.3 Suggested design air changes (N) (1/hour) (ASHRAE, 2011; Elsner *et al.* 2000 and Aldrich and Bartok, 1994).

New Construction	
Single glass lapped (unsealed)	1.25
Single glass lapped (laps sealed)	1.0
Plastic film covered	0.6 to 1.0
Structured sheet	1.0
Film plastic over glass	0.9
Old Construction	
Good maintenance	1.5
Poor maintenance	2 to 4

The solar gain on sunny days will replace some or all furnace heat needed to maintain temperature at the proper level. If solar gain exceeds heat loss, the greenhouse air temperature will rise and cooling may be required. The solar gain can be estimated by **Aldrich and Bartok (1994)**:

$$Q_s = \tau I_s A_f \quad (4.42)$$

Where:

τ is the transmittance of the greenhouse cover to solar radiation, (Table 4.4).

I_s is the intensity of solar radiation on a horizontal surface outside, W/m^2 .

A_f is the area of greenhouse floor, m^2 .

Transmittance will vary with angle of incidence (the angle between the sun's rays and a perpendicular to the surface), but an average value of 60% will give reasonable estimates. In Eq. 4.42, multiply rated (τ) by 0.6 if the angle of incidence is unknown.

Table 4.4 Transmissivity of glazing materials.^(c) (**Aldrich and Bartok, 1994**)

Transmissivity		
	Solar	Infrared
Temperature of radiation source (°C)	5538 °C	26.7 °C
Wavelength of radiation (micrometers) ^c	0.38 – 2.0	4.0 – 10.0
Material		
Window glass	0.85	0.02
Fiberglass	0.88	0.02
Acrylic	0.92	0.02
Polycarbonate	0.85	0.01
Polyethylene	0.92	0.81
Acrylic, double layer extrusion	0.83	< 0.02
Polycarbonate, double layer extrusion	0.77	< 0.01

(c) Values are for nominal thickness and single layer unless otherwise indicated.

Evapotranspiration rate in a greenhouse is affected by the solar radiation received by the crop and the stage of crop growth. The ratio of solar radiation to evapotranspiration for actively growing plants in a greenhouse averages about 0.5; that is, about one half the solar radiation received by the plant is used to evaporate water (**Aldrich and Bartok, 1994**):

$$Q_{ev} = E F Q_s \quad (4.43)$$

Where:

E is the ratio of evapotranspiration to solar radiation (= 0.5)

F is the floor use factor ratio of ground covered by plants to total ground area.

The peak demand of cooling is to be calculated from the following equation:

$$Q_{co} = Q_f + Q_s + Q_{ev} = Q_f + T I_s A_f (1 + E F) \quad (4.44)$$

Where:

Q_{co} is the cooling load, Watt.

and the peak demand of heating is to be calculated from the following equation:

$$Q_h = Q_c + Q_{inf} = AU(T_i - T_o) + \rho_{air} V C_p N (t_i - t_o) \quad (4.45)$$

Where:

Q_h is the heating load, Watt.

Microsoft office spread sheet 2013 program is used to running the geothermal energy model. Fig. 4.5 shows flow chart of greenhouse model.

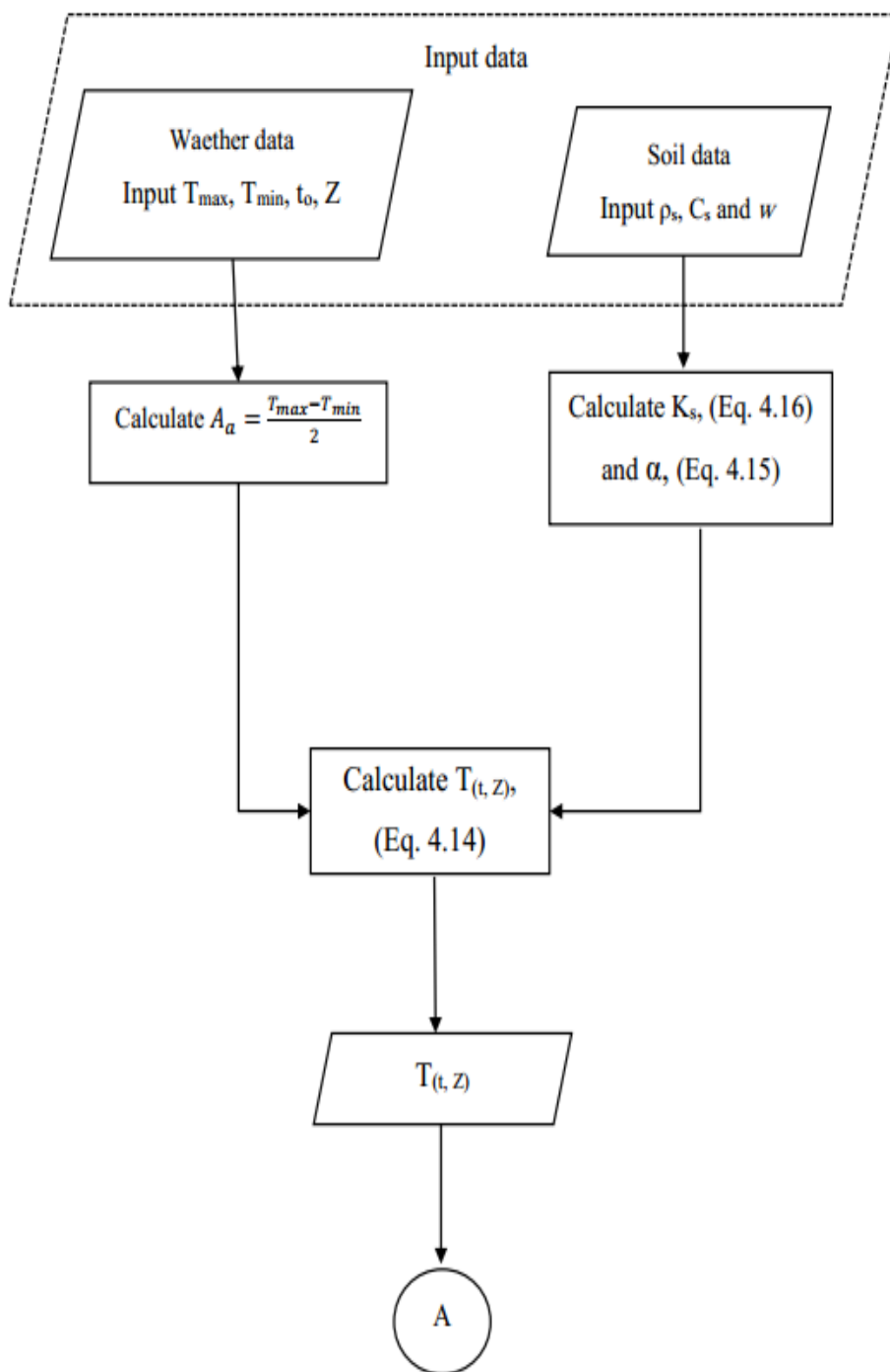


Fig. 4.2 Flow chart of soil temperature model.

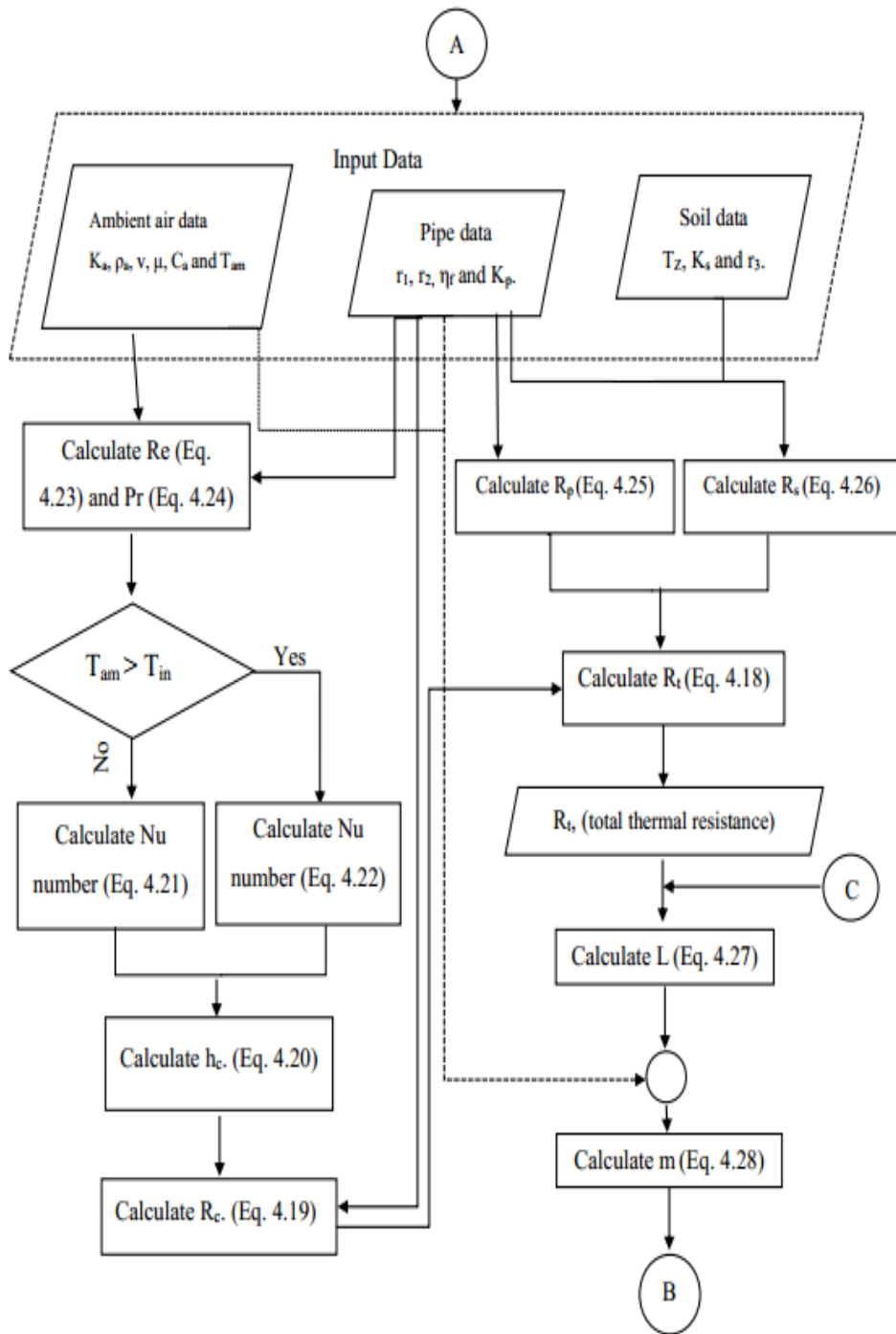


Fig. 4.3 Flow chart of ETAHE model.

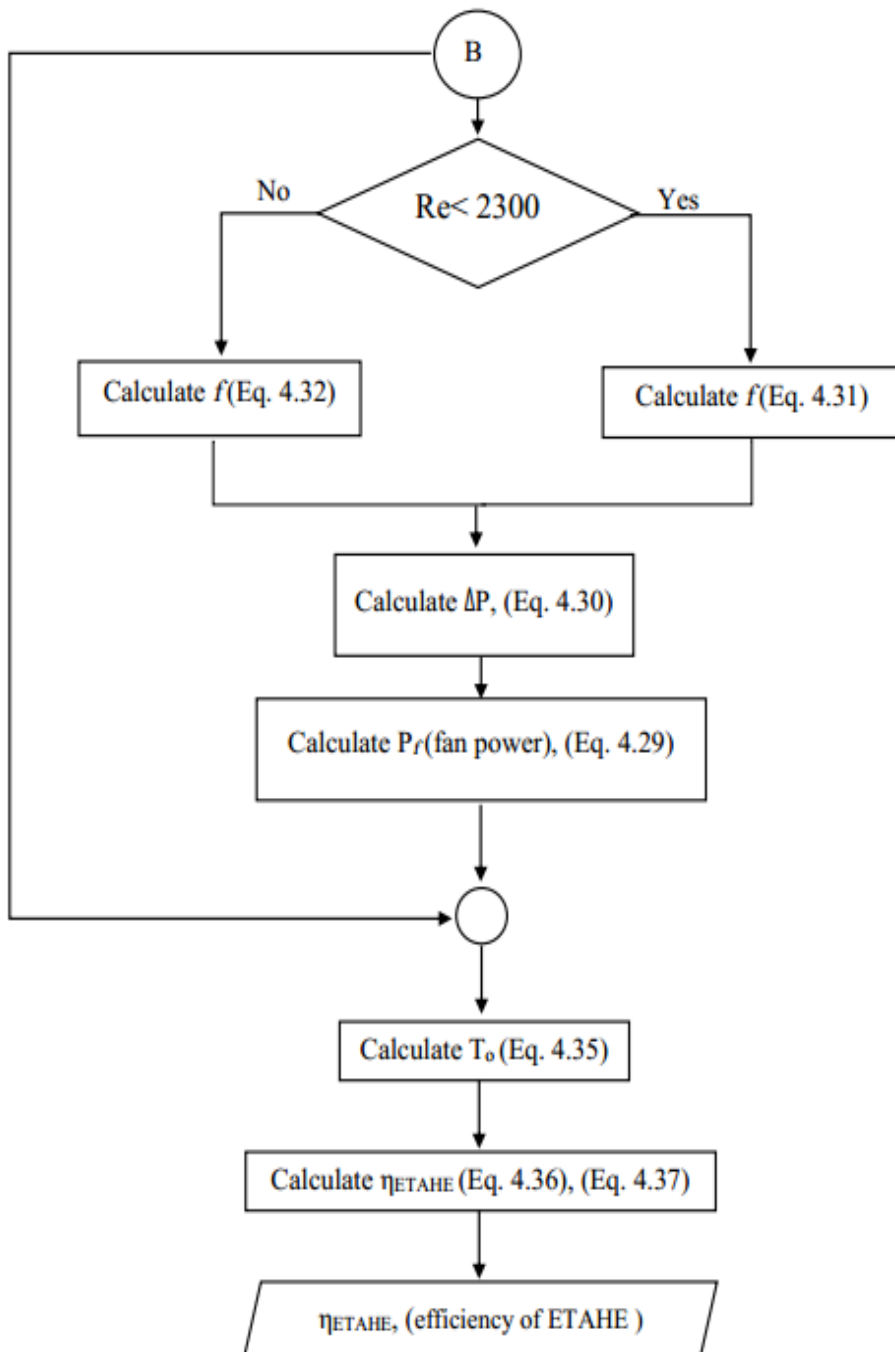


Fig. 4.3 Continued.

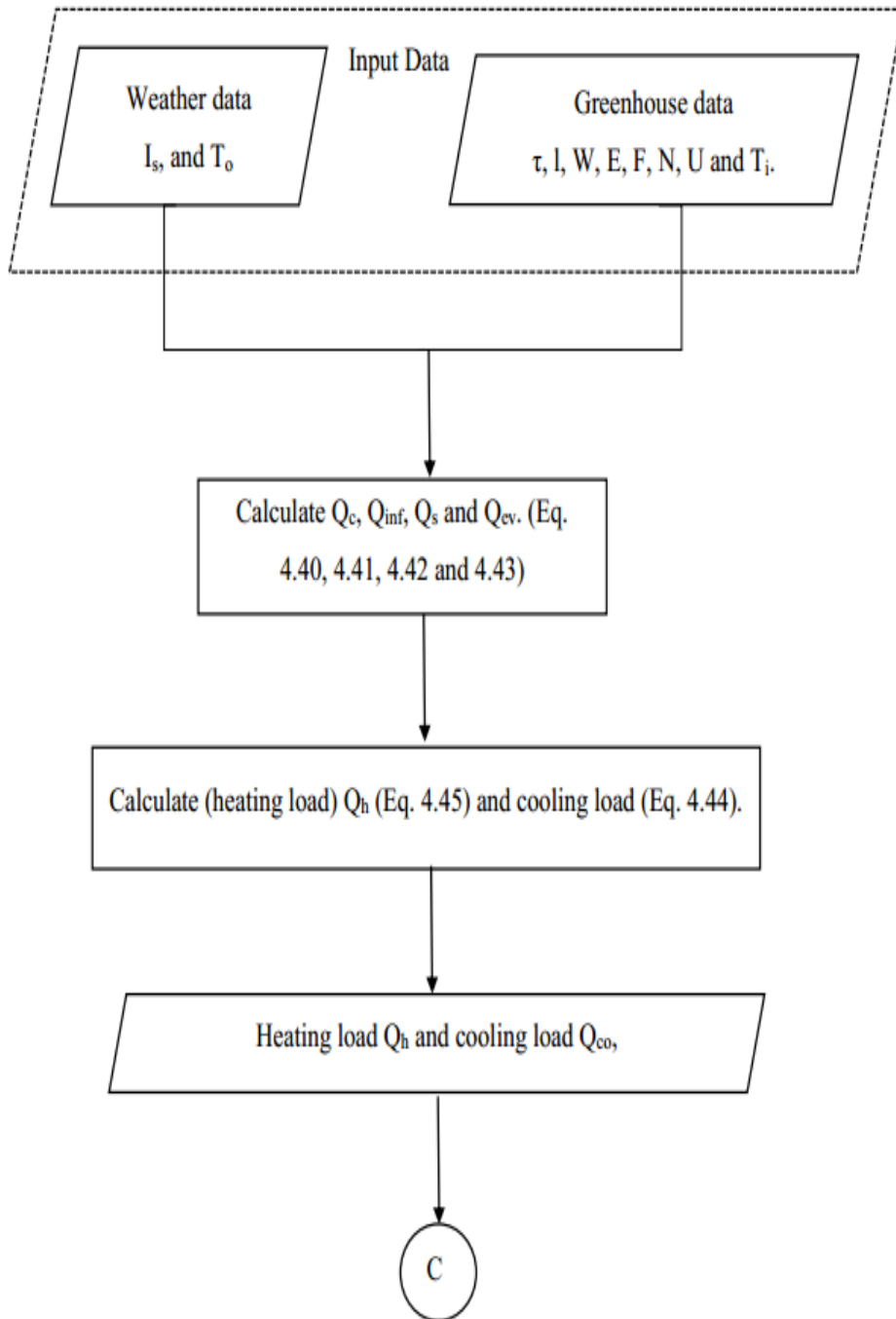


Fig. 4.5 Flow chart of greenhouse model.

4.1.4. Data inputs for model validation and experimentation

4.1.4.1. Input data of soil temperature model

Table 4.5 illustrates the input parameters used for validation the soil temperature model.

Table 4.5 Input parameters for calculation soil temperature.

Item	Field experiment	Work published by Kassem (1999) .
Soil type	Clay	Clay
Soil moisture content, %. (w)	19.70	-
Soil dry density (Bulk density), kg/m ³ . (ρ_s)	1190	-
Soil depth, m. (z)	2, 3, 4	1.5, 2
Dry Soil heat capacity, J/kg°C. (c_s)	730	-
Soil thermal diffusivity, m ² /day (SHRAE 2011). (α)	-	0.052
The mean ambient air temperature, °C. (T_{am})	21.6	20.08
The annual amplitude of the ambient air temperature, °C. (A_a)	10.7	6.36
The phase constant (days) since the beginning of the year of the highest average ambient air temperature, number. (t_o)	136	227

When the experimentation of model is carried out, the selected depths will be 0, 1, 2, 3, 4, 5, 6, 7, 8, 9 and 10 m.

4.1.4.2. Input data of earth to air heat exchanger model

The detailed input parameters for the ETAHE model used in validation are the same and are listed in Table 4.6.

Table 4.6 Input parameters for comparative validation of ETAHE model.

Item	Value
Pipe diameter (cm).	30
Pipe length (m)	24.7
Air velocity (m/s)	1.5
Ambient air temperature	25.56, 20.55°C
Soil temperature (°C)	18.89
Pipe depth (m)	2.13
Soil thermal conductivity (W/(m°C))	1.16
Soil thermal diffusivity (m ² /s)	0.00232

Using the developed ETAHE model, parametric studies were carried out to determine the effect of four important variables: pipe diameter, pipe length; pipe material and air velocity. These variables are influencing on the system inlet air temperature, the efficiency of ETAHE and the pressure drop.

- (i) **Pipe diameter:** previous research examined pipe diameter from 0.1 to 0.4 m. In the present work, it was decided to take the values of pipe diameter in the range from 0.1 to 0.3 namely 0.075, 0.10, 0.125, 0.15, 0.20, 0.25 and 0.30 m.
- (ii) **Pipe length:** previous research examined pipe length from 10 to 90 m. In the present work, it was decided to take the values of pipe

length in the range from 5 to 150 namely 5, 10, 30, 60, 90, 120 and 150 m.

(iii) Air velocity: previous research examined air velocity inside the pipe from 1 to 17 m/s. In the present work, it was decided to take the value of air velocity in the range from 1 to 20 m/s namely 1, 5, 8, 11, 14, 17 and 20 m/s.

(iv) Pipe material: previous research examined many of pipe material as metallic, concrete and plastic pipes. In the present work, it was decided to take two pipe materials: Polyvinyl Chloride (PVC) and steel with thermal conductivity 0.16 W/(m°C) and 54 W/(m°C), respectively.

4.1.4.3. Description of greenhouse as a case study

A typical gable even span greenhouse of dimensions $32 \times 8 \times 2$ m with gable angle 25° , is defined for designing the ETAHE for covering the heating and cooling requirements, with details as shown in Table 4.7.

The maximum air temperature over ten years from 1997 to 2006 is chosen as a summer design day for Kalubia climate conditions. It is set at 41°C . The minimum air temperature over ten years from 1997 to 2006 is chosen as a winter design day for Kalubia climate conditions. It is set at 5°C . These calculations performed on Moshtohor, Kalubia, Egypt.

Table 4.7 Details of greenhouse specifications and other details used for ETAHE model.

Item	Value
Length, m	32
Width, m	8
Height, m	2
Gable angle	25 °
Cover (from Table 4. 1)	Type: polyethylene Total thermal conductivity: 6.8W/m ² °C
Shade	50 %
Temperature inside greenhouse	Minimum: 18 °C and maximum: 22 °C
Solar radiation, W/m ² (from weather data)	1016
Air exchange rate (Infiltration rate), 1/h (from Table 4. 3)	0.75
The floor use factor	0.92

RESULTS AND DISCUSSIONS

5. RESULTTS AND DISCUSSIONS

5.1. Model validation

The system under study as previously explained consists of three models: soil temperature model, ETAHE model and greenhouse model. In this section the validation of the first and second models is presented.

5.1.1. Soil temperature model validation

The soil temperature model was validated using two sets of data. The first set was obtained by an experimental work which was described above. The results of the validation process experiment are shown in Table 5.1.

Data in Table 5.1 and Figs. 5- a, b and c show the comparison between the predicted and measured soil temperatures at different depths (2, 3 and 4 m). It could be seen that the measured soil temperature ranged from 19.50 to 22.95°C at 2 m depth, 18.61 to 21.83 °C at 3 m depth and from 19.50 to 20.40 °C at 4 m depth. As can be seen, the maximum differences between predicted and measured soil temperature at 2, 3 and 4 m depth were 4.09, 2.58 and 0.30 °C, respectively and the minimum differences between predicted and measured soil temperature at 2, 3 and 4 m depth were 0.44, - 0.73 and - 0.61 °C, respectively. The results showed good agreement where, the root mean squares of deviations at 2, 3 and 4 m depth were 2.65, 1.65 and 0.39 °C, respectively and the normalized root mean squares of deviations to the mean of the predicted data at the same depths were 0.14, 0.09 and 0.02 respectively.

Table 5.1 Measured data and predicted soil temperature.

Date	Soil temperature at various depths, m					
	2		3		4	
	Measured	Predicted	Measured	Predicted	Measured	Predicted
24/2/2012	21.58	18.71	21.6	19.24	19.54	20.14
25/2/2012	22.26	18.76	21.83	19.25	19.82	20.13
26/2/2012	22.09	18.81	21.51	19.27	19.7	20.13
27/2/2012	22.95	18.86	21.82	19.28	20.4	20.12
28/2/2012	22.09	18.91	21.66	19.29	19.85	20.12
29/2/2012	20.61	18.96	19.63	19.31	19.75	20.12
1/3/2012	21.14	19.01	19.46	19.32	19.5	20.11
2/3/2012	19.5	19.06	18.61	19.34	19.55	20.11
3/3/2012	21.4	19.12	18.86	19.35	19.58	20.11
4/3/2012	22.2	19.17	20.04	19.37	19.74	20.11
5/3/2012	21.36	19.23	20.27	19.39	19.93	20.10
6/3/2012	21.99	19.28	21.01	19.41	19.97	20.10
7/3/2012	22.13	19.34	21.23	19.43	20.14	20.10
8/3/2012	21.54	19.40	21.01	19.45	20.4	20.10
9/3/2012	20.53	19.45	20.45	19.47	19.71	20.10

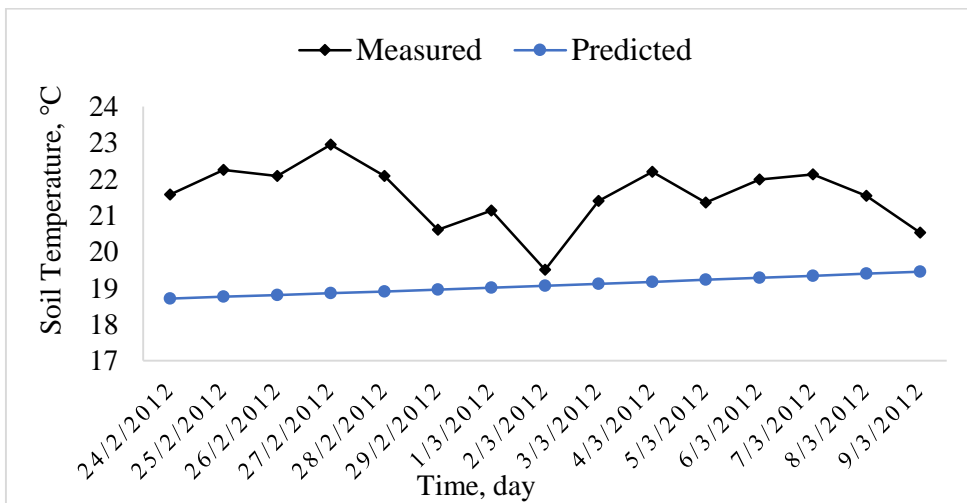


Fig. 5.1- a. The predicted and measured soil temperatures at 2 m depth.

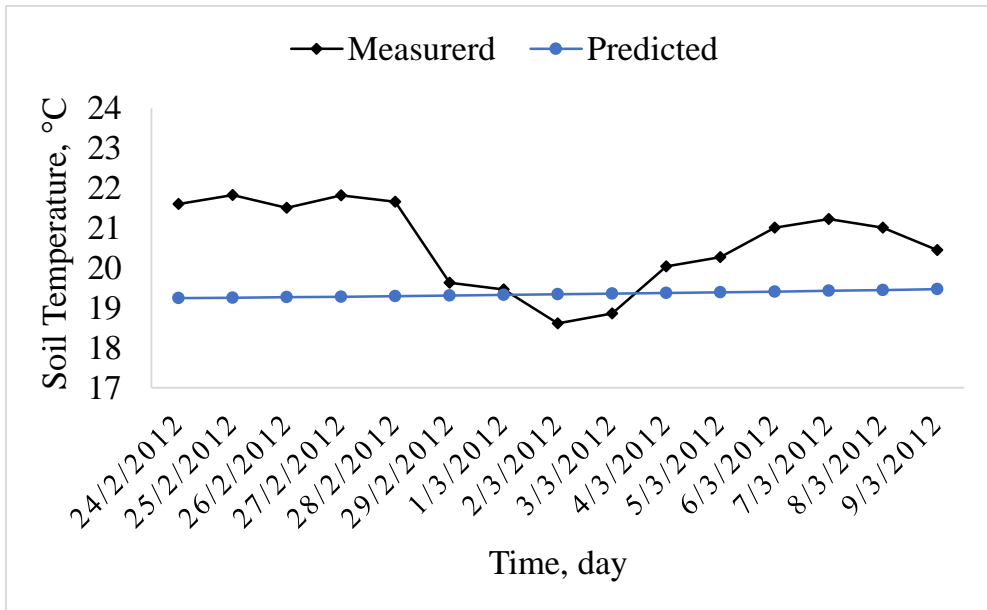


Fig. 5.1- b. The predicted and measured soil temperatures at 3 m depth.

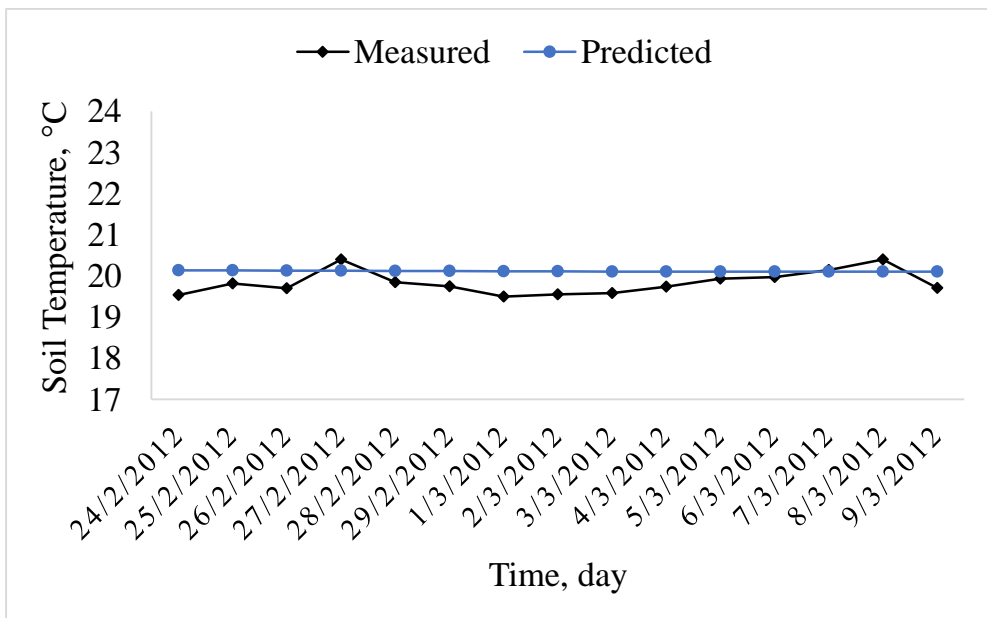


Fig. 5.1- c. The predicted and measured soil temperatures at 4 m depth.

The model was also validated using the data obtained by **Kassem (1999)** as shown in Table 5.2 and Figs. 5.2- a and b. It could be seen that, the results show good agreement where, the root mean squares of deviations at 1.5 and 2 m depths were 1.93 and 1.85 °C respectively and the normalized root mean squares of deviations to the mean of the predicted data at 1.5 and 2 m depths were 0.10 and 0.09 respectively.

Table 5.2 The predicted soil temperatures and measured by **Kassem, (1999)**.

Date	Soil temperature at Various depths, m			
	1.5		2	
	Measured	Predicted	Measured	Predicted
January	18.6	18.5	19.0	19.4
February	19.3	17.3	19.7	18.2
March	20.0	16.7	20.4	17.4
April	20.6	17.0	20.9	17.4
May	20.7	18.1	20.5	18.1
June	21.6	19.8	21.2	19.3
July	21.9	21.5	21.0	20.7
August	22.5	22.9	21.0	22.0
September	21.9	23.5	21.1	22.8
October	21.6	23.1	21.2	22.8
November	21.1	22.0	21.5	22.1
December	19.3	20.3	19.7	20.8

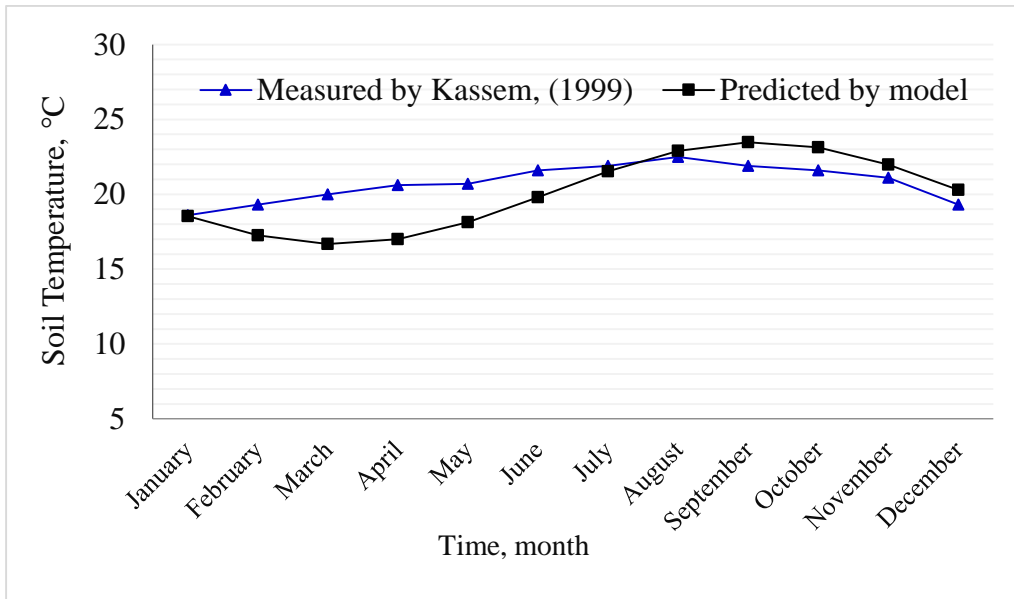


Fig. 5.2- a. The predicted soil temperatures compared to that measured by **Kassem, (1999)** at 1.5 m.

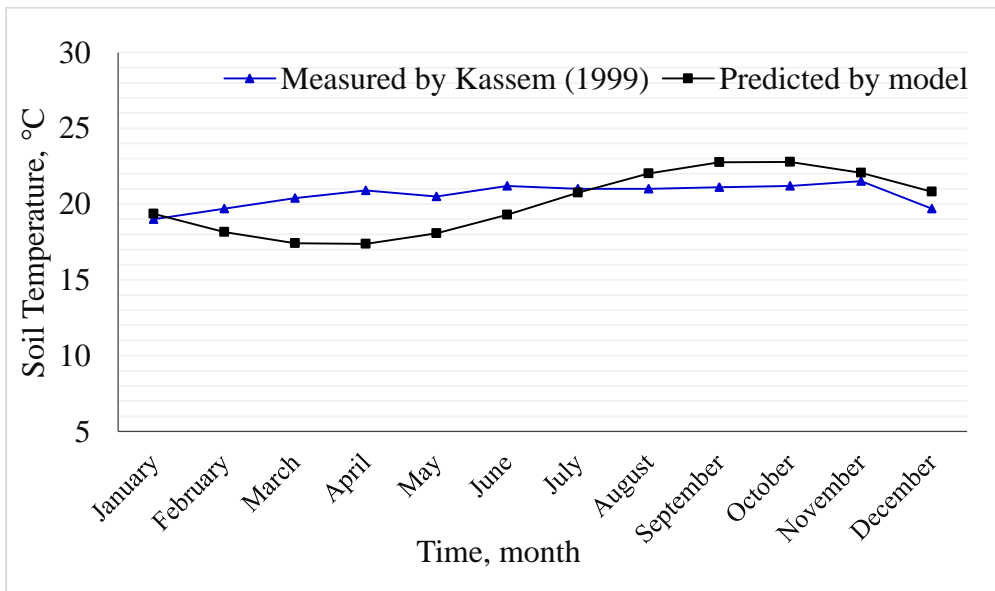


Fig. 5.2- b. The predicted soil temperatures compared to that measured by **Kassem, (1999)** at 2 m.

5.1.2. Earth to air heat exchanger model validation

The ETAHE model developed in the previous section was validated against the results of two theoretical models (**Al-Ajmi *et al.*, 2006; Lee and Strand, 2008**) and one experimental data (**Dhaliwal and Goswami, 1984**). **Al-Ajmi *et al.* (2006)** used similar model to the current developed model except ignoring the thermal resistance of the pipe and the calculation of Nu number is't the same and they studied the influence of fan on increasing the outlet air temperature. **Lee and Strand (2008)** used similar model to the current developed model except the calculation of Nu number and the outlet air temperature from the pipe are not the same.

Tables 5.3 and 5.4, Figs. 5.3 and 5.4 show the results for the experimental and tow theoretical studies using two different ambient air temperature conditions. As can be seen, the results show good agreement and have the values between the three studies under consideration. Where, using 25.56 °C ambient air temperature the root mean square of deviations between the model and experimental data by **Dhaliwal and Goswami (1984)** was 0.61 °C, between the model and theoretical data by **Al-Ajmi *et al.* (2006)** was 0.33 °C and between the model and theoretical data by **Lee and Strand (2008)** was 0.07 °C and where using 20.55 °C ambient air temperature the root mean square of deviations were 0.19, 0.06 and 0.02 °C respectively.

Table 5.3 ETAHE model validation at ambient air temperature 25.56 °C.

Axial distance from the pipe inlet (m)	Experimental data of Dhaliwal and Goswami (1984) , (°C)	Model of Al-Ajmi <i>et al.</i> (2006) results, (°C)	Model of Lee and Strand (2008) results, (°C)	ETAHE Model, (°C)
3.35	25.00	24.94	25.04	25.06
6.40	24.40	24.43	24.60	24.64
9.45	25.00	23.97	24.19	24.25
12.50	24.40	23.54	23.82	23.89
15.55	23.80	23.15	23.46	23.55
24.70	23.80	22.16	22.55	22.66

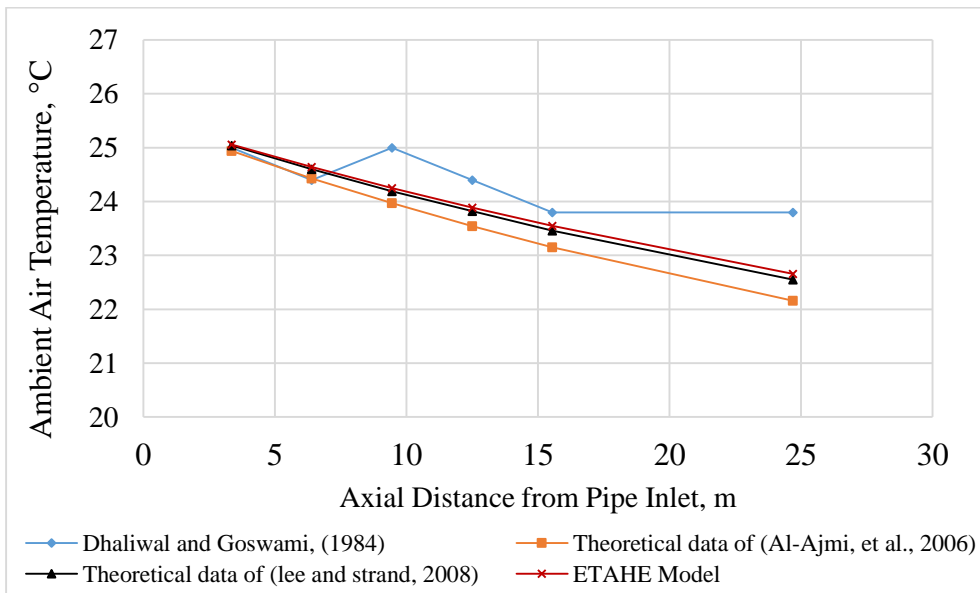


Fig. 5.3 ETAHE Model validation at ambient air temperature 25.56 °C.

Table 5.4 ETAHE model validation at ambient air temperature 20.55°C.

Axial distance from the pipe inlet (m)	Experimental data of Dhaliwal and Goswami (1984) , (°C)	Model of Al-Ajmi et al. (2006) results, (°C)	Model of Lee and Strand (2008) results, (°C)	ETAHE Model, (°C)
3.35	20.55	20.40	20.42	20.43
6.4	20.00	20.27	20.31	20.32
9.451	20.00	20.16	20.21	20.22
12.5	20.00	20.05	20.11	20.13
15.55	20.00	19.95	20.03	20.05
24.7	20.00	19.80	19.80	19.83

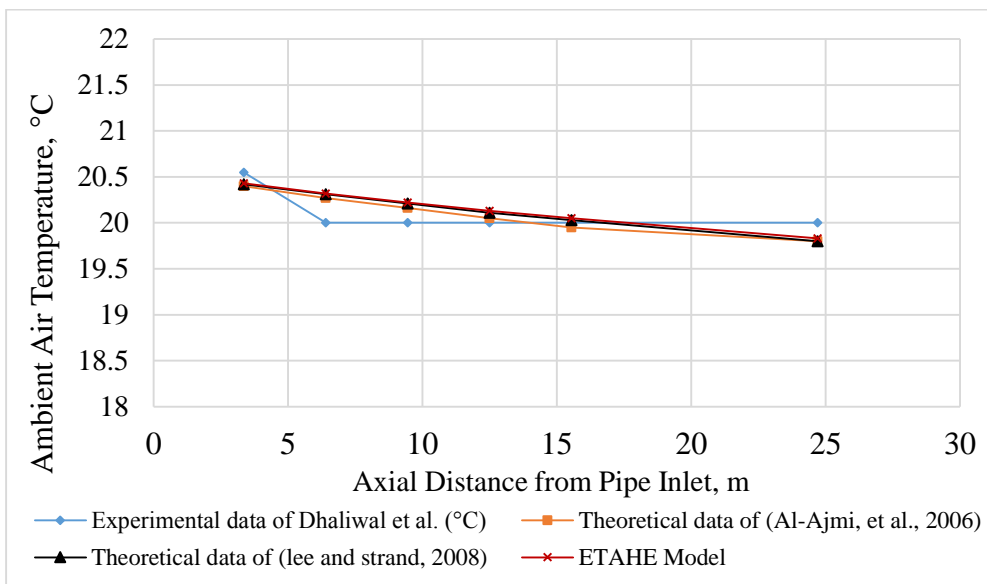


Fig. 5.4 ETAHE model validation at ambient air temperature 20.55°C.

5.2. Model experimentation

The effects of design important parameters significantly influence the performance of an ETAHE system are investigated through the parametric analysis for both heating and cooling. The effect of pipe diameter, pipe length, pipe material and air velocity on the system inlet air temperature, the efficiency of ETAHE and the pressure drop were investigated by the ETAHE model.

5.2.1. Soil temperature at various depths

Before installation of ETAHE, the optimal depth and the soil temperature at this depth should be determined. To achieve these two parameters, experimentation of the soil temperature model is performed at a wide range of soil depth starting from 0 to 10 m with 1 m intervals. The results are shown in Table 5.5.

Table 5.5 and Figs. 5.5 show the predicted soil temperatures at different soil depths during a whole year. It could be seen that the temperature fluctuations decreased with soil depth. Fig. 5.6 illustrates the amplitude of soil temperature at various depths. It could be seen that with increasing depth under soil surface the amplitude of temperatures decreased, where the maximum temperature at the soil surface during the year was 32.0 °C and the minimum was 11.0 °C. The amplitude of annual variation at soil surface was thus 10.6 °C. At 1 m depth it reduced to 6.5 °C, at 2 m to 3.9 °C, at 3 m to 2.4 °C, at 4 m to 1.5 °C, at 5 m to 0.9 °C, at 6 m to 0.5 °C, at 7 m to 0.3 °C, at 8 m to 0.2 °C, at 9 m to 0.1 °C, at 10 m to 0.1 °C. Attenuation of the annual wave is clearly evident, as it penetrates into the soil. The depth of 4 m under the ground level implies 1.5 °C amplitude of soil temperature, while a further deepness (5 m) allows only a minimal improvement 0.9 °C amplitude. Thus, a depth of

4 m is the preferable depth to installation an earth tube for geothermal energy system.

Table 5.5 Predicted soil temperature at various depths.

Month	Depth, m										
	0	1	2	3	4	5	6	7	8	9	10
January	16.6	16.2	17.7	19.4	20.7	21.4	21.8	21.8	21.8	21.7	21.7
February	21.8	18.7	18.3	19.2	20.2	21.0	21.5	21.7	21.7	21.7	21.7
March	27.0	21.9	19.9	19.7	20.1	20.7	21.2	21.5	21.7	21.7	21.7
April	30.8	25.1	21.9	20.6	20.4	20.7	21.1	21.4	21.5	21.6	21.7
May	32.2	27.4	23.8	21.9	21.1	20.9	21.1	21.3	21.5	21.6	21.6
June	30.7	28.1	25.2	23.0	21.8	21.3	21.2	21.3	21.4	21.5	21.6
July	26.7	27.0	25.5	23.8	22.5	21.8	21.4	21.4	21.4	21.5	21.5
August	21.3	24.5	24.8	24.0	23.0	22.2	21.7	21.5	21.5	21.5	21.5
September	16.0	21.2	23.2	23.5	23.1	22.5	22.0	21.7	21.6	21.5	21.5
October	12.3	18.0	21.2	22.5	22.7	22.5	22.1	21.8	21.7	21.6	21.6
November	11.0	15.8	19.3	21.3	22.1	22.3	22.1	21.9	21.8	21.6	21.6
December	12.6	15.1	18.0	20.1	21.4	21.9	22.0	21.9	21.8	21.7	21.6
Amplitude	10.6	6.5	3.9	2.4	1.5	0.9	0.5	0.3	0.2	0.1	0.1

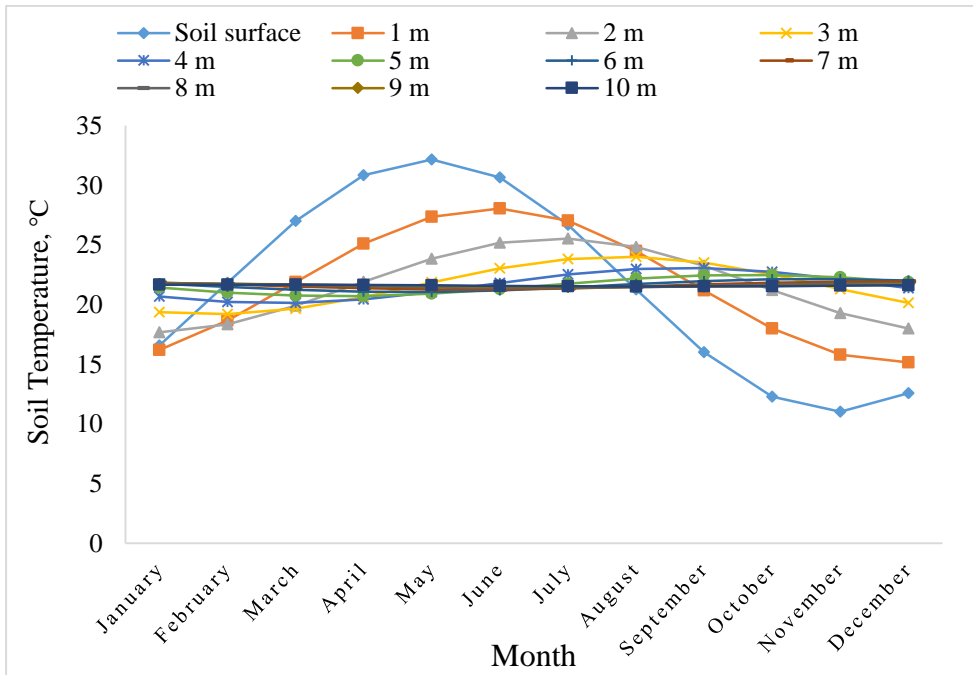


Fig. 5.5 Predicted soil temperature at various depths.

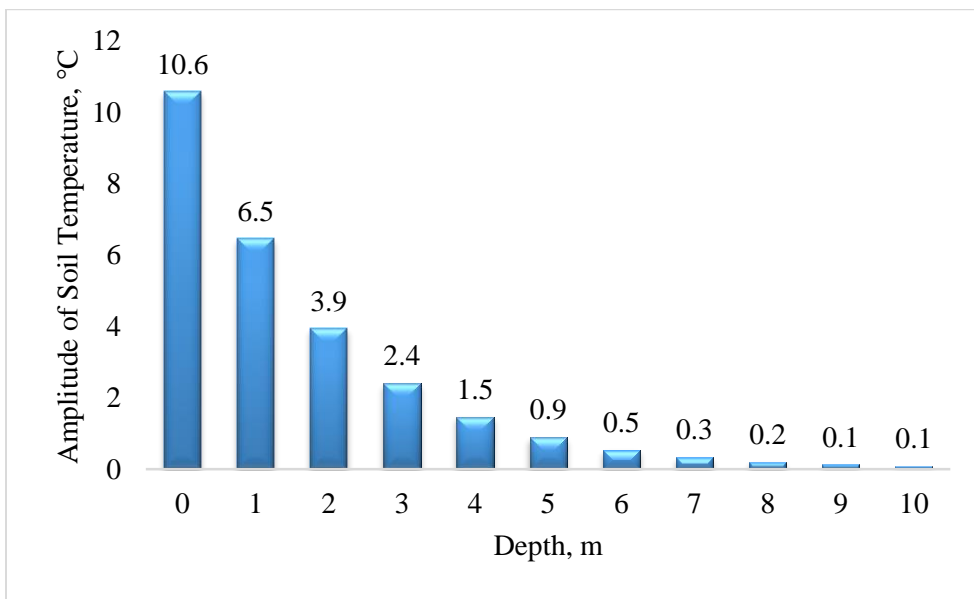


Fig. 5.6 Amplitude of predicted soil temperature at various depths.

5.2.2. Influence of various parameters on ETAHE system

Using the developed ETAHE model, parametric studies are carried out to determine the effect of four important variables: pipe diameter; pipe length; air velocity and pipe material. These variables are influencing on the system inlet air temperature, the efficiency of ETAHE and the pressure drop.

The “base case” values for each variable are assumed to be set at: 0.15 m for pipe diameter, 60 m for pipe length, 8 m/s for air velocity, and 4 m for pipe depth. In addition, when changing only one variable at every calculation process for parametric studies, the other variables are kept at those values.

5.2.2.1. Influence of pipe length

The calculations were performed for seven different pipe lengths, namely 5, 10, 30, 60, 90, 120 and 150 m. The diameter of the pipe was fixed at 0.15 m, placed at a depth of 4 m, while the air velocity inside the pipe is fixed at 8 m/s.

Table 5.6, Figs. 5.7, 5.8 and 5.9 show the effect of pipe length on the earth tube inlet air temperature at the highest ambient air temperature and the lowest air temperature, the efficiency of ETAHE and pressure drop. It could be seen that in cooling mode, as the pipe length increases, the inlet air temperature decreases, where the pipe length increased from 5 to 30 m, 30 to 90 m and 90 to 150 m the inlet air temperature decreased from 39.65 to 34.17 °C, 34.17 to 26.88 °C and 26.88 to 23.82 °C, respectively. The decreasing percentages were 14, 27 and 11 %, respectively. In heating mode as the pipe length increases, the inlet air temperature increases, where the pipe length increased from 5 to 30 m, 30 to 90 m and 90 to 150 m, the inlet air temperature increased from 6.16

to 10.34 °C, 10.34 to 17.08 °C and 17.08 to 19.7 °C, respectively. The increasing percentages were 40 %, 39 % and 13 %, respectively.

These results could be attributed to the fact that the longer pipe provides a longer path over which heat transfer between the pipe and the surrounding soil can occur given the same overall heat transfer coefficient of earth tube (**Lee and Strand, 2008**).

Table 5.6 Influence of pipe length on pressure drop, inlet temperature and efficiency of ETAHE at 0.15 pipe diameter and 8 m/s air velocity.

Pipe length, m	T _{inlet} -Heating, °C	T _{inlet} -Cooling, °C	Efficiency, %	Pressure drop, Pa
5	6.16	39.65	7	56.46
10	7.23	38.39	13	112.93
30	10.84	34.17	35	338.78
60	14.63	29.75	58	677.57
90	17.08	26.88	73	1016.35
120	18.67	25.02	82	1355.14
150	19.7	23.82	89	1693.92

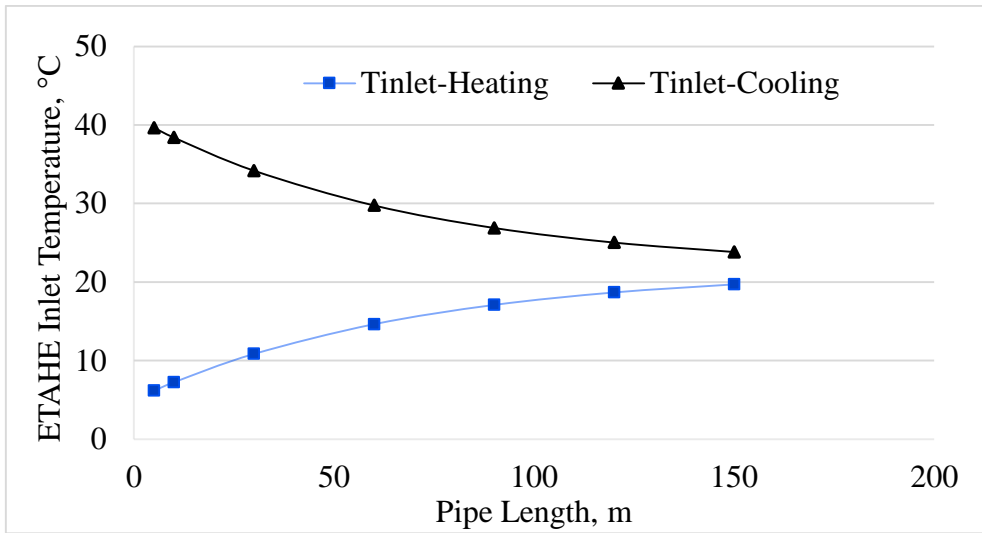


Fig. 5.7 Influence of pipe length on inlet air temperature in heating and cooling modes.

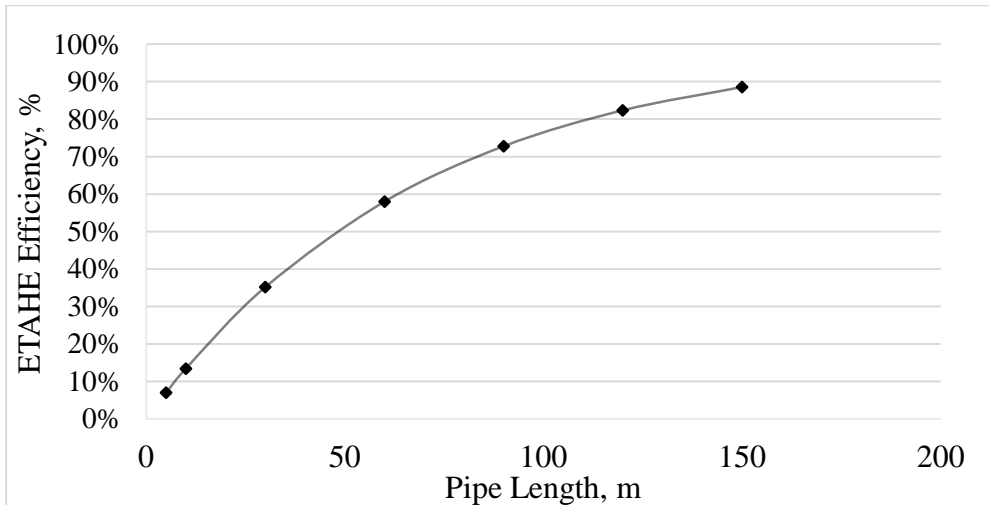


Fig. 5.8 Influence of pipe length on ETAHE efficiency.

Fig. 5.8 shows the effect of pipe length on the efficiency of ETAHE. It could be seen that as the pipe length increases, the efficiency of ETAHE increases, where the pipe length increased from 5 to 30 m, 30 to 90 m and 90 to 150 m, the efficiency of ETAHE increased from 7 to 35 %, 35 to 73 % and

73 to 0.89 %, respectively. The increasing percentages were 80, 52 and 18 %, respectively.

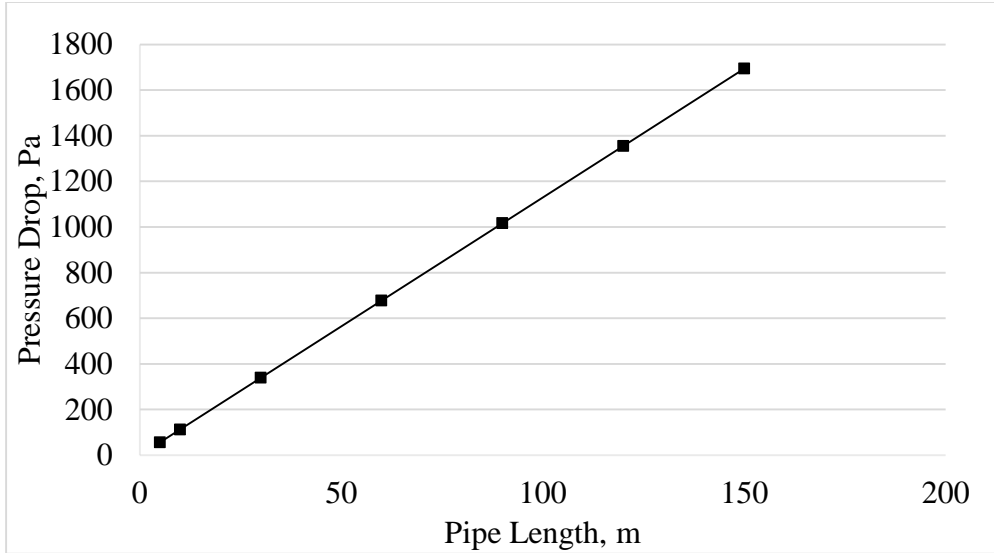


Fig. 5.9 Influence of pipe length on pressure drop.

Fig. 5.9 shows the effect of pipe length on the pressure drop. It could be seen that as the pipe length increases, the pressure drop increases, where the pipe length increased from 5 to 30 m, 30 to 90 m and 90 to 150 m the pressure drop increased from 56.46 to 338.78 Pa, 338.78 to 1016.35 Pa and 1016.35 to 1693.92 Pa, respectively. The increasing percentage was 83 %, 67 % and 40 %, respectively.

The results indicate that the optimal values of pipe length used as inputs to design an ETAHE should be greater than 30 m and not exceed 90 to 150 m. This is because of the length which is less than 30 m gives a little thermal efficiency and after a certain point around 90–150 m increasing the length does not result in much better performance, the improvements begin to level off and longest pipe required highest fan power due to the increases of pressure head.

The trend of this result was similar to those of other studies aimed out by *Ascione et al. (2011)*; *Deglin et al. (1999)*; *Ghosal and Tiwari (2006)*; *Lee and Strand (2008)* and *Santamouris et al. (1995)*.

5.2.2.2. Influence of pipe diameter

The calculations are performed for seven different pipe diameters, namely 0.075, 0.10, 0.125, 0.15, 0.20, 0.25 and 0.30 m. The length of the pipe is fixed at 60 m, placed at a depth of 4 m, while the air velocity inside the pipe is fixed at 8 m/s.

Table 5.7 and Figs. 5.10, 5.11 and 5.12 show the effect of pipe diameter on the ETAHE inlet air temperature at the highest ambient air temperature and the lowest air temperature, the efficiency of ETAHE and pressure drop. It could be seen that in cooling modem as the pipe diameter increases, the inlet air temperature increases, where the pipe diameter increased from 0.075 to 0.125 m, 0.125 to 0.20 m and 0.20 to 0.30 m the inlet air temperature increased from 22.85 to 27.49 °C, 27.49 to 32.97 °C and 32.97 to 36.59 °C, respectively. The increasing percentages were 17, 17 and 10 %, respectively. In heating mode, as the pipe diameter increases, the inlet air temperature decreases, where the pipe diameter increased from 0.075 to 0.125 m, 0.125 to 0.20 m and 0.20 to 0.30 m, the inlet air temperature decreased from 20.53 to 16.56 °C, 16.56 to 11.87 °C and 11.87 to 8.77 °C, respectively. The decreasing percentages were 19, 28 and 26 %, respectively.

These results could be attributed to that, larger pipe diameter results in a lower convective heat transfer coefficient on the pipe inner surface and a lower overall heat transfer coefficient of earth tube system (**Lee and Strand, 2008**).

Table 5.7 Influence of pipe diameter on pressure drop, inlet temperature and efficiency of ETAHE at 60 m pipe length and 8 m/s air velocity.

Pipe Diameter, m	T _{inlet} -Heating, °C	T _{inlet} -Cooling, °C	Efficiency, %	Pressure drop, Pa
0.075	20.53	22.85	94	1529.47
0.1	18.7	24.98	83	1103.86
0.125	16.56	27.49	70	842.95
0.15	14.63	29.75	58	677.57
0.2	11.87	32.97	41	489.48
0.25	9.96	35.20	30	374.25
0.3	8.77	36.59	23	304.58

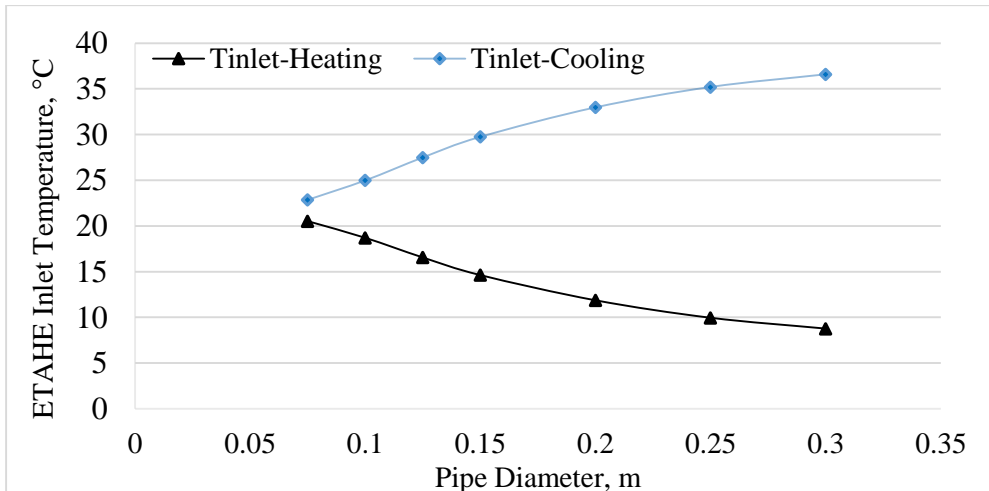


Fig. 5.10 Influence of pipe diameter on inlet air temperature in heating and cooling modes.

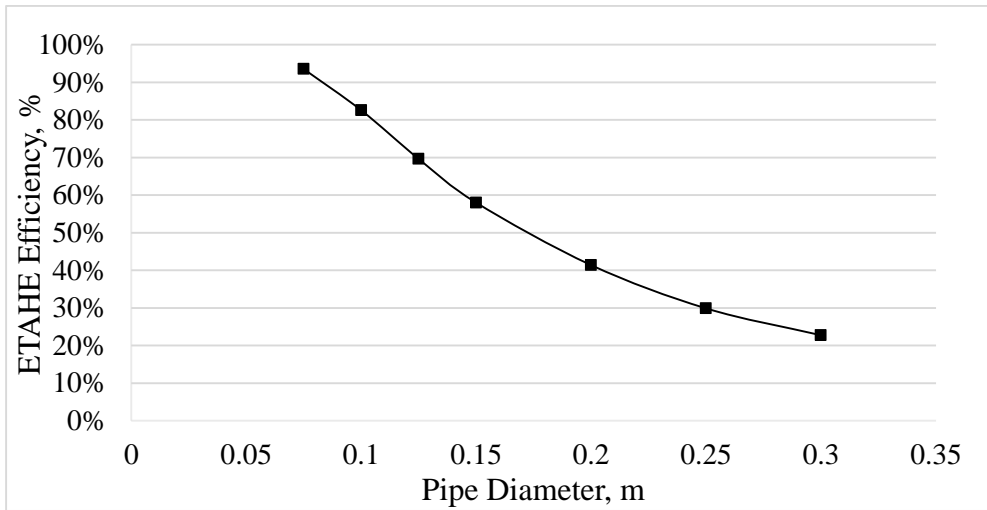


Fig. 5.11 Influence of pipe diameter on ETAHE efficiency.

Fig. 5.11 shows the effect of pipe diameter on the efficiency of ETAHE. It could be seen that as the pipe diameter increases, the efficiency of ETAHE decreases, where the pipe diameter increased from 0.075 to 0.125 m, 0.125 to 0.20 m and 0.20 to 0.30 m, the efficiency of ETAHE decreased from 94 to 70 %, 70 to 0.41 % and 0.41 to 0.23 %, respectively. The decreasing percentages were 26, 41 and 44 %, respectively.

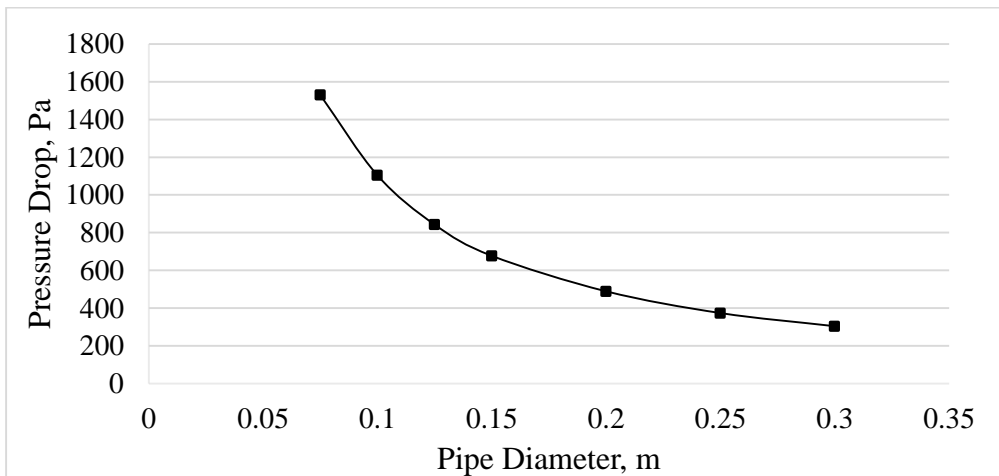


Fig. 5.12 Influence of pipe diameter on pressure drop.

Fig. 5.12 illustrates the effect of pipe diameter on the pressure drop. It could be seen that as the pipe diameter increases, the pressure drop decreases, when the pipe diameter increased from 0.075 to 0.125 m, 0.125 to 0.20 m and 0.20 to 0.30 m, the pressure drop decreased from 1529.47 to 842.95 Pa, 842.95 to 489.48 Pa and 489.48 to 304.58 Pa, respectively. The decreasing percentages were 45, 42 and 38 %, respectively.

The results indicate that an increase in the pipe diameter leads to a reduction in the convective heat transfer coefficient; this leads to a lower air temperature at the pipe outlet and thus reduces the system's heating capacity and a higher air temperature at the pipe outlet and thus reduces the system's cooling capacity. Smaller diameters are preferred from a thermal point of view, but they also correspond (at equal flow rate) to higher friction losses, so it becomes a balance between increasing heat transfer and lowering fan power. Generally, it is concluded that, the optimum pipe diameter ranged from 10 - 30 cm.

The trend of this result was similar to those of other studies **Ascione *et al.* (2011); Deglin *et al.* (1999); Ghosal and Tiwari (2006); Kondili and Kaldellis (2006); Lee and Strand (2008); and Thevenard (2007).**

5.2.2.3. Influence of air velocity

The calculations were performed for seven different air velocities, namely 2, 5, 8, 11, 14, 17 and 20 m/s. The length of the pipes was fixed at 60 m, with a pipe diameter of 0.15 m, buried at a depth of 4 m.

Table 5.8 and Figs. 5.13, 5.14 and 5.15 show the effect of air velocity on the ETAHE inlet air temperature at the highest ambient air temperature and the lowest air temperature, the efficiency of ETAHE and pressure drop. It could be seen that in cooling mode as air velocity

increases, the inlet air temperature increases, where the air velocity increased from 2 to 8 m/s, 8 to 14 m/s and 14 to 20 m/s, the inlet air temperature increased from 23.19 to 29.75 °C, 29.75 to 32.99 °C and 32.99 to 34.80 °C, respectively. The increasing percentages were 22, 10 and 5 %, respectively. In heating mode as the air velocity increases, the inlet air temperature decreases, where the air velocity increased from 2 to 8 m/s, 8 to 14 m/s and 14 to 20 m/s, the inlet air temperature decreased from 20.24 to 14.63 °C, 14.63 to 11.85 °C and 11.85 to 10.30 °C, respectively. The decreasing percentages were 28, 19 and 13 %, respectively.

Table 5.8 Influence of air velocity on pressure drop, inlet temperature and efficiency of ETAHE at 0.15 m pipe diameter and 60 m pipe length.

Air velocity, m/s	T _{inlet} - Heating, °C	T _{inlet} - Cooling, °C	Efficiency, %	Pressure drop, Pa
2	20.24	23.19	92	55.6
5	16.97	27.01	72	289.08
8	14.63	29.75	58	677.57
11	13.01	31.64	48	1209.29
14	11.85	32.99	41	1877.23
17	10.98	34.01	36	2676.44
20	10.3	34.8	32	3603.16

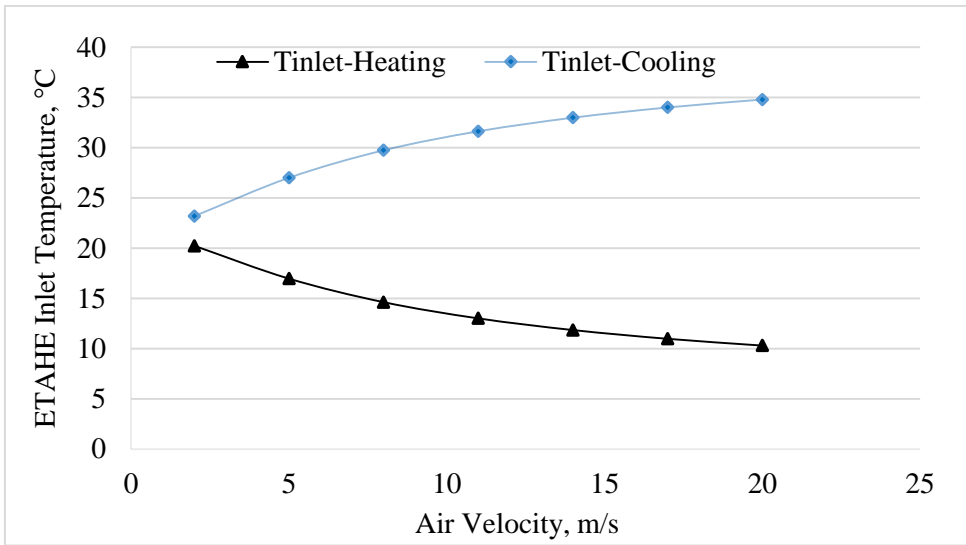


Fig. 5.13 Influence of air velocity on inlet air temperature in heating and cooling modes.

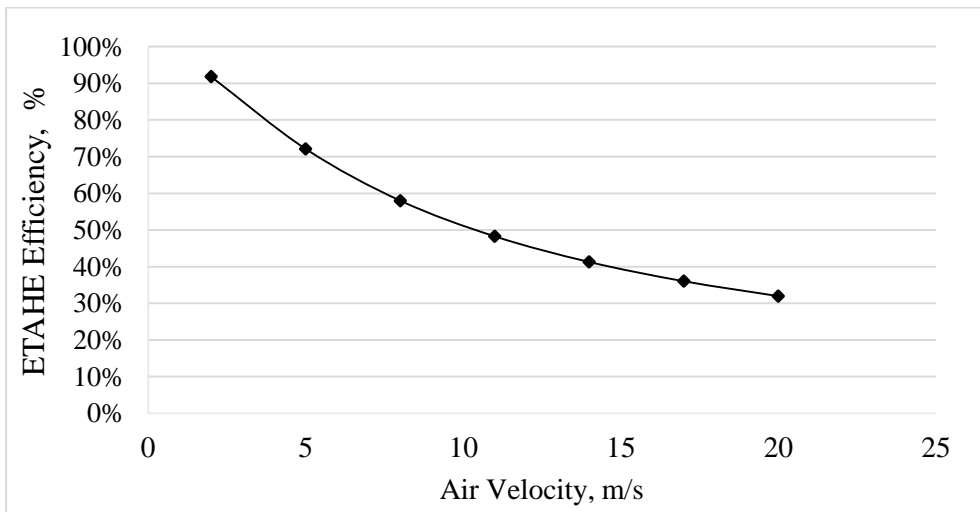


Fig. 5.14 Influence of air velocity on ETAHE efficiency.

Fig. 5.14 shows the effect of air velocity on the efficiency of ETAHE. It could be seen that as the air velocity increases, the efficiency of ETAHE decreases, where the air velocity increased from 2 to 8 m/s, 8 to 14 m/s and 14

to 20 m/s, the efficiency of ETAHE decreased from 92 to 58 %, 58 to 48 % and 48 to 32 %, respectively. The decreasing percentages were 37, 17 and 33 %, respectively.

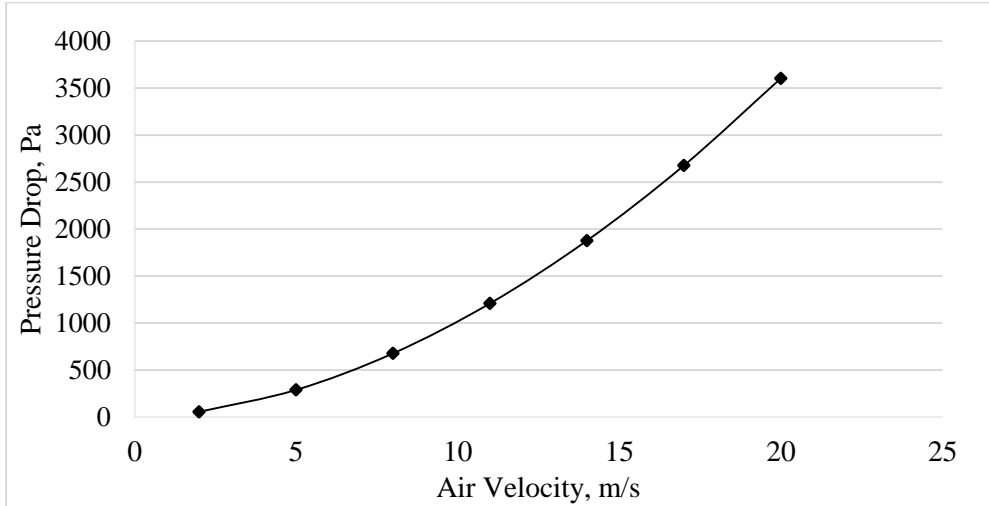


Fig. 5.15 Influence of Air velocity on pressure drop.

Fig. 5.15 shows the effect of air velocity inside the pipe on the pressure drop. It could be seen that as the air velocity increases, the pressure drop increases, where the air velocity inside the pipe increased from 2 to 8 m/s, 8 to 14 m/s and 14 to 20 m/s, the pressure drop increased from 55.60 to 677.57 Pa, 677.57 to 1877.23 Pa and 1877.23 to 3603.16 Pa, respectively. The increasing percentages were 92, 64 and 48 %, respectively.

These results indicate that the decreasing of air velocity causes an increase of thermal efficiency and diminution of pressure losses. Increased air velocity in the pipe leads to a slight decrease in outlet air temperature. This is mainly due to the increase in mass flow. It is concluded that high air velocities are not energy efficient.

5.2.2.4. Influence of pipe material

Table 5.9 and Figs. 5.16 and 5.17 show the effect of pipe material on both the ETAHE inlet air temperature at the highest ambient air temperature and the lowest air temperature and the efficiency of ETAHE. It could be seen that in cooling mode and heating mode there is a small difference between outlet air temperature from ETAHE in tow pipe materials PVC and steel, where the maximum absolute difference between outlet temperature with PVC pipe and steel pipe in cooling and heating modes was 1.80 and 1.54 °C, respectively and the minimum absolute difference was 0.59 and 0.51 °C, respectively.

Table 5.9 Influence of pipe material on inlet air temperature and efficiency of ETAHE at 0.15 m pipe diameter and 60 m pipe length.

Air velocity, m/s	PVC- T _{inlet} - Heating, °C	PVC- T _{inlet} - Cooling, °C	PVC- Efficiency, %	Steel- T _{inlet} - Heating, °C	Steel- T _{inlet} - Cooling, °C	Steel- Efficiency, %
2	20.24	23.19	92	20.75	22.6	95
5	16.97	27.01	72	18.25	25.52	80
8	14.63	29.75	58	16.14	27.98	67
11	13.01	31.64	48	14.55	29.84	58
14	11.85	32.99	41	13.34	31.26	50
17	10.98	34.01	36	12.39	32.36	45
20	10.3	34.8	32	11.63	33.25	40

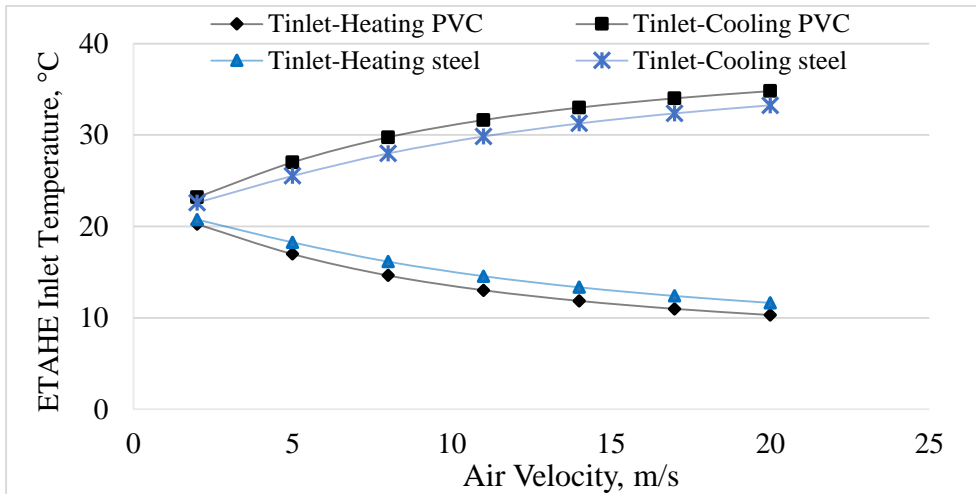


Fig. 5.16 Influence of pipe material on inlet air temperature.

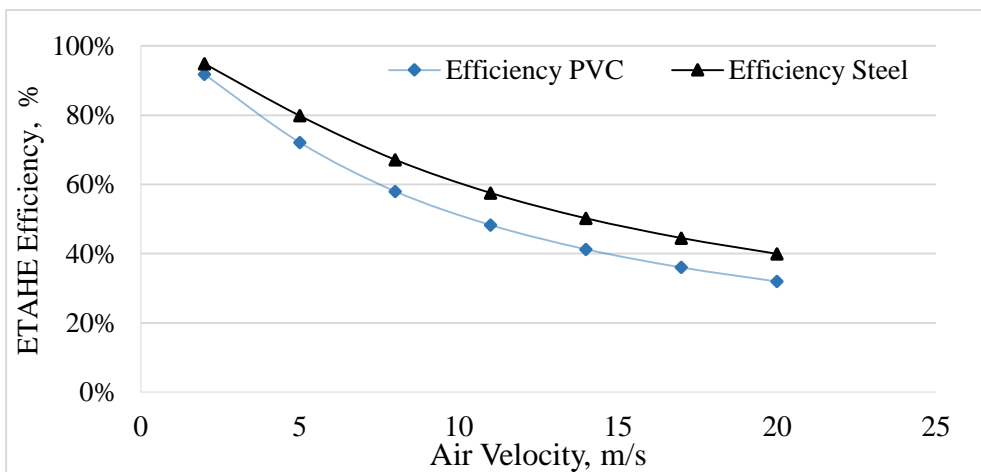


Fig. 5.17 Influence of pipe material on efficiency of ETAHE.

Fig. 5.17 shows the effect of pipe material on the efficiency of ETAHE. It could be seen that, there was a slight difference between the efficiency of ETAHE in both: using PVC pipe and steel pipe, where the maximum absolute difference between efficiency of ETAHE with PVC pipe and steel pipe was 9 % and the minimum absolute difference was 3 %.

These results could be attributed to that, plastic or metallic materials pipe lead to very similar energy performances. This takes place due to the small thickness of the pipe and the conductivity of the soil surrounding the pipe is the limiting factor. Therefore, the different thermal conductivity values scarcely influence the heat exchange, if the right depths and lengths are used (Ascione *et al.*, 2011).

The trend of this result is similar to those of other studies Ascione *et al.* (2011); Deglin *et al.* (1999) and Lee and Strand (2008).

5.2.3. Greenhouse as a case study

The current developed model used to design the ETAHE system to cover the heating and cooling requirements for any agricultural structure. Here greenhouse was taken as a case study. A typical gable even span greenhouse of 256 m² floor area was considered. The developed greenhouse model is used to predict the heating and cooling loads to be 42.91 kWh and 170.39 kWh respectively. The results for optimal design of ETAHE are obtained as shown in Table 5.10.

Table 5.10 The results obtained from geothermal energy model for greenhouse at 11 m/s air velocity and PVC pipe material.

Diameter, m	Pipe length, m		Costs of pipes (LE)		Total fan power, Watt	
	Heating	Cooling	Heating	Cooling	Heating	Cooling
0.10	1065.8	3621.3	17052.8	57940.8	3659.8	12435.0
0.125	998.0	3391.0	22954.0	77993.0	4124.6	14014.6
0.15	952.8	3237.3	30489.6	103593.6	4580.1	15562.4
0.20	897.8	3050.5	44441.1	150999.75	5414.2	18396.4
0.25	860.5	2923.9	74003.0	251455.4	6267.2	21295.0
0.30	836.7	2843.1	119648.1	406563.3	7050.0	23955.0

Table 5.13 shows the costs of pipes for ETAHE system for each diameter from 0.10 m to 0.30 m, in heating and cooling modes, respectively. It could be seen that with increasing diameter of pipe, the pipe costs increasing highly. Where the pipe diameter increased from 0.10 to 0.15 m and from 0.15 to 0.0.25 m, the cost of pipes increased from 17052.8 to 22954.0 LE and from 22954.0 to 74003.0 LE, in heating mode, respectively. The increasing percentages were 26% and 69%, respectively. In cooling mode, pipes cost increases as the pipe diameter increases, where the pipe diameter increased from 0.10 to 0.15 m and from 0.15 to 0.0.25 m, the cost of pipes increased from 57940.8 to 77993.0 LE and from 77993.0 to 251455.4 LE, respectively.

The results indicate that, to minimize the installation cost of ETAHE system for heating and cooling greenhouse under consideration, it is better to use smaller pipe diameters (from 0.10 to 0.30 m), because pipe diameter larger than this range leads to a little improvement in performance of ETAHE system and increases the installation cost. It also preferable to use a smaller air velocity which can be ranged from 5 to 15 m/s, because the air velocity less than 5 m/s required longer pipes and this leads to increase the costs and the air velocity larger than 15 m/s required high fan power and reduces the efficiency of the system. The results indicated that, using of an ETAHE system for heating greenhouse was more efficient and low cost compared to using it for cooling in all cases of pipe diameters. In case of using it for cooling, the remaining cooling requirements could be obtained by other cooling systems, e.g. evaporative cooling systems (fan-pad, fog/mist and roof evaporative cooling systems).

SUMMARY AND CONCLUSION

6. SUMMARY AND CONCLUSION

This study aimed to using geothermal energy in heating and cooling of agricultural structures. The greenhouse is taken here as a case study. To achieve that, geothermal energy system was analysed and restructured as three sub models: soil temperature model, ETAHE model and greenhouse model. Model development, validation and experimentation were performed. The most important results obtained could be summarized as follows:

6.1. Model validation

Geothermal energy system has been presented which consists of three sub models: soil temperature model, ETAHE model and greenhouse model. Soil temperature model was developed using previous researches and adjusted to suit Egyptian conditions. It was validated against two sets of data. The first set obtained by **Kassem (1999)** and the second set measured by field experiment carried out in the present work. The results shown good agreement with measurements in both cases. Where, the root mean squares of deviations of the first set at 1.5 and 2 m depths were 1.93 and 1.85 °C respectively and the normalized root mean squares of deviations to the mean of the predicted data at 1.5 and 2 m depths were 0.10 and 0.09 respectively and the root mean squares of deviations of the second set at 2, 3 and 4 m depth were 2.65, 1.65 and 0.39 °C, respectively and the normalized root mean squares of deviations to the mean of the predicted data at 2, 3 and 4 m depth were 0.14, 0.09 and 0.02, respectively. This soil temperature model was used as a component of ETAHE model.

Similarly an earth to air heat exchanger (ETAHE) model was developed. Its results were validated against the results of three other

studies: **Al-Ajmi, et al. (2006)**, **Lee and Strand (2008)** and **Dhaliwal and Goswami (1984)**. Using same inputs regarding ambient air temperatures which were 25.26 °C and 20.55 °C. It was found that the root mean square of the difference between the model results and their findings were 0.33 and 0.06 °C for **Al-Ajmi et al.**, 0.07 °C and 0.02 °C for **Lee and Strand** and 0.61 °C and 0.19 °C for **Dhaliwal and Goswami**. Therefore, the current model gave good agreement with these studies. It can be suitably used to predict the thermal performance of Earth to Air heat Exchanger (ETAHE) system.

6.2. Model experimentation

The developed model was used to study the influence of pipe length, pipe diameter, pipe material and air velocity inside the pipe on performance of ETAHE system and the cooling and heating potential of the ETAHE system for greenhouse. The results could be summarized as:

- **Pipe Length:** From the obtained results, the optimal values of pipe length used as inputs to design an ETAHE should be greater than 30 m and not exceed 90 to 150 m. This is because at the length which is less than 30 m gives a little thermal efficiency where as a length greater the certain point around 90–150 m does not result in much better performance as the improvements begin to level off and longest pipe required highest fan power due to the increases of pressure head.
- **Pipe diameter:** The results indicated that an increase in the pipe diameter leads to a reduction in the convective heat transfer coefficient. This leads to a lower air temperature at the pipe outlet and thus reduces the system's heating capacity. Higher air temperature at the pipe outlet reduces the system's cooling capacity. Smaller diameters are preferred from a thermal point of view, but (at equal flow rate) it causes higher friction losses, so it becomes a balance

between increasing heat transfer and lowering fan power. The optimum diameter was found to be 0.10 cm to 0.30 m.

- **Air velocity:** The results indicated that the diminution of air velocity causes an increase in thermal efficiency and diminution in pressure losses. Increased air velocity leads to a slight decrease in outlet air temperature in cooling mode. It is concluded that high air velocities are not energy efficient.
- **Pipe material:** plastic or metallic materials lead to very similar energy performances. This takes place due to the small thickness of the pipe and the conductivity of the soil surrounding the pipe is a limiting factor. Therefor the different thermal conductivity values scarcely influence the heat exchange, if the right depths and lengths are used.

6.3. Greenhouse as a case study

The current developed model used to design the ETAHE system to cover the heating and cooling requirements for any agricultural structure. Here greenhouse was taken as a case study. A typical gable even span greenhouse of 256 m² floor area was considered. The developed greenhouse model is used to predict the heating and cooling loads to be 42.91 kWh and 170.39 kWh respectively. Experimentation with the model has shown that, to minimize the installation cost of ETAHE system for heating and cooling greenhouse under consideration, it is better to use smaller pipe diameters (from 0.10 to 0.30 m), because pipe diameter larger than this range leads to a little improvement in performance of ETAHE system and increases the installation cost. It also preferable to use a smaller air velocity which can be ranged from 5 to 15 m/s, because the air velocity less than 5 m/s required longer pipes and this leads to increase the costs and the air velocity larger than 15 m/s

required high fan power and reduces the efficiency of the system. The results indicated that, using of an ETAHE system for heating greenhouse was more efficient and low cost compared to using it for cooling in all cases of pipe diameters. In case of using it for cooling, the remaining cooling requirements could be obtained by other cooling systems, e.g. evaporative cooling systems (fan-pad, fog/mist and roof evaporative cooling systems).

REFERENCES

7. REFERENCES

- Abdullahi, A., M. Andrew, and I. Kenneth. 2007.** The potential of earth-air heat exchangers for low energy cooling of buildings Paper presented at The 24th Conference on Passive and Low Energy Architecture. National University Singapore, Singapore, 2007.
- Al-Ajmi, F., D.L. Loveday, and V.I. Hanby. 2006.** The cooling potential of earth–air heat exchangers for domestic buildings in a desert climate. *Building and Environment* 41(3):235-244.
- Aldrich, R.A., and J.W. Bartok. 1994.** *Greenhouse Engineering*. 3rd revision August 1994 ed. Ithaca, New York 14852-4557: NRAES.
- Alghannam, A.O. 2012.** Investigations of Performance of Earth Tube Heat Exchanger of Sandy Soil in Hot Arid Climate. *Journal of Applied Sciences Research* 8(6):3044-3052.
- Ascione, F., L. Bellia, and F. Minichiello. 2011.** Earth-to-air heat exchangers for Italian climates. *Renewable Energy* 36: 2177-2188.
- ASHRAE. 2009.** *Handbook fundamentals*. Atlanta, GA: American Society of Heating, Refrigerating and Air-conditioning Engineers, Inc.
- ASHRAE. 2011.** *Handbook heating, ventilating, and air-conditioning application* Atlanta, GA: American Society of Heating, Refrigerating and Air-conditioning Engineers, Inc.
- ASHRAE. 2012.** *Handbook Heating, Ventilating, and Air-Conditioning system and equipment*. Atlanta, GA The American Society of Heating, Refrigerating and Air Conditioning Engineers, Inc.

- Bansal, V., R. Misra, G.D. Agrawal, and J. Mathur. 2012.** Performance evaluation and economic analysis of integrated earth–air–tunnel heat exchanger–evaporative cooling system. *Energy and Buildings* 55 (0):102-108.
- Barbier, E., and M. Fanelli. 1977.** Non-electrical uses of geothermal energy. *Prog. Energy Combustion Sci* 3:73-103.
- Beall, S.E., and G. Samuels. 1971.** The use of warm water for heating and cooling plant and animal enclosures. Oak Ridge National Laboratory ORNL-TM-3381.
- Ben Jmaa Derbel, H., and O. Kanoun. 2010.** Investigation of the ground thermal potential in Tunisia focused towards heating and cooling applications. *Applied Thermal Engineering* 30 (10): 1091-1100.
- BP p.l.c.,** BP (British Petroleum) Statistical Review of World Energy, London, United Kingdom, June 2014.
- Central Agency for Public Mobilization and Statistics (CAPMAS), Agriculturals sector. 2013.** Annual bulletin for estimates of the income from agricultural production. www.capmas.gov.eg.
- Central Agency for Public Mobilization and Statistics (CAPMAS), Agriculturals sector. 2013.** Annual bulletin for statistics of the cropping areas and plant production. In; <http://www.capmas.gov.eg>.
- Chel, A., and G. Kaushik. 2011.** Renewable energy for sustainable agriculture. *Agro. Sustain. Dev.* 31:91–118.
- Chow, T.T., H. Long, H.Y. Mok, and K.W. Li. 2011.** Estimation of soil temperature profile in Hong Kong from climatic variables. *Energy and Buildings* 43(12):3568-3575.
- Chung, S.O., and H. R. 1987.** Soil heat and water flow with a partial surface mulch. *Water Resour. Res* 23(12):2175–2186.

- Darkwa, J., G. Kokogiannakis, C.L. Magadzire, and K. Yuan. 2011.** Theoretical and practical evaluation of an earth-tube (E-tube) ventilation system. *Energy and Buildings* 43 (2-3): 728-736.
- Deglin, D., L.V. Caenegem, and P. Dehon. 1999.** Subsoil Heat Exchangers for the Air Conditioning of Livestock Buildings. *J. Agric. Engng Res* 73:179-188.
- Dhaliwal, A.S., and D.Y. Goswami. 1984.** Heat transfer analysis environment control using an underground air tunnel. *ASME Solar Energy Div., Las Vegas*:505-510.
- Dickson, M.H., and M. Fanelli . 2003.** Geothermal background, ed. M.H. Dickson, and M.A. Fanelli. London, UK, UNESCO Renewable Energy Series. Earthscan Publications Ltd, 1-28.
- Dickson, M.H., and M. Fanelli. 2004.** What is Geothermal Energy? www.geothermal-energy.org.
- Ekstrand, M.D., J.T. Riedl, and J.A. Konstan. 2011.** Collaborative filtering recommender systems. *Foundations and Trends in Human-Computer Interaction* 4:81-173.
- Elsner, B.v., D. Briassoulis, D. Waaijenberg, A. Mistrionis, C.v. Zabeltitz, J. Gratraud4;, G. Russo, and R. Suay-Cortes. 2000.** Review of Structural and Functional Characteristics of Greenhouses in European Union Countries: Part I, Design Requirements. *J. agric. Engng Res.* 75:1-16.
- Farghally, H.M., F.H. Fahmy, and M.A. H.EL-Sayed. 2010.** Geothermal Hot Water and Space Heating System in Egypt. Paper presented at International Conference on Renewable Energies and Power Quality (ICREPEQ'10). Granada (Spain), 23rd to 25th March, 2010.
- Florides, G., and S. Kalogirou. 2007.** Ground heat exchangers—A review of systems, models and applications. *Renewable Energy* 32(15):2461-2478.

- Ghosal, M.K., and G.N. Tiwari. 2006.** Modeling and parametric studies for thermal performance of an earth to air heat exchanger integrated with a greenhouse. *Energy Conversion and Management* 47(13-14):1779-1798.
- Ghosal, M.K., G.N. Tiwari, and N.S.L. Srivastava. 2004.** Thermal modeling of a greenhouse with an integrated earth to air heat exchanger: an experimental validation. *Energy and Buildings* 36(3):219-227.
- Goswami, D.Y., and K.M. Biseli. 1993.** Use of Underground Air Tunnels for Heating and Cooling Agricultural and Residential Buildings . Fact Sheet EES 78, a series of the Florida Energy Extension Service, Florida Cooperative Extension Service, Institute of Food and Agricultural Sciences, University of Florida.
- Hanaa, M.F., H.F. Faten, and A.H. Mohamed. 2010.** A simulation Model for Predicting the Performance of PV/Wind –Powered Geothermal Space Heating System in Egypt. *The Online Journal on Electronics and Electrical Engineering (OJEEE)* 2(4):321-330.
- Haytham, M.A., H.F. Fathallah, and A.H.E. Mohamed. 2013.** Geothermal hot water and space heating system in Egypt. Paper presented at 2nd International Conference on Energy Systems and Technologies. Cairo, Egypt, 18 – 21 Feb. 2013.
- International Geothermal Association (IGA). 2010.** Geothermal a natural choice, www.geothermal-energy.org.
- Kassem, A.M.M. 1999.** Possibilities of using soil heat as a renewable source for conditioning greenhouses. Ph. D Thesis, El-Mansoura University, Egypt.
- Kaushik, S.C., P.K. Bhargava, and S. Lal. 2013.** Earth–air tunnel heat exchanger for building space conditioning: a critical review. *Nanomaterials and Energy* 2(4):216-227.

- Kersten, M.S. 1949.** Final report laboratory research for the determination of the thermal properties of soils.
- Kharseh, M. 2009.** Reduction of Prime Energy Consumption in the Middle East by GSHP Systems. PhD, Luleå University of Technology (LTU).
- Kondili, E., and J.K. Kaldellis. 2006.** Optimal design of geothermal–solar greenhouses for the minimisation of fossil fuel consumption. *Applied Thermal Engineering* 26(8-9):905-915.
- Kumar, R., S. Ramesh, and S.C. Kaushik. 2003.** Performance evaluation and energy conservation potential of earth–air–tunnel system coupled with non-air-conditioned building. *Building and Environment* 38(6):807-813.
- Kusuda, T., and P.R. Archenbach. 1965.** Earth temperature and thermal diffusivity at selected stations in the United States. *ASHRAE Transaction* 71(1):61-74.
- Labs, K. 1992.** Ground cooling, in: J. Cook (Ed.), *Passive Cooling*. MA, MIT Press, Cambridge.
- Lashin, A., and A. Nassir . 2010.** Some Aspects of the Geothermal Potential of Egypt Case Study: Gulf of Suez-Egypt. Bali, Indonesia, *Proceedings World Geothermal Congress 2010*.
- Lee, K.H., and R.K. Strand. 2008.** The cooling and heating potential of an earth tube system in buildings. *Energy and Buildings* 40(4):486-494.
- Lee, K.H., and R.K. Strand. 2006.** Implementation of an earth tube system into EnergyPlus Program. Paper presented at *Proceedings of the SimBuild 2006 Conference*. Boston MA, USA, 2006.
- Lund, J.W. 2010.** Direct Utilization of Geothermal Energy. *Energies* 3:1443-1471.

- Lund, J.W., D.H. Freeston, and T.L. Boyd. 2011.** Direct utilization of geothermal energy 2010 worldwide review. *Geothermics* 40:159–180.
- Maerefat, M., and A.P. Haghghi. 2010.** Passive cooling of buildings by using integrated earth to air heat exchanger and solar chimney. *Renewable Energy* 35(10):2316-2324.
- Mands, E., and B. Sanner. 2005.** Shallow geothermal energy. <http://www.ubeg.de/Downloads/ShallowGeothEngl.pdf> (accessed on 12 April 2012).
- Mihalakakou, G. 2002.** On estimating soil surface temperature profiles. *Energy and Buildings* 34:251-259.
- Mihalakakou, G., J.O. Lewis, and M. Santamouris. 1996.** On the heating potential of buried pipes techniques- application in Ireland. *Energy and Buildings* 24:19-25.
- Mihalakakou, G., M. Santamouris, and D. Asimakopoulos. 1992.** Modelling the earth temperature using multiyear measurements. *Energy and Buildings* 19:1-9.
- Misra, R., V. Bansal, G.D. Agrawal, J. Mathur, and T. Aseri. 2013.** Transient analysis based determination of derating factor for earth air tunnel heat exchanger in summer. *Energy and Buildings* 58:103-110.
- Mongkon, S., S. Thepa, P. Namprakai, and N. Pratinthong. 2014.** Cooling performance assessment of horizontal earth tube system and effect on planting in tropical greenhouse. *Energy Conversion and Management* 78:225-236.
- Ogunlela, A.O. 2003.** Modelling soil temperature variations. *J.Agric.Res,Dev.2*, Faculty of Agriculture, University of Ilorin.
- Ozgener, L. 2011.** A review on the experimental and analytical analysis of earth to air heat exchanger (EAHE) systems in Turkey. *Renewable and Sustainable Energy Reviews* 15(9):4483-4490.

- Ozgener, O., and L. Ozgener. 2011.** Determining the optimal design of a closed loop earth to air heat exchanger for greenhouse heating by using exergoeconomics. *Energy and Buildings* 43(4):960-965.
- Ozgener, O., and L. Ozgener. 2010.** Exergoeconomic analysis of an underground air tunnel system for greenhouse cooling system. *International Journal of Refrigeration* 33(5):995-1005.
- Paepe, M.D., and A. Janssens. 2003.** Thermo- hydraulic design of earth- air heat exchanger. *Energy Buildings* 35:389-397.
- Popiel, C., J. Wojtkowiak, and B. Biernacka. 2001.** Measurements of temperature distribution in ground. *Experimental Thermal and Fluid Science*. 25(301-309).
- Ryan, J., G. Estefan, and A. Rashid. 2007.** Soil and plant analysis laboratory manual: ICARDA.
- Santamouris, M., G. Mihalakakou, C.A. Balaras, A. Argiriou, D. Asimakopoulos, and M. Vallindras. 1995.** Use of buried pipes for energy conservation in cooling of agricultural greenhouses. *Solar Energy* 55(2):111-124.
- Sethi, V.P., and S.K. Sharma. 2008.** Survey and evaluation of heating technologies for worldwide agricultural greenhouse applications. *Solar Energy* 82(9):832-859.
- Sharan, G., J. Kamalesh, and S. Anand. 2005.** Greenhouse cultivation in a hot arid area. www.iimahd.ernet.in (accessed on 8 June 2013).
- Sharan, G., and R. Jadhav. 2002.** Soil temperature regime at Ahmedabad. *Journal of Agricultural Engineering*, 39:1, January-March.
- Stecher, D., and K. Klingenberg. 2008.** Design and performance of the Smith House, a passive house. *ASHRAE Trans.* 114(1):209-217.
- Thevenard, D. 2007.** Bibliographic Search on The Potential of Earth Tubes. Numerical Logics Inc:Waterloo, Canada. available on line

www.energy.gov.yk.ca/pdf/biblio_search_earth_tubes_v3_1.pdf
(accessed on 12 April 2012).

- Thevenard, D.** Earth tube ventilation systems - applicability in the Canadian climate. Numerical Logics Inc, 31 March 2011.
- Thorhallsson, S., and A. Ragnarsson . 2008.** Multipurpose use of geothermal energy. Tianjin, China, UNU-GTP, TBLRREM and TBGMED.
- Tiwari, G.N., M.A. Akhtar, A. Shukla, and M. Emran Khan. 2006.** Annual thermal performance of greenhouse with an earth–air heat exchanger: An experimental validation. *Renewable Energy* 31(15):2432-2446.
- U.S. Energy Information Administration. 2014.** Country Analysis Brief: Egypt. August 2014, U.S. Department of energy.
- Zhao, M.Z. 2004.** Simulation of earth-to-air heat exchanger systems. M.Sc Thesis, Concordia University, Montreal, Quebec, Canada.

ARABIC SUMMURY

الملخص العربي

تهدف هذه الدراسة إلى استخدام الطاقة الأرضية في تسخين وتبريد المنشآت الزراعية. تم أخذ البيت المحمي كحالة دراسة. لتحقيق هذا تم تحليل وبناء نظام الطاقة الحرارية الأرضية والذي يتكون من ثلاثة نماذج: نموذج حرارة التربة، نموذج المبادل الحرارى الأرضى ونموذج البيت المحمي واختبار صلاحيته وتجريبه والنتائج الهامة المتحصل عليها يمكن تلخيصها كالتالى:

أولاً: اختبار صلاحية النموذج:

يتكون نظام الطاقة الحرارية الأرضية من ثلاثة نماذج: نموذج حرارة التربة، نموذج المبادل الحرارى الأرضى، نموذج البيت المحمي. تم تطوير نموذج حرارة التربة باستخدام الأبحاث السابقة وتم تعديلها لتلائم الظروف المصرية، كما تم اختبار صلاحيته مع مجموعتين من البيانات. المجموعة الأولى أجراها قاسم (1999) والمجموعة الثانية تمت عن طريق تجربة حقلية أجريت خلال هذه الدراسة، وأعطت نتائج النموذج موافقة جيدة مع القياسات فى كلتا الحالتين. حيث كان متوسط الجذر التربيعى للإختلافات لمجموعة البيانات الأولى عند أعماق 1,5 و 2 متر هي 1,93 و 1,85 درجة مئوية على الترتيب وكان متوسط الجذر التربيعى للإختلافات منسوباً إلى متوسط درجة الحرارة المتوقعة عند أعماق 1,5 و 2 متر هي 0,10 و 0,09 على الترتيب. وكان متوسط الجذر التربيعى للإختلافات لمجموعة البيانات الثانية عند أعماق 2,3 و 4 متر هي 2,65 و 1,65 و 0,39 درجة مئوية على الترتيب وكان متوسط الجذر التربيعى للإختلافات منسوباً إلى متوسط درجة الحرارة المتوقعة عند أعماق 2,3 و 4 متر هي 0,14، 0,09 و 0,02. واستخدم نموذج حرارة التربة كمكون فى نموذج المبادل الحرارى الأرضى.

بالمثل تم تطوير نموذج المبادل الحرارى الأرضى (ETAHE) واختبار صلاحية نتائجه مع نتائج ثلاث دراسات أخرى: Al-Ajmi, et al. (2006), Lee and Strand (2008) و Dhaliwal and Goswami (1984) باستخدام نفس المدخلات فيما يتعلق بدرجة حرارة الهواء الخارجية والتي كانت 25,26 و 20,56 درجة مئوية وقد وجد أن متوسط الجذر التربيعى للفرق بين نتائج النموذج ونتائجهم هو 0,33 و 0,06 درجة مئوية بالنسبة لـ Al-Ajmi, et al.، 0,07 و 0,02 درجة مئوية بالنسبة لـ Lee and Strand، 0,61 و 0,19 بالنسبة لـ Dhaliwal and Goswami. لذلك فقد أظهر النموذج الحالى توافق جيد مع هذه الدراسات. لذا يمكن أن يستخدم للتنبؤ بالأداء الحرارى للمبادل الحرارى الأرضى.

ثانياً: تجريب النموذج:

النموذج الذى تم تطويره لدراسة تأثير كل من طول الأنبوبه وقطرها وسرعة الهواء بداخلها وكذلك مادة الأنبوبه علي أداء المبادل الحراري الأرضي، جهد التبريد والتسخين له عند استخدامه للبيوت المحمية.
يمكن تلخيص النتائج كالتالى:

- **طول الأنبوبية:** من النتائج المتحصل عليها القيمة المثلي لطول الأنبوبية المستخدم كمدخل في تصميم النظام يجب أن يزيد عن ٣٠ متر ولا يزيد عن ٩٠ إلى ١٥٠ متر وذلك بسبب أن الطول الأقل من ٢ متر يعطى كفاءة حرارية منخفضة والطول الأكبر من ٩٠ إلى ١٥٠ متر لا يحسن كثيراً من الأداء الحراري والطول الأكبر يلزمه مضخة ذات قدرة عالية نتيجة زيادة الفاقد في الضغط.
- **قطر الأنبوبية:** أشارت النتائج إلى أن زيادة قطر الأنبوبية يؤدي إلى تقليل معامل إنتقال الحرارة بالحمل وذلك يؤدي إلى إنخفاض درجة حرارة الهواء عند مخرج الأنبوبية مما يقلل من سعة التسخين للنظام، ودرجة حرارة هواء أعلى عند المخرج مما يقلل من سعة التبريد للنظام. ولكن الأقطار الأقل أفضل من الناحية الحرارية ولكن يتبعها فواقد احتكاك أعلى لذلك يجب عمل موازنة بين زيادة إنتقال الحرارة وتقليل قدرة المروحة. القطر الأمثل يتراوح ما بين ١٠ سنتيمتر و ٣٠ سنتيمتر.
- **سرعة الهواء:** أشارت النتائج إلي أن الانخفاض في سرعة الهواء داخل الأنبوبية يسبب زيادة في الكفاءة الحرارية للمبادل الحراري الأرضي ويقلل من فواقد الضغط. زيادة سرعة الهواء داخل الأنبوبية يؤدي إلى انخفاض طفيف في درجة حرارة الهواء الخارج أثناء التبريد. سرعة الهواء العالية يتبعها انخفاض في الطاقة المتحصل عليها.
- **مادة الأنبوبية:** استخدام أنابيب بلاستيكية أو معدنية تؤدي الى كفاءة طاقة متماثلة جداً، وذلك يحدث نتيجة السمك الصغير للأنبوبية كما أن الموصلية الحرارية للتربة المحيطة للأنبوبية تعتبر عامل ضعيف ، لذلك الاختلاف في قيم معامل انتقال الحرارة بالتوصيل نادراً ما يؤثر على انتقال الحرارة إذا استخدم العمق والطول الصحيحين.

البيت المحمي كحالة للدراسة:

استخدم نموذج البيت المحمي المطور للتنبؤ باحتياجات التدفئة والتبريد لبيت محمي جملوني متناظر الجوانب ذو مساحة أرضية مقدارها ٢٥٦م^٢ وكانت على الترتيب ٤٢,٩١ كيلو وات ساعة و ١٧٠,٣٩ كيلو وات ساعة. وتجريب النموذج تبين أن لتقليل تكلفة الإنشاء لنظام

المبادل الحرارى الأرضى يفضل استخدام أقطار أنابيب صغيرة (من ٠,١٠ إلى ٠,٣٠ م) وذلك لأن القطر الأكبر من هذا المدى يؤدي إلى تحسين صغير فى كفاءة النظام ويزيد من تكلفة الإنشاء. كذلك يفضل استخدام سرعات هواء يمكن أن تتراوح من ٥ إلى ١٥ م/ث ، لأن السرعات الأقل من ٥ م/ث تتطلب أنابيب أطول مما يؤدي إلى زيادة التكلفة. والسرعات الأعلى من ١٥ م/ث تتطلب مروحة ذات قدرة عالية وتقلل من كفاءة النظام. وقد أشارت النتائج إلى أن استخدام نظام المبادل الحرارى الأرضى لتسخين البيت المحمى يكون كافى وأقل تكلفة مقارنة باستخدامه للتبريد مع كل أقطار الأنابيب ، وفى حالة استخدامه للتبريد فإن النسبة المتبقية من التبريد يمكن تغطيتها باستخدام نظم تبريد أخرى مثل نظم التبريد التبخيرى (نظام المروحة والوسادة، نظام الضباب ونظام التبريد التبخيرى للسطح).

المستخلص

تهدف هذه الدراسة الى استخدام الطاقة الأرضية فى تدفئة وتبريد المنشآت الزراعية. وفى هذه الدراسة تم أخذ البيوت المحمية كحالة دراسة تحت الظروف المصرية. يتكون نظام الطاقة الحرارية الأرضية من ثلاثة نماذج: نموذج حرارة التربة، نموذج المبادل الحرارى الأرضى ونموذج للبيت المحمى. تم تطوير نموذج حرارة التربة باستخدام الدراسات السابقة وتم تطويرها لتلائم الظروف المصرية، وقد تم اختبار صلاحية هذا النموذج باستخدام مجموعتين من البيانات. المجموعة الأولى أجراها قاسم (١٩٩٩) والمجموعة الثانية تمت عن طريق تجربة حقلية أجريت خلال هذه الدراسة، وأعطت نتائج النموذج موافقة جيدة مع القياسات فى كلتا الحالتين. حيث كان متوسط الجذر التربيعى للفروق لمجموعة البيانات الأولى عند أعماق ١,٥ و ٢ متر هى ١,٨٣ و ١,٨٥ درجة مئوية على الترتيب. وكان متوسط الجذر التربيعى للفروق لمجموعة البيانات الثانية عند أعماق ٢, ٣ و ٤ متر هى ٢,١٩، ١,٩١، و ٠,٧٢ درجة مئوية على الترتيب. واستخدم نموذج حرارة التربة كمكون فى نموذج المبادل الحرارى الأرضى وبالمثل تم تطوير نموذج المبادل الحرارى الأرضى (ETAHE) واختبار صلاحية نتائجه مع نتائج ثلاث دراسات أخرى وقد أظهر النموذج الحالى توافق جيد مع نتائج هذه الدراسات. لذلك يمكن أن يستخدم للتنبؤ بالأداء الحرارى للمبادل الحرارى الأرضى. استخدم النموذج الذى تم تطويره لدراسة تأثير كل من طول الأنبوب، قطرها وسرعة الهواء بداخلها على أداء المبادل الحرارى الأرضى وجهد التبريد والتسخين عند استخدامه للبيوت المحمية تحت الظروف المصرية. وأوضحت النتائج أن القيمة المثلى لطول الأنبوب المستخدم كمدخل فى تصميم النظام يجب أن لا يقل عن ٣٠ متر ولا يزيد عن ٩٠ إلى ١٥٠ متر. والقطر الأمثل يتراوح ما بين ٠,١٠ متر و ٠,٣٠ متر. الانخفاض فى سرعة الهواء داخل الأنبوب بسبب زيادة فى الكفاءة الحرارية للمبادل الحرارى الأرضى يقلل من فواقد الضغط. استخدام أنابيب بلاستيكية أو معدنية تؤدى الى كفاءة طاقة متماثلة جداً. استخدم نموذج البيت المحمى المطور للتنبؤ باحتياجات التدفئة والتبريد لبيت محمى جملونى متناظر الجوانب ذو مساحة أرضية مقدارها ٢٥٦م^٢ وكانت على الترتيب ٤٢,٩١ كيلو وات ساعة و ١٧٠,٣٩ كيلو وات ساعة. وبتجريب النموذج تبين أن لتقليل تكلفة الإنشاء لنظام المبادل الحرارى الأرضى يفضل استخدام أقطار أنابيب صغيرة (من ٠,١٠ إلى ٠,٣٠ متر) وذلك لأن القطر الأكبر من هذا المدى يؤدى إلى تحسين صغير فى كفاءة النظام ويزيد من تكلفة الإنشاء. كذلك يفضل استخدام سرعات هواء يمكن أن تتراوح من ٥ إلى ١٥ م/ث ، لأن السرعات الأقل من ٥ م/ث تتطلب أنابيب أطول مما يؤدى إلى زيادة التكلفة.

والسرعات الأعلى من ١٥ م/ث تتطلب مروحة ذات قدرة عالية وتقلل من كفاءة النظام. وقد أشارت النتائج إلى أن استخدام نظام المبادل الحرارى الأرضى لتسخين البيت المحمى يكون كافى وأقل تكلفة مقارنة باستخدامه للتبريد مع كل الحالات من أقطار أنابيب وسرعات هواء، وفى حالة استخدامه للتبريد فإن النسبة المتبقية من التبريد يمكن تغطيتها باستخدام نظم تبريد أخرى مثل نظم التبريد التبخيرى (نظام المروحة والوسادة، نظام الضباب ونظام التبريد التبخيرى للسطح).

الكلمات الدالة: الطاقة الأرضية، درجة حرارة التربة، نموذج المبادل الحرارى الأرضى، المنشآت الزراعية، البيت المحمى، احتياجات التدفئة والتبريد.

صفحة الموافقة على الرسالة

استخدام الطاقة الأرضية فى تسخين وتبريد المنشآت الزراعية

رسالة مقدمة من

شعبان جابر علي جودة

بكالوريوس العلوم الزراعية (هندسة زراعية)
كلية الزراعة - جامعة بنها (٢٠١٠)

للحصول على درجة الماجستير فى العلوم الزراعية (هندسة زراعية)
وقد تمت مناقشة الرسالة والموافقة عليها:

اللجنة:

أ.د / محمد هاشم حاتم
أستاذ الهندسة الزراعية المتفرغ
كلية الزراعة - جامعة القاهرة

أ.د / زكريا عبد الرحمن الحداد
أستاذ الهندسة الزراعية المتفرغ
كلية الزراعة بمشتهر - جامعة بنها

أ.د عادل حامد بهنساوى
أستاذ ورئيس قسم الهندسة الزراعية
كلية الزراعة بمشتهر - جامعة بنها

أ.د / سمير أحمد على
أستاذ الهندسة الزراعية
كلية الزراعة بمشتهر - جامعة بنها

د / طه حسن مختار عاشور
أستاذ الهندسة الزراعية المساعد
كلية الزراعة بمشتهر - جامعة بنها

تاريخ المناقشة: / / ٢٠١٥

استخدام الطاقة الأرضية فى تسخين وتبريد المنشآت
الزراعية

رسالة مقدمة من

شعبان جابر علي جودة

بكالوريوس العلوم الزراعية (هندسة زراعية)
كلية الزراعة - جامعة بنها (٢٠١٠)

لجنة الإشراف العلمى:

-  أ.د / زكريا عبد الرحمن الحداد
أستاذ الهندسة الزراعية المتفرغ
كلية الزراعة بمشهر - جامعة بنها
-  أ.د عادل حامد بهنساوى
أستاذ ورئيس قسم الهندسة الزراعية
كلية الزراعة بمشهر - جامعة بنها
-  أ.د / سمير أحمد على
أستاذ الهندسة الزراعية
كلية الزراعة بمشهر - جامعة بنها

استخدام الطاقة الأرضية فى تسخين وتبريد المنشآت الزراعية

رسالة مقدمة من

شعبان جابر على جودة
بكالوريوس العلوم الزراعية (هندسة زراعية)
كلية الزراعة - جامعة بنها (٢٠١٠)

للحصول على درجة
الماجستير فى العلوم الزراعية
(هندسة زراعية)

قسم الهندسة الزراعية
كلية الزراعة - جامعة بنها

٢٠١٥